UNIVERSITÀ POLITECNICA DELLE MARCHE

FACOLTÀ DI MEDICINA E CHIRURGIA

DIPARTIMENTO DI MEDICINA SPERIMENTALE E CLINICA (DIMSC)

Corso di Dottorato in "Human Health"

XXXVII° ciclo

Titolo:

"OXYTOCIN AND LEPTIN CROSSTALK IN THE REGULATION OF THE ENERGY BALANCE"

"L'INTERAZIONE TRA OSSITOCINA E LEPTINA NELLA REGOLAZIONE DEL BILANCIO ENERGETICO"

Dottoranda:

Dott.ssa Chiara Galli

Relatore:

Prof. Antonio Giordano

Correlatore:

Dott.ssa Georgia Colleluori

Anno accademico:

2023/2024

List of abbreviations

AT	-	Adipose Tissue
Amy	-	Amygdala
α-Msh	-	Alpha-melanocyte stimulating hormone
AgRP	-	Agouti related protein
ARC	-	Arcuate nucleus
Avp	-	Arginine vasopressin
BAT	-	Brown adipose tissue
BBB	-	Blood brain barrier
BMI	-	Body mass index
CART	-	Cocaine and amphetamine- regulated transcript
CCK	-	Cholecystokinin
CNS	-	Central nervous system
CSF	-	Cerebrospinal fluid
CRH	-	Corticotrophin-releasing hormone
DAB	-	3,3'-diaminobenzidine
DIO	-	Diet-induced obesity
DMV	-	Dorsal motor nucleus of the vagus
DVC	-	Dorsal vagal complex
EIA	-	Enzyme immunoassay
ELS	-	Early Life Stress
ERK	-	Extracellular signal–regulated kinases
GI	-	Gastro-intestinal
GK	-	Glucokinase
gWAT	-	Gonadal white adipose tissue
HFD	-	High fat diet
iBAT	-	Interscapular brown adipose tissue
ICV	-	Intracerebroventricular
IHC	-	Immunohistochemistry
iWAT	-	Inguinal white adipose tissue
InsR	-	Insulin receptor
IP	-	Intraperitoneal
IRS	-	Insulin receptor substrate
JAK-STAT	-	Janus kinase - signal transducer and activator of transcription
K^{atp}	-	ATP-sensitive potassium channel
LBN	-	Limited bedding and nesting
LC-MS	-	Liquid chromatography and mass spectrometry
Lep	-	Leptin
Lepr	-	Long isoform leptin receptor
LH	-	Lateral hypothalamus
MAPK	-	Mitogen-activated protein
MBH	-	Mediobasal hypothalamus
Mc3r	-	Melanocortin 3 receptor
Mc4r	-	Melanocortin 4 receptor
mPC	-	Medial prefrontal cortex

ME	-	Median eminence
MS	-	Maternal separation
mTOR	-	Mammalian target of rapamycin
NaC	-	Nucleus Accumbens
NPY	-	Neuropeptide Y
NTS	-	Nucleus of the solitary tract
Oxt	-	Oxytocin
Oxtr	-	Oxytocin receptor
P	-	Postnatal day
POMC	-	Pro-opiomelanocortin
PI3K	-	Phosphatidylinositol-3-OH kinase
PVN	-	Paraventricular nucleus
PWS	-	Prader-Willi syndrome
qPCR	-	Quantitative real-time PCR
RIA	-	Radioimmunoassay
SOCS3	-	Suppressor of cytokine signalling 3
SON	-	Supraoptic Nucleus
Th	-	Tyrosine Hydroxylase
VMH	-	Ventromedial hypothalamus
VTA	-	Ventral Tegmental Area
WAT	-	White adipose tissue
WB	-	Western blot
WHO	-	World Health Organization

Index

1. ABSTRACT **8**

2. INTRODUCTION

2.1 The central regulation of the energy balance **9**

2.2 The anorexigenic adipokine leptin: central signalling pathways **12**

2.3 The neuro-endocrine oxytocin system: morphological distribution and connectivity, mechanisms of transport and physiological functions **15**

2.4 The central oxytocin system: a hormone mediating the anorexigenic effects of leptin **18**

2.5 The role of the supraoptic nucleus of the hypothalamus in the regulation of the energy balance **21**

2.6 Oxytocin role in the adipose tissue metabolism and obesity: a link with leptin resistance **25**

2.7 Endogenous oxytocin quantification: a methodological issue in obesity research **28**

2.8 Oxytocin and leptin during postnatal development: early life stress and obesity vulnerability in adulthood **30**

3. AIM OF THE STUDY **34**

4. MATERIALS AND METHODS

4.1 Animal cares **35**

4.2 Sample size **36**

4.3 Genotyping of transgenic mouse lines **36**

4.4 Tissue processing and morphological analysis **36**

4.5 Peroxidase immunohistochemistry **37**

4.6 Immunofluorescence and confocal microscopy **39**

4.7 Morphometric analysis **40**

4.8 Leptin "time-course" experiment **41**

4.9 Liquid-Chromatography and Mass Spectrometry **42**

4.10 Real-time PCR **44**

4.11 Western Blot **46**

4.12 Stimulated Emission Depletion Microscopy **47**

4.13 Fluorescent In-situ Hybridization **48**

4.14 Single-cell RNA sequencing **50**

4.15 Stereotaxic surgery **50**

4.16 Calcium imaging **51**

4.17 High-Fat Diet **53**

4.18 Early Life Stress **54**

4.19 Statistical Analysis and softwares **54**

4.20 Tables **55**

5. RESULTS

5.1 Oxytocin neurons distribution in the paraventricular and supraoptic nucleus is sexually dimorphic and changes during the postnatal development **60**

5.2 Leptin activates oxytocin neurons in the supraoptic nucleus **62**

5.3 Leptin induces oxytocin plasma release in a time-dependent and sexually dimorphic manner **66**

5.4 Leptin increases the expression of the oxytocin receptor in the white adipose tissue **71**

5.5 Leptin receptor is not express by oxytocin neurons **73**

5.6 Pro-opiomelanocortin neurons project to melanocortin 4-negative oxytocin neurons in the supraoptic nucleus **75**

5.7 Leptin does not affect calcium signalling in the supraoptic nucleus **79**

5.8 Oxytocin hypothalamic synthesis and plasma secretion in mice exposed to high-fat diet **83**

5.9 Oxytocin secretion in plasma in mice exposed to Early Life Stress **86**

6. DISCUSSION **88**

7. CONCLUSIONS **98**

8. BIBLIOGRAPHY **98**

9. ACKNOWLEDGMENTS **111**

1. Abstract

Oxytocin (Oxt) is a hormone produced by the paraventricular (PVN) and supraoptic (SON) nuclei of the hypothalamus, known to mediate the central anorexigenic effects of the adipokine leptin (Lep), as well as to promote adipose tissue (AT) lipolysis in periphery. Here, we sought to address whether Oxt neurons could directly respond to Lep and if any such regulatory cascade would increase Oxt levels in plasma. Adult C57BL/6J mice were intraperitoneally injected with recombinant leptin (0.5 mg/kg) or saline. We found that Lep induced c-Fos, but not p-Stat3, activation mainly in Oxt neurons of the SON. Furthermore, Lep administration resulted in increased Oxt plasma levels time-dependently and with a sex-dimorphic pattern and in increased Oxt receptor (Oxtr) protein levels in AT. However, Lep receptor (Lepr) is not expressed by Oxt neurons and Lep perfusion failed to induce Ca^{2+} signalling in SON neurons, *ex-vivo*. At the same time, we revealed that melanocortin 4 receptor (Mc4r) is not expressed by Oxt neurons, although pro-opiomelanocortin (POMC) neurons, which are known to express Lepr, abundantly innervated Oxt neurons in the SON. Therefore, we have characterized a Lep-dependent Oxt secretory pathway driven in SON neurons. As Oxt system is shaped during postnatal development and may affect vulnerability to obesity in adulthood, we exposed mice to "early life stress" protocol (ELS) (from postnatal day 2-P2 to P9) and adult mice to 12-weeks of high fat diet (HFD) to assess Oxt circulating levels. We found that endogenous Oxt system is not significantly altered by ELS in mice at P21 but is affected by HFD in adulthood. In conclusion, our study points to the existence of a novel neuroendocrine pathway underlying the crosstalk between Lep and Oxt

and possibly implicated in the regulation of the energy balance, hence of critical relevance for the study of obesity.

2. Introduction

2.1 The central regulation of the energy balance

The regulation of the energy balance refers to the physiological mechanism behind the homeostasis between energy intake and energy expenditure. The regulation of the energy balance is mediated by the central nervous system (CNS), primarily by the hypothalamus, a diencephalic structure surrounding the third ventricle, with a crucial role in the regulation of the body homeostasis [1]. The de-regulation of such energy homeostasis is associated with the development of obesity. [2]

Obesity is recognized by the World Health Organization (WHO) as a chronic, complex and multifactorial disease defined by excessive fat deposits that can impair health [3]. According to the WHO, in 2019 overweight and obesity caused around 5 million deaths [4]; obesity is in fact the fifth leading cause of death worldwide and is significantly associated with an increased risk in the development of cardiovascular disease, type 2 diabetes, and cancer [4]. Due to its global expansion, high numbers of death and current lack of a therapeutic target, obesity has been declared as a global pandemic [5].

Since the regulation of the energy balance largely occurs in the brain, obesity has been defined as a disease of the CNS [2, 6, 7]. Several studies focused on molecules targeting neural pathways behind the regulation of the energy balance to tackle new promising therapeutic approach [8, 9].

The main region within the hypothalamus involved in energy balance regulation is the Arcuate Nucleus (ARC) [2]. The ARC regulates the “hunger-

satiety" circuit and is composed of two population of neurons promoting antagonistic effects on feeding behaviour [10]. The anorexigenic population, which is deputed to inhibit food intake and promote satiety, is the pro-opiomelanocortin (POMC) and cocaine- and amphetamine-regulated transcript (CART) [11]. An opposite role is undertaken by the orexigenic neurons co-releasing Neuropeptide Y (NPY) and agouti related protein (AgRP), which promote hunger and food consumption [12]. In rodent studies, direct optogenetic or pharmacogenetic activation of NPY-AgRP neurons *in-vivo* rapidly increased food intake [13, 14], while chemogenetic activation of POMC neurons in the ARC resulted in a long-term suppression of food-intake [15]. POMC and NPY neurons in the ARC, are classified as primary order neurons and thus the anorexigenic/orexigenic responses are integrated within other hypothalamic circuits located in the ventromedial (VMH) and lateral (LH) hypothalamic nuclei, named secondary order neurons [16], which contribute to suppress/promote food intake and energy expenditure.

Interestingly, recent studies have demonstrated that satiety circuits are composed by an additional nucleus: the paraventricular nucleus of the hypothalamus (PVN), which act as a bridge connecting ARC with other extra-hypothalamic regions involved in the regulation of the energy balance [17]. The PVN's role in energy balance regulation, will be further discussed in another paragraph of this thesis.

The nucleus of the solitary tract (NTS) is an extra-hypothalamic region receiving signals from the gastrointestinal (GI) system, such as the cholecystokinin (CCK), which is a gastrointestinal hormone released postprandially to act as a peripheral signal of satiety [18]. Then, the NTS integrates this anorexigenic signal to the ARC [6]. Of note, the NTS contains also an extra-hypothalamic source of POMC neurons, which are involved in

food intake regulation [15]. The chemogenetic stimulation of POMC neurons in the NTS was found to evoke an acute response of food suppression, in contrast to what observed in the ARC[15], thus suggesting that POMC neurons regulate feeding by integrating long-term signals in the ARC and short-term satiety signals in the NTS.

Importantly, food consumption is not only the result of the interaction between the circuits regulating the homeostatic feeding but also of those responsible for the hedonic eating [7]. Therefore, several mesolimbic, subcortical and prefrontal regions are known to play a pivotal role in food consumption and thus, in energy balance regulation [19]. For instance, ARC neurons were found to project to the amygdala (Amy) [20, 21], a nucleus processing both the emotional behaviour and the energy balance regulation [21] and the activation of the circuit ARC ^{POMC} → Amy resulted in reduced short-term food intake [20]. Furthermore, regions belonging to the limbic system such as the ventral-tegmental area (VTA) and nucleus accumbens (Nac) were demonstrated to promote to the reward-associated and palatable food intake, since they are part of the dopamine circuits [22, 23]. It was observed that the modulation of some dopamine neural circuits, such as those of VTA → Nucleus accumbens (Nac) or medial prefrontal cortex (mPC) → NaC , was associated with altered eating behaviour or the developing of food addiction [23, 24].

Therefore, the central regulation of the energy balance is the result of a complex interaction between different brain regions, which integrate specific stimuli to promote a proper hunger/satiety balance.

However, the stimuli governing energy balance originate in response to the energy state from the peripheral organs, which then create a crosstalk with the CNS [25]. One of the most studied peripheral signals, regulating the energy

balance and playing a critical role in obesity, is the adipose-derived hormone Leptin (Lep). Lep is released by the adipose tissue (AT) and reaches the CNS where it exerts its powerful anorexigenic role [26].

2.2 The anorexigenic adipokine leptin: central signalling pathways

Lep was discovered as the product of the *ob* gene in 1994 by Zhang et al. [27]. Mutation of the Lep gene in Lep-deficient mice (ob/ob) was associated with an obese phenotype [28]. Indeed, Lep is a protein primarily produced by adipocytes of the white adipose tissue (WAT) [27, 29], proportionally with fat mass [30]. Lep circulating levels reflect the filling state of adipose tissue (AT) depots and thus relate directly to the body's long-term energy stores [31]. Moreover, the finding that Lep was produced by WAT contributed to entail a change in the vision of this tissue, which had been considered an inert storage of energy reserves until that time. After Lep discovery, WAT gained recognition as an endocrine organ [32] able to release a wide range of protein signals and factors termed “adipokines” [33].

Once secreted into peripheral circulation, the adipokine Lep signals through the long isoform of the leptin receptor (Lepr) and exerts most of its effects acting on the brain [34]. It indeed serves as the main peripheral signal in the regulation of the energy balance, interacting with a multitude of highly interconnected neuronal populations [25]. It has a central anorexigenic role that is mainly exerted through action on the hypothalamic ARC, where it inhibits orexigenic NPY-AgRP neuron, while it activates anorexigenic POMC-CART neurons [34].

Lepr can be categorized into two major groups: short and long isoforms of the receptor [35]. Lep was demonstrated to bind to the short and long form receptors with the same affinity, although only the long form can transmit Lep signalling and thus induce the intracellular responses [36]. Compared to the short form, the long form has a large intracellular domain consisting of 304 residues and has several putative "Janus kinase/signal transducer and activator of transcription" (JAK/STAT) binding sites [37]. JAK-STAT is the main signalling pathway through which Lep regulates food intake and energy homeostasis in the hypothalamus [37, 38]. The mammalian STAT family has seven members (STAT1-STAT4, STAT5a-b, STAT6) among which STAT3 is recognized as the major player in the Lep-induced anorectic effects [39, 40]. Indeed, Lep administration in rodents was shown to induce Stat3 phosphorylation in the main regions involved in the regulation of the energy balance, such as the ARC, the VMH and the NTS [38, 41]. Furthermore, the specific knock-out of the tyrosine residue in Lepr-mediating Stat3 activation, induced an hyperphagic and obese phenotype in mice [39], thus strengthening the pivotal role of Stat3 in the regulation of the energy balance mediated by Lep.

However, JAK-STAT is not the only transduction pathway involved in the regulation of the energy balance mediated by Lep: the central administration of Lep was demonstrated to activate the insulin receptor substrate (IRS)–phosphatidylinositol 3-OH kinase (PI3K) signalling (Fig. 1) in the mediobasal hypothalamus (MBH) [42]. Furthermore, PI3K was observed to integrate insulin and Lep signalling in hypothalamic cultures [42], although mice with impaired PI3K signalling in POMC neurons had normal body weights *in vivo*, thus suggesting that PI3K signalling in the ARC is not critical for the Lep-mediated regulation of the energy balance [43].

In contrast, several studies demonstrated the role of the mitogen-activated protein (MAPK) in the Lep-mediated regulation of the energy balance, among which the extracellular signal-regulated kinase 1/2 (Erk 1/2) was specifically induced by Lep (Fig. 1) in the ARC [37, 44, 45]. Furthermore, a pharmacological blockade of hypothalamic Erk1/2 was found to reverse the anorectic and weight-reducing effects of Lep [46].

Importantly, several papers demonstrated that Erk signalling mediates the activation of the downstream signal c-fos [35, 37, 44]. c-Fos is part of the "immediate early genes" which are activated transiently and rapidly in response to specific cellular stimuli [47]. The study of c-Fos has been always widely employed in neuroscience as a marker of cell activation and the staining of these proteins was considered as an extremely useful technique for functional anatomical mapping under specific stimuli [48]. Lep was found to activate c-Fos in the ARC [49-51] and in the PVN [50, 52], thus supporting the activation of Erk1/2 - cFos signalling in the Lep-mediated regulation of food intake and energy balance.

The Lep signalling in the brain is thus pivotal for the central regulation of the energy balance and lack of functional Lep or Lepr, is the first cause of genetic obesity in humans [53, 54]. Obesity phenotype was indeed observed in ob/ob mice [28] and in those mice lacking the intracellular domain of the long form of Lepr, named db/db [40].

The first evidence of a "Lep insensitivity" in obesity was observed when exogenous Lep failed to reduce food intake and body weight in obese mice [55], where Lep circulating levels are known to be high [34]. Together, these evidences suggest that hyperleptinemia coupled with impairments in the Lep

system induce a state of “resistance” to Lep signalling, which is associated with obesity disease and other metabolic disorders [56].

Among the potential mechanisms for Lep resistance, defects in Lep signalling in hypothalamic neurons expressing Lepr were hypothesized to be involved in obesity [57]. Leptin signalling is negatively regulated by many intracellular proteins, including the “suppressor of cytokine signalling 3” (SOCS3) which normally provides a negative feedback regulatory mechanism on JAK-STAT signalling to prevent over-activation of the Lepr-associated pathways [57, 58]. However, SOCS3 expression was found to be increased in obese rodents [57] and the hypothalamic inactivation of SOCS3 retained sensitivity to exogenous Lep administration in obese mice [59]. This evidence suggest that elevate SOCS-3 activity in leptin-responsive neurons is a potential mechanism for Lep resistance [57].

The whole central mechanism behind Lep resistance remained to be determined and several processes, including impaired Lep transport, may be involved in these phenomenon [60].

2.3 The neuro-endocrine oxytocin system: morphological distribution and connectivity, mechanisms of transport and physiological functions

Oxt is a neuropeptide produced by magnocellular and parvocellular neurons located in the PVN and in the supraoptic nucleus (SON) of the hypothalamus [61]. Magnocellular neurons are found in the PVN and the SON and mainly project to the neurohypophysis, where Oxt is released into the circulation; parvocellular neurons are mainly located in the PVN but are also scattered in

other hypothalamic and extrahypothalamic areas and project to different hindbrain regions, such as the NTS [61, 62].

Oxt was discovered in the 1909, when Sir Henry H. Dale applied an extract from the posterior pituitary gland to an uterus of a cat and observed that it induced uterine contractions [63]. Therefore, the name originated from the greek “oxys” and “tokos”, meaning “quick birth” [61].

Besides its primary role as the “hormone of labour”, Oxt displays a wide range of physiological functions: it promotes milk ejection, stimulates maternal cares and social bonding and regulates response to stress, anxiety, and depression [64-67].

Furthermore, Oxt modulates food intake and acts as an anorexigenic hormone [17, 68]. The complex role of Oxt in the regulation of the energy balance, will be the main object of this thesis and discussed in depth in the next paragraphs.

The widespread effects of Oxt reflects the complexity of this system in the CNS, where it acts as neuromodulator, mainly by two complementary mechanisms: 1) somatodendritic release and 2) axonal transmission [69].

Somatodendritic Oxt release mediates localized effects in the hypothalamus and neighbouring brain areas, fine-tuning the sensitivity of the Oxt system, while axonal transmission extends Oxt signalling to remote brain regions [61, 70]. In specific, several studies in mice demonstrated that magnocellular Oxt neurons in the PVN/SON release Oxt somatodendritically in the posterior pituitary, while parvocellular Oxt neurons in the PVN send out axonal projections to several extrahypothalamic regions, such as the forebrain limbic regions (e.g., mPC, Nac, Amy, bed nucleus of the stria terminalis, hippocampus).

However, recent investigations in rats [71] demonstrated that also magnocellular Oxt neurons project to extrahypothalamic regions (e.g. the cerebral cortex) [69, 72], thus highlighting a possible interspecies differences in morphological patterns and connectivity of Oxt neurons [69], which must be taken into account while investing the Oxt system.

Interestingly, Oxt axons and/or dendrites were also found in the proximity of the third ventricle and among ependymal cells in direct contact with the cerebrospinal fluid (CSF), thus suggesting that Oxt neurons may directly release the neuropeptide into the third ventricle and/or act as biochemical sensors [73, 74]. Furthermore, Oxt receptor (Oxtr) has been detected in various brain areas, including those where Oxt neuron projections were not documented [61]. Such mismatch, together with the Oxt detection in the CSF, suggests that Oxt signalling may involve synaptic and volume transmission [69, 75]. The dendritic Oxt release was demonstrated to occur independently of neuron spiking activity and to allow Oxt action on different target cells, even far from the area of secretion, thus operating across a broader spatial and temporal scale [69].

Then, it is likely that different transport modalities work together: the somatodendritic transmission establishes a baseline and fine-tunes excitation, while axonal release and volume/synaptic transmission provide precise control over timing and location, efficiently targeting Oxtr in distant brain regions [69, 76].

In this context, it should be stressed that Oxt and the regulation of Oxtr expression is mediated by sex steroids, hence sex dimorphism should always be considered when investigating the Oxt system [77, 78]. Compared to males, female mice display a higher number of Oxt-immunoreactive neurons in the

PVN and the SON and more Oxt projections to several brain mesolimbic areas [79]. However, a study of Oxt^{Cre};Z/AP mice, where Oxt neurons are labelled with alkaline phosphatase, documented similar Oxt projections in both sexes [80].

Another possible confounder is the close homology between Oxt and the arginine vasopressin (Avp) hormone, which is synthetized in the PVN and SON [61] in response to osmotic balance and blood pressure regulation [81]. These two neuropeptides are similar in structure, differing by only two amino acids, as well as their receptors [82]. Furthermore, they are both involved in social behaviour and in the regulation of the stress-response by modulating the hypothalamic-pituitary-adrenal axis [61, 83]. Interestingly, previous studies demonstrated that Oxt and Avp can also activate each other's receptors, particularly when present at high levels, resulting in a crosstalk between these two neuropeptides [82]. Therefore, it is pivotal to consider Avp when investigating the Oxt system.

2.4 The central oxytocin system: a hormone mediating the anorexigenic effects of leptin

In 1989, Arletti et al. described for the first time that Oxt administration (intraperitoneally-IP or intracerebroventricularly-ICV) decreased food intake in rats, by reducing meal size and time spent eating [84]. Furthermore, exogenous Oxt administration in both mice and rats led to sustained weight suppression by reducing food intake, increasing or maintaining energy expenditure and improved glucose homeostasis [85-87]. Oxt and Oxtr knockout (-/-) mice were shown to develop late-onset obesity [88, 89], with increased abdominal fat pads and fasting plasma triglycerides. These findings

in animals, indicated that Oxt might be a novel therapeutic target for the treatment of obesity and metabolic disorders [68].

Further evidence emerged when patients suffering from Prader-Willi syndrome (PWS), were found to have impairments in Oxt neurons in the PVN [90, 91]. The main clinical characteristic of PWS is a sever hyperphagic obesity, which was associated with a significant decrease in the number of Oxt-expressing neurons in the PVN [90], thus suggesting that endogenous Oxt is a powerful anorexigenic molecule [17].

At the same time, accumulate evidence suggested that Oxt neurons in the PVN may mediate the central anorexigenic effect of the adipokine Lep [17, 92-95].

Perello et al. showed that ICV injection of Lep can induce p-Stat3 activation in Oxt neurons in the PVN projecting to the NTS (PVN Oxt → NTS) [93]. Furthermore, the injection of an Oxtr antagonist in the fourth ventricle (close to the NTS) blunted the Lep plus CCK -induced activation of c-Fos [95]. Consistently, Oxtr was abundantly detected in the NTS [95, 96] and the Oxt content in the dorsal vagal complex (including the NTS) was found to increase in response to Lep intraperitoneal administration (1 mg/kg) in mice [97]. In addition, the administration of an Oxtr antagonist into the NTS was found to blunt the effect of Lep in decreasing food intake [97].

Altogether, these evidence supports the hypothesis that Oxt neurons in the PVN are a component of a Lep-sensitive signalling circuit between the ARC and the NTS, thus integrating adiposity signalling of Lep with that produced by meal-related satiety signals in the brainstem [95, 98].

Studies in rodents demonstrated that Oxt neurons in the PVN also project to POMC and NPY-AgRP neurons in the ARC (PVN Oxt → ARC), where Oxtr

is expressed [17, 99]. The *ex-vivo* administration of Oxt was shown to increase the Ca^{2+} activity in POMC neurons in the ARC and the ICV injection of Oxt in the ARC resulted in reduce food intake in rats [99]. At the same time, Lep-sensitive ARC neurons were reported to project to PVN (ARC → PVN) [92] and Lepr expression was described in Oxt neurons of PVN and SON by IHC in rats [100]. In addition, the "alpha-melanocyte stimulating hormone" (α-Msh) derived from POMC neurons, was demonstrated to directly activate magnocellular Oxt neurons of the PVN in rats [101]. Once secreted, the α-Msh binds to the melanocortin 4 receptor (Mc4r) and *Mc4r mRNA* was reported to be expressed in the PVN in both humans [102] and rodents, although in the latter the Mc4r-expressing cells were not Oxt neurons [103], thus suggesting that Lep may directly target Oxt neurons in the PVN through Lepr.

Therefore, Oxt neurons may be involved in a complex neural network integrating peripheral afferents: the circuit PVN Oxt → NTS pathway may integrate the vagal afferent [92], while the ARC → PVN Oxt pathway may be under the influence of peripheral humoral factors, such as Lep [92].

Importantly, several studies reported that Oxt neurons in the PVN remains sensitive to Lep also in rodent models of Lep resistance: Perello et al. [104] showed that in diet-induced obese (DIO) rodents, which developed Lep-resistance, Lep administration failed to induce p-Sta3 in the ARC but not in Oxt neurons in the PVN [93]. Furthermore, Wu et al. observed that mice were more sensitive to develop DIO and Lep-resistance in a sex-dimorphic way, when Oxt neurons were ablated [94].

Therefore, altogether this evidence suggest that Oxt may mediate and enhance the anorexigenic effect of Lep by a specific Lep-Oxt circuit involving the PVN.

The disruption of such crosstalk may be involved in the development of Lep-resistance and obesity.

2.5 The role of the supraoptic nucleus of the hypothalamus in the regulation of the energy balance

Several studies regarding the role of Oxt in the regulation of the energy balance have largely focused on the PVN [95], while Oxt neurons in the SON were historically not associated with this role [17]. SON neurons are known to be activated by several stimuli and involved in multiple physiological functions such as lactation [105], body temperature regulation [106], osmotic balance [107, 108] and pain response [109]. Furthermore, they are also the main source of neuropeptides (Oxt, Avp) release in circulation [110].

Although SON neurons were poorly investigated in the context of the regulation of the energy balance, there are evidences reporting that c-fos expression was increased after feeding in the SON [92] and Oxt neurons in this region were responsive to anorexigenic peripheral signals, such as the CCK [111]. Concurrently, the presence of the insulin receptor (InsR) was described in the SON [112, 113], which raised the possibility that these neurons may regulate food intake and glucose metabolism, consistently with the anorexigenic role of Oxt [114-116].

The paper from Song et al. [114] revealed the presence of the enzyme glucokinase (GK) and the ATP-sensitive potassium channel (K^{atp}) in the SON, (both recognized as "glucose sensors" [117-119]) and demonstrated that SON neurons directly respond to glucose and insulin by increasing Ca^{2+} activity and Oxt release, thus functioning as "metabolic sensors".

Interestingly, the article from Sladek et al. [115] reported that Oxt neurons in the SON may become resistant to glucose/insulin in lactating rats as a strategy to maximize the energy stores necessary for lactation [115]. At the same time, experiments *in-vitro* suggest that Oxt neurons in the SON remained responsive to insulin in DIO rats [115].

Furthermore, Oxt neurons in the SON are reported to express Lepr [100]. However, few articles investigated the direct [120-122] or indirect [123] effect of Lep in the SON: in rodents, Lep induced mainly an inhibitory response in SON neurons when administered *ex-vivo* to hypothalamic brain slices [120], while neuronal activation was observed by injecting Lep directly into systemic circulation *in vivo* [122]. Importantly, Lep failed to induce an excitatory response in SON neurons in both pregnant and in DIO rats [120, 122], thus suggesting that Lep-sensitivity in SON may be reduced during particular conditions, such as pregnancy and obesity. However, these studies did not investigate whether Lep resistance specifically affected the neuronal response of Oxt neurons in the SON.

Furthermore, Mc4R and Mc1R were found to be expressed in Oxt neurons of the SON, and the central administration of α-Msh was reported to activate these neurons [123, 124].

Importantly, α-Msh is released by POMC terminals originating from ARC/NTS, but it has not yet been demonstrated whether POMC neurons [99] send projections to Oxt neurons in the SON (ARC/NTS → SON).

Interestingly, as for the PVN, SON neurons were observed to project to the ARC (SON → ARC) [17, 99]. *Therefore, a complex and still unveiled neural network may exists linking POMC neurons in the ARC and Oxt neurons in the SON, possibly mediating the crosstalk between Lep and Oxt.*

Of note, Oxt neurons in the SON express Oxtr and receive several axonal projections from parvocellular Oxt neurons of the PVN, which is a mechanism hypothesized to mediate the regulation of Oxt release [125]. Therefore, is of importance to consider that Oxt neurons in the SON are strongly related to those residing in the PVN and they could play synergically by integrating different central/peripheral stimuli (e.g. CCK in the PVN and Lep in the SON). Furthermore, the expression of Lepr in Oxt neurons of the PVN [100] could indirectly mediate the action of Lep in Oxt neurons of the SON.

Grouping all the evidence together, the molecular setting (Lepr, InsR, GK, K^{atp}) coupled with the response to peripheral molecules, such as Lep, suggest that SON neurons may have a role in the regulation of the energy balance. Since Oxt is recognized as an anorexigenic neuropeptide mediating the effect of Lep [93], it is possible that the role of the SON in the regulation of the energy balance is mediated by Oxt neurons [114].

However, several questions are still opened regarding the crosstalk between Lep and Oxt in the SON (Fig. 1) and is still not known whether:

1) Oxt neurons in SON are activated by Lep.

2) Oxt neurons in SON are directly targeted by Lep through Lepr.

3) Oxt neurons in SON receive POMC projections by the ARC.

4) Oxt neurons in SON respond to POMC-derived α-Msh through Mc4r.

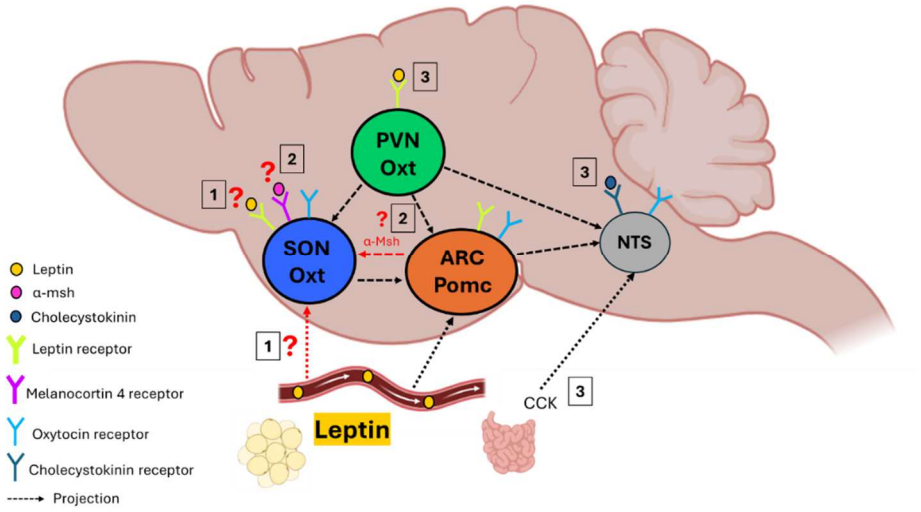

Figure 1: *Central pathways linking Oxt neurons of the SON to the regulation of the energy balance mediated by Lep.* Oxt neurons of the SON are reported to express Lepr. However, it is not known whether the adipose-derived Lep, which is transported to the SON through the bloodstream, directly targets Oxt neurons by binding to Lepr (**1**). Oxt neurons in SON project to POMC neurons in the ARC, which express Oxtr and it is unknown whether POMC neurons send back projections to Oxt neurons in the SON, where Mc4r is reported to be expressed. Therefore, a further possible mechanism of interaction between Lep and Oxt may rely on the α-Msh release by POMC neurons and binding to Mc4r in the SON (**2**). In addition, Oxt neurons in the SON express Oxtr and receive projection from the PVN, which is targeted by Lep through Lepr and project to the NTS, which express the receptor for the gut-hormone CCK and integrates gut-derived anorexigenic signals with the Lep-mediated pathway in the ARC (**3**). SON=supraoptic nucleus of the hypothalamus; PVN=paraventricular nucleus of the hypothalamus; Oxt=oxytocin; Oxtr= oxytocin receptor; ARC=arcuate nucleus; Leptin= Lep; Lepr=leptin receptor; POMC=pro-opiomelanocortin neurons; Melanocortin 4 receptor=Mc4r; α-Msh=α-Melanocyte-stimulating hormone NTS=nucleus of the solitary tract; CCK=cholecystokinin. This picture was created by using the Scientific Image and Illustration Software: www.biorender.com.

2.6 Oxytocin role in the adipose tissue metabolism and obesity: a link with leptin resistance

The anorexigenic effect of Oxt rely on its central activity, resulting in decreased body weight and improved metabolic health [17]. However, Oxt was discovered to regulate body weight not only by modulating food intake in the CNS, but also by directly acting on AT [88, 126-128]. Oxtr is abundantly expressed in WAT, in both the subcutaneous and visceral depots [129] and Oxt treatment was shown to induce fatty acid uptake and lipolysis *in vitro* [130, 131].

Assinder et al. [126] observed that Oxt directly promote lipolysis on 3T3-L1 adipocytes and increased the secretion of the adipokine Lep, which was previously demonstrated to promote lipolysis in AT [132].

These results were confirmed *in vivo,* where Oxt has a powerful anti-obesogenic effect by directly acting on AT [131]. Deblon et al. found that ICV administration of Oxt in DIO rats, resulted in decreased body weight and increased lipolysis and β-oxidation, while no variation in lipogenesis and fat storage was reported [85]. Importantly, this study also demonstrated that the central Oxt administration was responsible for decreased Lep levels in plasma, a result which was quite in contrast to what observed *in vitro* [126]. Indeed, the role of Oxt in inducing/suppressing Lep release and the consequent role of Oxt in promoting or limiting Lep-mediated lipolysis is still debated [126] and the mechanism behind Lep-Oxt crosstalk in AT is not fully elucidated [17].

The exogenous administration of Oxt was shown to successfully treat obesity in rodent models of Lep resistance, such as ob/ob and db/db mice, which resulted in decreased body weight and improved glucose homeostasis [17]. Furthermore, Altirriba et al. [128] reported that, Oxt treatment in ob/ob mice

resulted in increased expression of enzymes involved in futile cycling of the fatty acids, suggesting that Oxt may induce energy dissipation in AT.

Interestingly, Oxtr expression was reported to be increased in db/db mice, where Oxt treatment had a strong effect in inducing lipolysis and in reversing the obesity-induced inflammation in adipocytes, further suggesting that Oxt functioning in AT is enhanced in Lep-resistant mice [127].

All together these evidence highlight the role of Oxt in overcoming Lep-resistance in rodents, overall improving the metabolic health in obesity [17]. However, the whole mechanism behind this process is still currently unknown.

Importantly, Oxt administration and its role in body weight regulation was tested also in human patients [68, 131]. A randomized, placebo-controlled study of 24 IU of Oxt delivered intranasally four times per day in overweight or obese men and women, demonstrated that Oxt led to substantial weight loss over 8 weeks [133]. However, the data regarding the role of Oxt in treating obesity disease are still controversial, since a recent randomized, placebo-controlled trial in adults with obesity, showed that intranasal Oxt administered four times daily for 8 weeks did not reduce body weight [134].

A further huge gap in literature is represented by the study of the role of the endogenous Oxt system in AT metabolism, body weight regulation and in obesity disease. Of note, Oxt is secreted not only by the PVN/SON but also by peripheral organs, such as in the myenteric and submucous ganglia along the GI tract [135], where Oxt was demonstrated to modulate gastric/intestinal motility and inflammation [136] . Importantly, a recent paper from Li et al. showed a novel mechanism of endogenous Oxt secretion from the sympathetic nerves of the AT, which was demonstrated to synthetize and release Oxt locally to promote lipolysis in both rodents and humans [137]. However, this

study did not provide further evidence regarding the absence of the hypothalamic contribution to the Oxt release in mediating the lipolysis in AT. [137].

Further studies are needed to establish the role of endogenous Oxt system in obesity and to disentangle the physiological basis behind the crosstalk between Oxt and Lep in AT (Fig. 2).

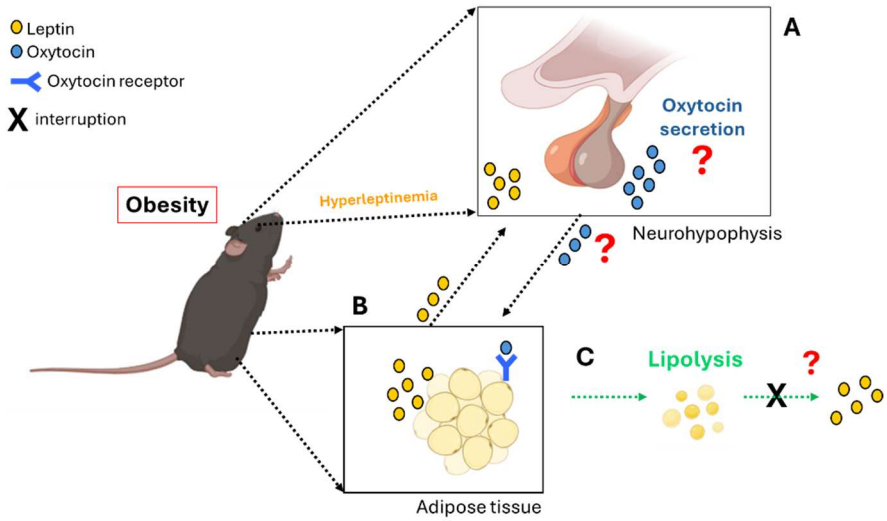

Figure 2: *Lep-Oxt crosstalk in obesity*. Obesity is associated with hyperleptinemia. However, it is not known whether Lep secretion by the AT may affect the endogenous Oxt release by the neurohypophysis in obesity (**A**). Furthermore, it is not known whether endogenous Oxt system regulates lipolysis during obesity by binding to Oxt receptor in the AT (**B**). The Oxt-mediated lipolysis may result in decreased Lep secretion by the AT to counteract Lep-resistance in obesity (**C**). AT= adipose tissue; Lep=leptin; Oxt=oxytocin. This picture was created by using the Scientific Image and Illustration Software: www.biorender.com.

2.7 Endogenous oxytocin quantification: a methodological issue in obesity research

Oxt treatment has a powerful anti-obesogenic effect. However, data regarding the endogenous Oxt levels in both rodent models and human subjects with obesity are discordant [131]. In rodents, plasma Oxt levels were reported to be decreased in high fat diet (HFD)-fed mice [138], which also developed Lep resistance and the same result was observed in obese Zucker rats [139]. In human studies, mean Oxt levels in serum were reported to be higher in overweight men and women compared with healthy normal-weight controls [140, 141]. Furthermore, mean Oxt concentration was positively associated with body mass index (BMI), fat mass and lean mass in premenopausal women across a wide body weight range [141]. In contrast, other studies reported an opposite result with reduced fasting levels of serum Oxt in patients with obesity who had also insulin resistance, dyslipidaemia and hypertension [142, 143].

The discrepancy in these observations could be attributed to the differences in subject characteristics (healthy lean vs. overweight/obese, with or without metabolic syndrome and diabetes), as well as in the methods employed to measure Oxt levels [68, 131]. Indeed, in interpreting data regarding Oxt concentration in serum/plasma, it is important to recognize that measurement of Oxt levels in blood samples is controversial and rigorous validations of the commercially available assays have never been performed [144].

In 1970, the measurement of peripheral Oxt was facilitated by the advent of radioimmunoassay (RIA) [145], which was used also for measuring Avp [146, 147]. Since both Oxt and Avp have a low-molecular weight, extraction was shown to be necessary to concentrate Oxt and Avp levels [148]. Using such

methods, researchers have determined that in healthy women and men, normal Oxt and Avp concentrations in plasma are ~<10 pg/ml, in the range of ~1–3 pg/ml for most people, and for many people are below the lower limit of detection [146, 148, 149].

The later development of the enzyme immunoassay (EIA) methods, which not required the extraction phase [145, 148], yielded concentrations of Oxt which were two orders of magnitude higher than those obtained in analogous samples using RIA with extraction [145, 148]. The same phenomenon was observed in rodents, where EIA quantified Oxt levels in blood that were higher than those previously published [145, 150]. In contrast, for the quantification of Avp in biological samples, the RIA has remained the most widely employed technique [147, 151, 152].

McCullough et al. reported that the commercial RIA has a huge lack of sensitivity for Oxt, since most of the samples' values fell below the assay's detection limit [145]. The same limitations of these methods may affect Avp quantification by RIA.

Since Oxt in blood may undergo structural modifications, due to Oxt degradation or binding with plasma proteins, the EIA method without extraction may detect these macromolecules and thus lead to the overestimation of the Oxt concentration in plasma [145, 153]. McCullough et al. [145] revealed at least two macromolecular species in plasma that showed Oxt-like immunoreactivity in the un-extracted plasma measured by EIA.

However, despite the inconsistency of the results, RIA and EIA are still widely used for Oxt and Avp quantification in blood in both rodents and humans samples [137], although they are not the unique solution.

An alternative is represented by the Liquid chromatography and mass spectrometry (LC–MS), which is recognized as the gold-standard technique to measure both Oxt and Avp in blood due to its high sensitivity, selectivity and specificity [151, 153-156]. Structurally similar peptides could be chromatographically separated by LC, while the MS allows unambiguous identification/quantification of the molecule by first recording the molecular mass of a compound and then creating a "molecular fingerprint" by fragmenting the compound into smaller parts. Different LC-MS protocols have been optimized to quantify Oxt in plasma/serum of humans [153, 155, 156] or rats [155, 156], while most of them were tested only in human plasma for Avp [151, 154]. Brandtzaeg et al. [153] reported a standardized method in humans and rats to free Oxt from plasma protein binding and to further amplify the sensitivity of the method. Furthermore, the addition of a stable isotope (deuterated Oxt or Avp) during LC–MS analysis, enables accurate corrections for any loss of analytes or gain in signal strength due to concentration [68].

In conclusion, all these results suggest that measuring Oxt or Avp in plasma by RIA or EIA samples should be discontinued and replaced by the LC-MS, due to its high sensitivity and specificity. Measuring Oxt in blood by LC-MS is of critical importance in the study of the endogenous Oxt system in physiological conditions and during obesity.

2.8 Oxytocin and leptin during postnatal development: early life stress and obesity vulnerability in adulthood

The maturation of the central neural circuitries involved in the regulation of the energy balance is not completed at birth and is shaped during early postnatal life [157]. In mammals, postnatal ages are denoted by critical

developmental periods during which organs and neural systems are highly plastic [158, 159]. In this timeframe, adverse nutritional, social, and environmental cues may program body metabolism to maximize energy intake to cope with hostile conditions. Accordingly, the prevalence of obesity is higher among individuals exposed to early life stress (ELS) during both the pre- and postnatal periods [160, 161]. In rodents, only thermogenic brown adipose tissue (BAT) is present at birth to sustain pups' survival, whereas WAT progressively develops during the first postnatal weeks [157, 162]. This timing may reflect an evolutionary strategy aimed at adjusting metabolic functions to environmental cues, such as maternal care and food availability.

Therefore, obesity is rarely due to only environmental and/or genetic factors, while it rather result from the interaction between the individual's biological characteristics and the environment in which he/she lives in [163]. For this reason, obesity is recognized as a preventable disease [163].

Clinical observations and studies by psychiatrists and paediatricians, such as John Bowlby and Donald Winnicott, emphasized the crucial role of early life experiences, in particular the relationship between the infant and the mother, in the proper brain development and in individual's health [164].

Rodent studies demonstrated that early adverse experiences may have a strong impact on the way the Oxt system is shaped. Oxt neurons progressively increase from postnatal day 2 (P2) to P21, reaching maturation by the second postnatal week [165]. In contrast, Oxt axons reach their targets only in early adulthood, when Oxtr is already widely expressed in various regions [61].

Importantly, Oxt-synthesizing neurons were found to play a fundamental role in their own maturation: local Oxt release activates Oxtr expressed on Oxt neurons, resulting in further Oxt discharge. These data explained how deeply

early variations in Oxt levels can impact the maturation of Oxt neurons [75, 165]. It is hence possible that postnatal environmental stimuli affect Oxt production and the development of the Oxt system, resulting in the exclusive maintenance of neural pathways necessary to face external conditions.

At the same time, Lep was detected in circulation during early life, even though WAT achieves maturation during the first postnatal weeks [166]. In early life, Lep was recognized to exert a trophic action on the developing brain and in peripheral organs [157]. Studies on ob/ob and db/db mice, demonstrated that the brain displayed lower cell density, altered hypothalamic dendritic orientation, and immature glial and synaptic protein expression patterns [166, 167]. The finding that in ob/ob mice, such alterations could be normalized with Lep injection in early life but not in adulthood supports the key role of Lep during the critical neurodevelopment periods [167-169]. Notably, several hypothalamic nuclei progressively acquire Lep responsiveness (p-STAT3 activation) in the first postnatal days (up to PND 15) when adipokine does not regulate the energy balance yet [170], thus suggesting that during this developmental stage, Lep actually exerts a neurotrophic role. Deficient Lep signalling in early life resulted in an altered number of axonal projections from the ARC (AgRP and POMC neurons) to the PVN [168, 171] and in ob/ob mice, this alteration was restored by Lep administration on PND 4 to 12 [168].

During early life parental–offspring interactions exert a critical role on offspring's neural networks development [172]. In rodents' studies, ELS was usually reproduced by maternal separation (MS), which consisted in separating pups from their dam for 180 min per day, or by limiting the nesting and bedding material (LBN), a procedure that resulted in disorganized maternal

care and hence stress among pups. However, compared to the MS protocol, the LBN procedure impacted the development of the offspring with minimal external intervention from the investigator and strongly reproduced the quality of care that often characterizes depressed, severely stressed, or drug abusing human mothers [173].

Early adversity usually results in reduced circulating Oxt in humans [174]. A recent meta-analysis documented lower plasma Oxt and a reduced or negative response to intranasal Oxt administration among individuals who experienced childhood adversity [175]. Interestingly, the LBN protocol resulted in altered development of Oxt system in rats, by changing Oxt neurons, Oxtr expressing cells and Oxt projections in age- and sex- dependent manner [176].

At the same time, LBN in rodents resulted in a short- and long-term reduction in plasma Lep and in its WAT expression in both sexes [177]; higher plasma Lep and increased Lep mRNA expression in gonadal, but not inguinal WAT, have been described in females exposed to ELS plus HFD [178]. Of note, a recent meta-analysis found a reduction in circulating Lep due to acute stress [179].

Therefore, ELS may lead to a dysfunctional neurometabolic programming, by affecting the development of the neural and peripheral circuits behind the Lep-Oxt crosstalk, thus predisposing to obesity vulnerability in adulthood [157] (Fig. 3). Further studies targeting the Lep-Oxt crosstalk during early-life in shaping neural circuits regulating energy balance, would be of paramount importance to shed light on the etiopathogenetic basis of obesity and may offer new targets for intervention and prevention.

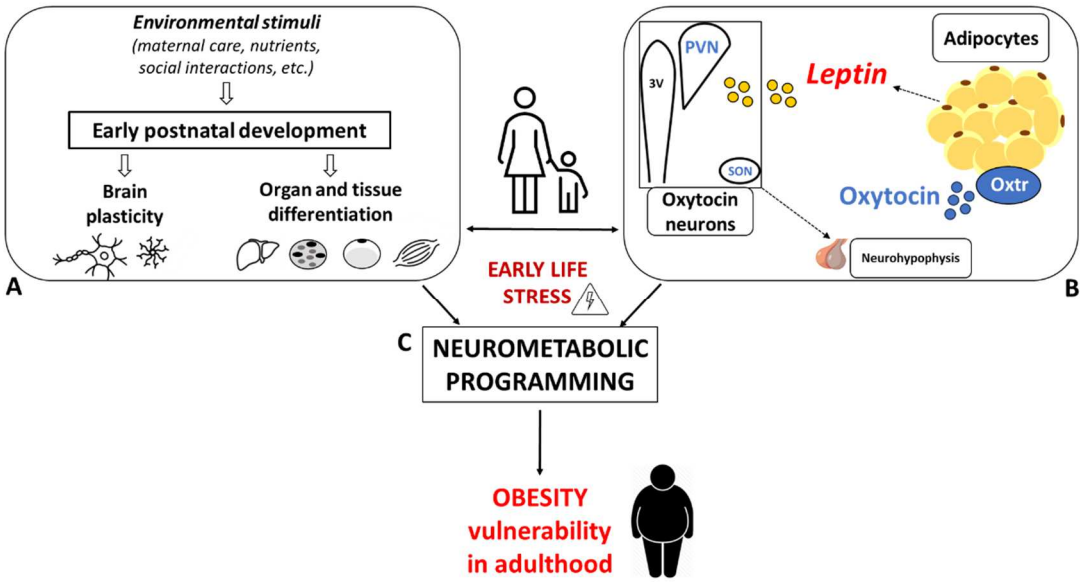

Figure 3: *Schematic representations of the pathways linking ELS to vulnerability to adult obesity*. This figure is taken from Colleluori et al. [157] (A). Impact of environmental stimuli on the early postnatal development of various organs involved in the regulation of the energy balance (e.g., brain, liver, brown and white adipose tissues, and skeletal muscle). (B) Oxt neurons in the PVN and the SON project to the neurohypophysis and release Oxt into the peripheral circulation. Then, peripheral Oxt target AT where Oxtr is expressed. Adipocytes are the main source of Lep, the master regulator of the energy balance, which is reported to act in the PVN and the SON Oxt neurons (C). Early adverse experiences may affect brain development, metabolically relevant organs differentiation, and Oxt and Lep systems maturation. In this condition, dysfunctional neurometabolic programming and homeostatic and hedonic feeding centres maturation may occur, ultimately enhancing the vulnerability to obesity in adulthood. AT= adipose tissue; Oxt=oxytocin; Oxtr= oxytocin receptor; Lep= leptin; PVN= paraventricular nucleus; SON= supraoptic nucleus.

3. Aim of the study

Oxt is an anorexigenic hormone with a powerful anti-obesogenic effect. The anorexigenic effect of Oxt is supposed to be mediated by the crosstalk with the adipokine Lep, although the whole mechanism behind this phenomenon has

not been fully elucidated. The main objective of this study is to measure the response of Oxt neurons to Lep peripheral administration, by quantifying Oxt release in plasma. In addition, we aim to assess whether Lep administration can induce any signalling activation in Oxt neurons in both PVN/SON and to elucidate the neural mechanism behind Oxt neurons response to peripheral Lep, by confirming data in literature regarding the expression of Lepr and Mc4r in both PVN/SON. Furthermore, we aim to assess the presence of POMC neurons projections in PVN/SON, to further explore whether Lep target Oxt neurons directly, by Lepr, or indirectly by POMC neurons projecting to Mc4r-expressing cells. Then, we aim to investigate the endogenous Oxt system during HFD and ELS to study how possible alterations in the Lep-Oxt crosstalk may predispose to obesity vulnerability. All the experiments will focus on sex dimorphism, to highlight a possible sex-dependent response of the Oxt system.

4. Materials and Methods

4.1 Animal cares

Three to eight-weeks old mice C57BL/6 (males and females) were purchased from Charles River (Calco, Italy). C57BL/6J-Tg (Pomc -EGFP)1Low/J (#009593) and Tg(Pomc1-cre)16Lowl/J (#005965) male mice were purchased from Jackson Laboratory (Bar Harbor, ME, USA) and bred with C57BL6/J female mice to establish the colony. Mice were housed individually in plastic cages and maintained on a 12:12-h light-dark cycle at 22-23 °C with free access to standard diet and water. Mice were handled daily one week before the experiments. Prior to sacrifice, all the animals were anaesthetized with

intraperitoneal injection of 2,2,2-tribromoethanol (Avertin) (Sigma-Aldrich, Saint Louis, MO, USA), then killed and processed for the analyses.

4.2 Sample size

The number of mice used for each analysis is reported in *Table 1*.

4.3 Genotyping of transgenic mouse lines

Eartags were collected from 4-weeks old mice. One hundred µl of PCRBIO Rapid Extract Lysis Kit (PCR Biosystems, London, UK; # PB15.11-24) were added to each sample and DNA was isolated by boiling the eartags for 75 min at 75°C and then for 10 minutes at 95°C with a ThermoShaker (GrantBio, Cambridge, CB, UK). Two µl of isolated genomic DNA were used for the genotyping PCR by the TaKaRa Taq™ PCR kit (Takara Bio Inc., Kansai, JPN; #HR001A), using protocols described on the website of The Jackson Laboratory (Genotyping protocols: Standard-PCR). Primers used are listed in *Table 2*.

4.4 Tissue processing and morphological analysis

Morphological analyses were conducted to assess first:

1) Oxt neurons quantification at the post-natal day 21 (p21), during development, and in adulthood at p60 in both PVN and SON by immunohistochemistry (IHC).

Then:

2) p-Stat3 and **c-Fos** response to Lep administration in Oxt neurons of PVN-SON of p21 and p60 mice by immunofluorescence (IF) and confocal microscopy.

Animals used for morphological analyses 1) and 2) were sacrificed by intracardiac perfusion. Briefly, the chest cavity was opened by an incision below the sternum to gain access to the heart and inject the fixative solution of 4% paraformaldehyde (PFA), made in 0.1 M phosphate buffer (PB) at pH 7.4, into the left ventricle, while the right atrium was cut to drain blood from the heart. Then, brain was removed from the skull and post-fixed in 4% PFA for 24h at 4 °c. To isolate the hypothalamus, after a quick wash in PB, the entire brain was processed through a brain matrix to discard the caudal region containing cerebellum and the hindbrain, and the rostral region containing the olfactory areas (both bulb and cortex). Then, brain (5 mm thick) was cut using a vibratome (Leica VT1000S) into 40 µm tick coronal slices containing the PVN, SON, or ARC and placed "free-floating" in 1X Phosphate-Buffered Saline (PBS) solution. In all experiments, ARC was used as a positive control for Lep-response and Lepr distribution. For the morphological characterization of Tyrosine hydroxylase (Th) and Oxt expression in the adipose depots and in the GI tract, the iWAT, gWAT, stomach and duodenum were collected as described for the previous morphological analyses. After the 24h of post-fixation in 4% PFA made in TP, organs were dehydrated, paraffin embedded and then cut by a microtome in 3.5-µm-thick sections.

4.5 Peroxidase immunohistochemistry

Immunohistochemistry (IHC) was used for morphological analyses 1) and 2) in hypothalamic sections. Fort the analysis 2), IHC for p-Stat3 was performed in ARC of both saline and lep-treated mice as a positive control for Lep treatment. Briefly, free-floating sections were reacted with 1% NaOH and 1% H2O2 (20 min), 0.3%glycine (10 min), and 0.03% sodiumdodecylsulfate (10

min). After rinsing in 1x PBS, they were blocked with 3% normal goat serum (Vector Laboratories, Burlingame, CA, USA; # S-1000-20; in 0.2% TritonX-100 ; 60 min) and incubated with the primary antibodies for Oxt, p-Stat3 and c-Fos (*Table 3*) at appropriate dilutions in 1x PBS, overnight at 4˚C. The next day, after a thorough rinse in PBS, sections were incubated in 1:200 biotinylated anti-guinea pig or anti-rabbit secondary antibodies (Vector Laboratories, Burlingame, CA, USA; #BA-7000-1.5; #BA-1000-1.5) for 30 minutes at room temperature (RT), rinsed in PBS, and incubated in avidin-biotin peroxidase complex (ABC Elite, Vector Laboratories; #PK-6100) for 1h at RT. After washing several times in PBS, sections were finally incubated for 1 minute in 3,3'-Diaminobenzidine (DAB) solution (Vector Laboratories; #SK-4100) at RT. After IHC staining, sections were mounted on slides, air-dried, dehydrated in ethanol, cleared with xylene, and mounted with Eukitt (Bio-Optica S.p.A, Milan, Italy). IHC reactions were analysed by using a Nikon Eclipse E600 microscope (Nikon; Sesto Fiorentino, Florence, Italy) with a camera mounted to obtain the images. Pictures were taken at a magnification of 20x and 40x and brightness and contrast of the final images were adjusted using the Photoshop 6 software (Adobe Systems, Mountain View, CA).

IHF was further performed for the study of the expression of Th and Oxt in adipose depots and GI tract. Briefly, sections were deparaffinized in xylenes, hydrated, and incubated with 30% H2O2 (diluted to 3% in dH20) for 5 min at room temperature to block endogenous peroxidase. Then, sections were washed in PBS 1x (2 × 7 min) and incubated in 3% normal rabbit or goat serum (Vector Laboratories; #S-5000-20; #S-1000-20; in 1x PBS) for 20 min at RT to block nonspecific sites. Sections were incubated overnight at 4°C with the primary antibody against Th and Oxt (Table 3). The next day, after a thorough rinse in PBS, sections were incubated in 1:200 biotinylated secondary anti-

sheep or anti-guinea pig (Vector Laboratories, Burlingame, CA, USA;#BA-6000-1.5; #BA-1000-1.5) for 30 minutes at RT, rinsed in PBS, and incubated in avidin-biotin peroxidase complex (ABC Standard, Vector Laboratories; #PK-4000) for 1h at RT. After washing several times in PBS, sections were finally incubated in DAB solution for 30 seconds (Vector Laboratories; #SK-4100). After IHC staining, sections were mounted on slides, dehydrated and mounted with Eukitt (Bio-Optica S.p.A, Milan, Italy).

Negative controls were obtained in each instance by using PBS 1X instead of the primary antibody to assess the background originated from the non-specific binding of the secondary antibodies. IHC reactions were analysed by using a Nikon Eclipse E600 microscope. Pictures were taken at a magnification of 100x to search for fibres and brightness and contrast of the final images were adjusted using the Photoshop 6 software (Adobe Systems).

4.6 Immunofluorescence and confocal microscopy

Double-labelled confocal microscopy was used for morphological analysis 2). Free-floating sections were processed according to the above-described protocol for IHC, up to incubation with the primary antibodies for Oxt, p-Stat3 and c-Fos (*Table 3*). The next day, after 3 washes in 1x PBS and additional incubation with 4% donkey serum (Jackson ImmunoResearch; , Bar Harbor, MA, USA # 017-000-001) for 30 minutes at RT, sections were incubated in fluorophore-linked secondary antibodies (*Table 4*) solution in PBS for 1h at RT. Nuclear staining was performed using the fluorescent dye TO-PRO-3 Iodide (642 nm of excitation wavelength) (Invitrogen by Thermo Fisher, MA, USA; #T3602), in 1x PBS for 15 min at RT. Sections were subsequently washed twice with 1x PBS, mounted on standard glass slides, air-dried, and covered using Vectashield mounting medium (Vector Laboratories; # H-1000-

10). Colocalization between Oxt and p-Stat3 or c-Fos was analysed by a motorized Leica DM6000 microscope at 40X and 60X magnifications. Fluorescence was detected with a Leica TCS-SL spectral confocal microscope equipped with an Argon and He/Ne mixed gas laser. Fluorophores were excited with the 488,543, and 649 nm lasers and imaged separately. Images (1024 × 1024 pixels) were obtained sequentially from two channels using a confocal pinhole of 1.1200 and stored as TIFF files. The brightness and contrast of the final images were adjusted using Photoshop6 (AdobeSystems, MountainView, CA, USA).

4.7 Morphometric analysis

Morphometry was performed for:

1) Quantification of Oxt neurons in PVN and SON by IHC for oxytocin antibody, by summing the number of Oxt neurons in two coronal sections of both PVN and SON.

2) Quantification of Oxt neurons responsive to Lep by c-Fos activation in SON: morphometry was performed after IF and confocal microscopy for Oxt and c-Fos antibodies and by counting the total number of Oxt neurons and Oxt neurons colocalizing with c-Fos in two coronal sections containing the anterior and posterior part of both PVN and SON. The number of c-Fos responsive Oxt neurons, was obtained my normalizing the total number of Oxt neurons for the number of colocalizations with c-Fos.

For both the analysis, the neuronal counting was made at 40x magnification. Results are given as mean ± standard error of the mean (SEM).

4.8 Leptin "time-course" experiment

Between 8:00-9:00 am of the day of the experiment, male and female C57BL/6 mice were housed individually, food deprived and left with *ad libitum* water. Animals were sacrificed between 12:00 p.m and 14:00 p.m., since circadian oxytocin levels in plasma increase physiologically between 8:00 a.m. and 12:00 p.m, while they stabilize in the afternoon and decrease during the dark phase [180]. In addition, the week before the start of the experiment, female mice were observed once daily to assess the estrous cycle as described elsewhere and, to avoid experimentation during estrous [181, 182]. The day of the experiment, animals were given a single intraperitoneal injection (IP) of recombinant mouse leptin (Sigma-Aldrich, Saint Louis, MO, USA; 0,5 mg/kg of body weight) or vehicle (pyrogen-free saline), accordingly to body weight (range between 100-150 µl). Then, animals were anesthetized with 300 mg/kg 2,2,2-tribromoethanol and sacrificed by decapitation at 45 minutes (min), 1 hours and 30 min (1.5h), 3h and 6h after treatments to collect blood, hypothalamus and adipose tissues. Blood was collected before decapitation by intracardiac puncture while the animals were anesthetized and was then placed inside 1,5 ml-tubes containing 100 µl of EDTA (Sigma-Aldrich; 0.5M, pH8). All the samples were immediately stored in ice and processed within 1.5h. Plasma was separated by centrifugation at 3000 rpm for 10 min using a refrigerated (4°C) centrifuge. The whole hypothalamus (about 5 mm thick) was obtained by removing through a surgical blade the cerebellum and the hindbrain, the anterior regions containing the olfactory areas and the lateral and dorsal regions containing cortex, hippocampus, amygdala and the thalamus. Nissl staining was performed on few samples to ensure the presence of paraventricular and supraoptic nuclei in the whole hypothalamic fraction before collecting those necessary for the present experiment. For the adipose depots,

the WAT was harvested from the inguinal depot (iWAT) as representative of subcutaneous WAT. The gonadal WAT (gWAT) was dissected out from the epididymal (male mice) and parametrial (female mice) fat pads, both representative of visceral WAT. The interscapular depot was dissected out for studying the brown adipose tissue (iBAT). After the dissection, all the samples were quickly frozen in liquid nitrogen and stored at -80 °C.

4.9 Liquid-Chromatography and Mass Spectrometry

Samples preparation: to improve the precision and accuracy of the result of Oxt quantification, a stable-isotope labelled-Oxt was added as an internal standard (IS) prior to LC analysis, by adding 5 µL of oxytocin-(leucine-5,5,5-d3, glycine-2,2-d2) trifluoroacetate salt (Merck, Burlingtone, MA, USA; # 900169-1MG; at 10 µg/L) to 100µL of plasma. To create a calibration curve, oxytocin acetate salt hydrate ≥97% for HPLC (Merck; #O6379) was used. For Avp quantification, [Arg^8]-Vasopressin acetate salt (Merck; # V9879) was used for the calibration curve, and LC was performed without adding an IS.

Oxytocin quantification:

Samples were added with 120 µL of H3PO4 and shaken for 45 minutes at room temperature. After the addiction of 600 µL of acetonitrile (ACN), sample was kept at -20°C for 30 min and then centrifugated at 14000 rpm for 10 minutes at 4°C. Supernatant was transfer in a tube and evaporated to approximately 300 µL at 45°C and under a gentle stream of nitrogen. After adding 3 mL of water, sample was purified by the solid-phase extraction (SPE) columns Strata-X 33 µm Polymeric Reversed Phase 60 mg/3 mL (Phenomenex, Torrance, CA, USA; # 8B-S100-UBL) . SPE columns were conditioned with 3 mL of methanol and 3 mL of water. Samples were loaded into the columns and were first washed with 3 mL of water and then with 3 mL of ACN 5%. Analytes were eluted with

3 mL of ACN 70% and solutions were evaporated till dryness in evaporating centrifuge. Residues were resuspended in 200 µL of ACN 10% containing 0.1% of formic acid (FA) and transfer to a new 2 mL tube. After the addiction of 700 µL of ACN, samples were kept at -20°C overnight and then centrifugated at 14000 rpm for 10 min at 4°C. The supernatant (850 µL) was evaporated under gently nitrogen stream at 45°C and residues were suspended in 100 of ACN 10% containing 0.1% of FA. The nano-LC RLSC coupled to a Q-Exactive system (Thermo Fisher Scientific, Waltham, Massachusetts, United States) was used for the analyses. Acclaim PepMap RSLC 75 µm x 25 cm column (Thermo Fisher Scientific, Waltham, Massachusetts, United States) was used for chromatographic separation employing H_2O and ACN both containing 0.1% of FA as mobile phase A and B respectively. Gradient initiated with 2% of mobile phase B maintaining this condition for 2 minutes and then the mobile phase B increased to 30% in 63 minutes. The final step increased the percentage of mobile phase B to 72% in 12 minutes and this condition was maintained for 6 min. The flow rate was 0.3 µL/min, column temperature and samples were set at 40°C and 16°C respectively. 5 µL of sample was injected. For the acquisition, ESI (+) source was using target-SIM/dd-MS2 experiment for analytes detection. Resolution, AGC target, maximum injection time and isolation window were set at 140000 (FWHM@200 m/z), 1e6, 400 ms and 2.0 m/z respectively for full scan experiment. For dd-MS2 experiment resolution, AGC targeted, maximum injection time, isolation window, collision energy (NCE), minimum AGC target, apex trigger and dynamic exclusion were set 35000 (FWJM@200 m/z), 5e5, 150 ms, 1 Da, 10-20-35 NeV, 8e2, 1-3 s and 2 s respectively.

Vasopressin quantification: 100 µL of plasma sample was incubated under agitation with 120µL of 4% H3PO4 solution in 2mL low protein binding tubes

at room temperature and in the dark. After 45 minutes of incubation, 600 µL of cold acetonitrile was added and the samples were vortexed and placed at -20°C for 30 minutes for protein precipitation. Then, samples were centrifuged for 10 minutes at 14000 rpm and 4°C, the supernatant was transferred into 15 mL tubes and was evaporated under nitrogen at maximum temperature of 45°C to remove organic solvent. 3 mL of 4% H3PO4 solution was added and the analytes were extracted with Waters Oasis WCX (150 mg/6 mL) columns (Waters Corporatio, Milford, MA, USA). The samples were loaded on the columns after the conditioning with 6 mL of CH3OH and 6 mL of H2O and the columns were washed with 5 mL of 4% NH4OH solution and 5 mL of 10% CH3OH solution. The analytes were eluted with 3 mL of 90% of Acetonitrile solution with 1% of Trifluoroacetic acid and the elute was recovered in 5 mL Eppendorf tubes. Then, samples were evaporated to dryness in an evaporating centrifuge at 45°C and were regained with 100 µL of 5% CH3OH solution containing 0.1% of HCOOH. The samples were filtered with LCR filters (Merck; #SLLGR04NL) and analyzed in Thermo NanoLC-Q-Exactive instrument.

4.10 Real-time PCR

Gene expression analysis was performed in both hypothalamus and adipose tissues to investigate the time-response of *Oxt* and *Oxtr* gene expression to Lep administration. RNA extraction was made by using phenol-chloroform-guanidinium thiocyanate method. Briefly, each sample was added with 500 µl of Trizol (Invitrogen, Waltham, MA, USA) and a sterile and RNAse free zirconium grinding bead was placed in each tube to perform tissue homogenization by TissueLyser (Qiagen, Hilden, Germany) for 5 minutes at 50 Hertz. Samples were then passed through a 22-gauge (0.7 mm) needle,

attached to a sterile plastic syringe, until a homogeneous lysate was achieved (~5 times). Samples were added with chloroform (Sigma-Aldrich) and then centrifuged for 15 minutes at 12000 rpm at 4 °c. An equal volume of 70% ethanol was added to the isolated supernatant. RNA extraction was performed using the Total RNA Purification Kit (Norgen Biotek, Thorold, ON, CA; #17250) combined with the RNase-Free DNase I Kit (Norgen, #25720) to remove genomic DNA. The quality and quantity of total RNA was evaluated using a Nanodrop Spectrophotometer (Fisher Scientific, Hampton, NH, USA). One µg RNA was reverse-transcribed with the High-Capacity cDNA RT Kit with RNase Inhibitor (Applied BioSystems, Waltham, MA, USA; #4374966) in a total reaction volume of 20 µl. The cDNA library was then used for quantitative real-time PCR (qPCR). For SYBR® Green gene expression assays: pairs of PCR primers were designed by Primer3 (web version 4.1.0) and the NCBI Primer Blast software, and then customized by ThermoFisher (Waltham, MA, USA; # 10336022) (*Table 5*). The quantitative analysis of gene expression was performed with Universal SYBR Green Master Mix (Applied Biosystem; #4309155). For TaqMan gene expression assays: RT-qPCR was performed using TaqMan Master Mix (Applied BioSystems; # 4304437) and probes (Applied Biosystem;#4453320) (*Table 5*).

All reactions were carried out by the Step One Plus Real-Time PCR system (Applied BioSystems) using 50 ng RNA on a final reaction volume of 10 µl.

The thermal cycling conditions for SYBR® Green assays followed the standard cycling mode for designed primers with a $T_m \geq 60$: 1 cycle at 50 °C for 2 minutes, 1 cycle at 95 °C for 2 minutes and 40 cycles at 95 °C for 3 seconds followed by 60 °C for 30 seconds. A dissociation step (melt curve stage) of 95°C for 15 seconds, 60 °C for 1 minutes and 95 °c for 15 seconds, was added in continuous at the end of the cycling stage. For TaqMan assays thermal

conditions were initial incubation at 95°C for 10 min followed by 40 cycles of 95°C for 15 s and 60°C for 20 s.

A control reaction without reverse transcriptase in the amplification mixture was performed for one sample to rule out genomic contamination. All samples were run in duplicate. Samples not containing the template were included as negative controls in all experiments. TATA box-binding protein (TBP) and β-actine were used as endogenous controls to normalize gene expression. Relative mRNA expression was determined by the ΔCt method ($2^{-\Delta Ct}$).

4.11 *Western Blot*

Protein expression analysis was performed to assess Oxtr expression in adipose tissues, 3h after Lep administration. Samples were weighed and added with a quantity of RIPA buffer (in µl) equal to double the weight of each sample. Then, proteins were isolated by adding Aprotinin (Merck; #A6106) and PMSF proteinase inhibitor (Thermofisher; # 36978) and using the TissueLyser at 50 Hertz for 1 minutes repeated for 3 times. After centrifugation at 14000g for 20 min at 4°c, the infranatant containing soluble proteins was collected. Proteins were quantified using a Bradford protein assay (Bio-Rad; # 5000001). Protein denaturation and reduction were performed by adding the samples with 4X LDS Sample Buffer (Invitrogen; B0007) and 10X Sample Reducing Agent (Invitrogen; B0009). An equal number of proteins were loaded in precast polyacrylamide gels Bis-Tris Plus, 4-12%, 10 wells (Invitrogen; NW04120BOX) and proteins were separated using sodium dodecyl sulfate polyacrylamide gel electrophoresis (SDS-PAGE) and transferred onto nitrocellulose membranes using a trans-blot turbo transfer system (Bio-Rad). To check loading and transfer efficiency, membranes were visualized with Ponceau S solution (Santa Cruz Biotechnology, Santa Cruz, CA, USA; #SC-

301558). Membranes were then incubated in a blocking solution (Invitrogen) for 5 minutes to block non-specific binding of the antibodies and incubated with the primary antibody for oxytocin receptor (*Table 3*) (in TBS-T; overnight at 4°c). Membranes were washed thoroughly with TBS-T and incubated with the anti-mouse 1:5000 (Jackson ImmunoResearch; #715-036-150) in TBS-T for 1 h at RT. Membranes were developed using clarity ECL substrate (Bio-Rad; #170-5060). Protein levels were assessed in at least three separate experiments per molecule by densitometric analysis using a Chemidoc imaging system and ImageLab software (Bio-Rad). Quantitation of immunoreactive bands was performed using the Bio-Rad Image Lab software. Results were expressed as fold changes in relative protein expression compared with the control group. Where appropriate, membranes were stripped, washed and re-probed for total protein content.

4.12 Stimulated Emission Depletion Microscopy

Stimulated Emission Depletion Microscopy (STED) microscopy was used for the study of POMC fibers distribution in SON. Free-floating sections by C57BL/6J-Tg (Pomc -EGFP)1Low/J were processed as described for confocal microscopy, until the use of primary antibodies for Oxt and GFP protein (*Table 3*). Antibody against GFP, was used to enhance the green-fluorescent signal. The staining was developed with secondary antibodies Abberior STARRED (Abberior GmbH; # STRED-1002-20UG) and Abberior STARGREEN (Abberior GmbH; # STGREEN-1002-20UG) both diluted1:200 in 1x PBS and incubated at RT for 90 min. Cellular nuclei were labelled with DAPI (Akoya Biosciences, Marlborough, MA, USA; #FP1490) diluted 1:1000 in 1x PBS for 10 minutes at RT. Slices were covered with coverslips 0,17 mm thick, mounted with the mowiol mounting medium and imaged with a Nikon A1R microscope

with 100x oil immersion. STED imaging was performed with a STEDYCON microscope *(*Abberior GmbH ,GÖ, Germany). Images were acquired with NIS-Elements (Nikon) and analyzed by STEDYCON (Abberior GmbH) acquisition software. Confocal microscopy for Oxt (in red) and GFP was also employed to increase the sample size and performed as described for the previously described morphological analyses.

4.13 Fluorescent In-situ Hybridization

-Tissue processing and cryopreservation for frozen sections

Lepr and Mc4r *mRNA* distribution in SON was investigated by fluorescence RNA *in-situ* hybridization with the RNA scope technology in frozen hypothalamic sections. To obtain the hypothalamus, mice were anesthetized and perfused with 4% PFA to collect brain as described above. After 24 hours of post-fixation in 4% PFA at 4 °C, hypothalami were isolated from the whole brain by using the brain matrix. Then, tissues were subjected to 3 steps in sucrose at increasing concentration gradient (10%, 20% and 30%) diluted in 1x PBS, to induce the cryopreservation of the samples. For each step, tissues were left in sucrose overnight at 4 °C. Then, hypothalami were included in O.C.T embedding medium (Sakura Finetek Italy S.r.l, VE, Italy) and cut by a cryostat (Leica) (holder temperature (T): -20 °C ; chamber T: -25 °C) in 15 mm thick sections containing: PVN/SON as target regions and ARC as positive control. Frozen sections were mounted on Menzel Gläser Super-Frost Plus slides (Thermo Scientific, Waltham, MA) and dried at -20 °c for 120 minutes prior to start the RNA Scope.

-RNA Scope

RNA scope (ACDBio, Bio-Techne, Minneapolis, MN) was performed using specific RNA probes (*Table 6*) according to the manufacturer's instructions. Frozen sections were first baked at 60 °c for 30 minutes and then dehydrated. Sections were subsequently incubated with H_2O_2 at RT for 10 min, rinsed twice in deionized water and subsequently submerged in Target Retrieval Buffer (ACDBio) at 95 and 97ºC for 15 min. Slides were washed in deionized water for 15 s and dehydrated in 100% ethanol for 30 s. After air drying, a hydrophobic barrier was drawn using ImmEdge barrier pen and sections were incubated with Protease Plus (both from ACDBio) for 30 min at 40ºC. The subsequent hybridization, amplification and detection steps were performed according to the manufacturer's instructions (Multiplex Fluorescent Detection kit v2, ACDBio). Both a 3-plex negative and a 3-plex positive control probes were processed in parallel with target probes. All incubation steps were performed at 40ºC using the ACD HybEz hybridization system (ACDBio). Sections were stained with TO-PRO3, mounted with ProLong Gold Antifade Mountant (Thermo Fisher) and stored at 4ºC in the dark. Sections were viewed under a motorized Leica DM6000 microscope at different magnifications (40x and 60x). Fluorescence was detected with a Leica TCS-SL spectral confocal microscope equipped with an Argon and He/Ne mixed gas laser. Fluorophores were excited with the 488, 543, and 649 nm lines and imaged separately. Images (1024 × 1024 pixels) were obtained sequentially from two channels using a confocal pinhole of 1.1200 and stored as TIFF files. The brightness and contrast of the final images were adjusted using Photoshop6 (AdobeSystems, MountainView, CA, USA).

4.14 Single-cell RNA sequencing

Data on Lepr expression in Oxt magnocellular neurons were shared with us by Prof. Tibor Harkany (Center For Brain Research, Medical University of Vienna) and originated from the Single cell RNA sequencing (scRNA-seq) database used for a previous publication [183] in C57BL6/N mice from embryonic day 15 (E15.5) to P23. Thus, embryos were removed by caesarean sections, postnatal animals were transcardially perfused and hypothalamic cells were lysed, as explained in detail in the original article [183]. For the preparation of cDNA libraries, cells were re-suspended in PBS (0.01M, pH7.4) and concentrated to a range of 105-700 cells/µl. Thirty-three µl of the cell suspension together with 1 µl cellular spike-ins (lymphocytes) were added to the reverse transcription mix. cDNA synthesis, library preparation and sequencing were performed accordingly to the 10x Genomics Chromium Single Cell Kit (version 2). High-throughput RNA sequencing was on an Illumina HiSeq3000 instrument.

Sample sizes for scRNA-seq experiments: n = 8 (E15.5), n = 7 (E17.5), n = 4 (P0), n = 4 (P2), n = 3 (P10), n = 3 (P23).

4.15 Stereotaxic surgery

Animals were anesthetized by IP injection with a mixture of ketamine (Richter, Kasendorf, DE; #A6A066) at 50 mg/kg and xylazine (Le Vet Pharma, Oudewater, NE; #15H044) at 4 mg/kg. After anaesthesia, mice were mounted in a stereotaxic frame (RWD Life Science, TX, USA) with anaesthesia maintained with isoflurane (1.5%; 0.6 l min−1 flow rate) through a snout mask. Viral particles were delivered with a micropipette (Drummond) mounted on either a Quintessential Stereotaxic Injector (Stoelting) or an R-480 nanolitre microinjection pump (RWD Life Science) at a speed of 100 nl min−1. The

pipette was slowly withdrawn 5 min after AAV delivery. Male and female Tg (Pomc 1-cre) 16Lowl were bilaterally injected with a *Cre*-dependent AAV-EF1a-DIO-GCaMP6f-P2A-nls-dTomato (250 nl; Addgene #51083) in the ARC at the following coordinates (all relative to bregma): anterior–posterior (AP): −1.45 mm, medio-lateral (ML): ± 0.25 mm, dorso-ventral (DV): −5.8 mm. Mice were processed 15 days after virus delivery. Male and female C57BL/6 mice were bilaterally injected with a AAV-hSyn1-GCaMP6f-P2A-nls-dTomato (150 nl; Addgene #51085) in the SON at the following coordinates (all relative to bregma): AP: -0.60 , ML: ± 1 , DV: -5.5 . Mice were processed 7 days after virus delivery.

4.16 Calcium imaging

Eight- to ten-week-old male and female Tg (Pomc 1-cre) 16Lowl and Oxt<tm1.1(cre) Dolsn> mice were anesthetized with sodium-penthobarbital (30mg/ml) and perfused with N-methyl-D-glucamine (NMDG)-HEPES artificial cerebrospinal fluid (aCSF) containing (in mM): 93 NMDG, 3 KCl, 1.2 NaH2PO4 *2H2O, 20 HEPES, 3 Na-Pyruvate, 5 Na-Ascorbate, 30 NaHCO3, 25 D-Glucose, 8 MgSO4, 0,5 CaCl2 (300 mOsm, pH7.4). After perfusion, mice were decapitated, and the brain rapidly removed and put in ice-cold oxygenated (O2 95% / CO2 5%) NMDG-HEPES aCSF. After removal of the cerebellum, the brain was glued and 300µm-thick coronal slices containing the SON (optic tract and third ventricle-3V) and ARC (median eminence and 3V) were cut using a vibratome (VT1200S; Leica). Slices were allowed to recover at room temperature for 2h, placed in submerged wells in oxygenated a-CSF composed by (in mM): 90 NaCl, 3 KCl, 1.2 NaH2PO4 *2H2O, 20 HEPES, 3 Na-Pyruvate, 5 Na-Ascorbate, 30 NaHCO3, 25 D-Glucose, 2 MgSO4, 1.5 CaCl2, 0.5 L-glutathione (300 mOsm, pH7.4). Leptin (Sigma-Aldrich, Saint Louis, MO,

USA; 250-500 nM) was diluted in a recording aCSF composed by (in mM): 124 NaCl, 2.5 KCl, 1.2 NaH2PO4*2 H2O, 5 HEPES, 24 NaHCO3, 12.5 D-Glucose, 2 MgSO4 , 1.5 CaCl2 (300-mOsm, pH 7.4). Slices were observed with a 10x objective using a AxioExaminer D1 microscope (Zeiss). GFP fluorescence was detected under blue illumination at 470 nm and images collected with a sCMOS Prime 95B camera (Teledyne Photometrics, Tucson, USA), using VisiView image acquisition software (Visitron Systems GmbH, Puchheim, Germany). Regions of interest (ROI) were drawn around individual cell bodies in infrared and/or fluorescent images. Changes in GCaMP6 fluorescence intensity were measured by plotting the intensity of ROI (minus background) over time, initial resting state fluorescence (F0) was computed before leptin application and subsequent fluorescence values (F-F0=△F) normalized to this (△F/F0).

-Immunofluorescence and confocal microscopy on thick sections.

After Ca^{2+} recording, brain slices 300µm-thick containing ARC and SON, were fixed with 4% PFA overnight at 4°c. Afterwards, slices were washed 4 times for thirty minutes in 0,1M PB and blocked with a solution made of 2.5% Bovine Serum Albumine (BSA), 5% Normal Donkey Serum (NDS) and 0.5% Triton prepared in 0.1M PB at room temperature for 4 hours. Then, primary antibodies for Oxt and Cre-recombinase (*Table 3*) were diluted in 0.1% BSA, 1% NDS, 0.5% Triton and 5% Dimethyl Sulfoxide for 3 days at 4°c. Then, slices were washed 4 times for 30 minutes in 0.1M PB and incubated with secondary antibodies (Table 3) diluted 1:200 and Hoecst 33,342 diluted 1:10000 (Thermofisher; #H1399), both in 2% BSA overnight at 4°c. Finally, sections were washed 4 times for 3 minutes in 0.1M PB, shortly rinse in water and then mounted with Mowiol mounting medium. Sections were imaged on an

LSM880 confocal microscope (Zeiss) and processed with the ZEN software (Zeiss).

4.17 High-Fat Diet

Four-week-old animals, purchased from Charles Rivers were housed with two mice per cage and allowed to acclimatize for 1 week. Then, animals were divided into 2 experimental groups: one group was fed with a normal diet (ND) (7% fat, 61% carbohydrates,19% proteins; Research Diets, New Brunswick, NJ, USA; #D11112201), while the second group was fed with HFD (45% fat, 35% carbohydrates, 20% proteins; Research Diets; #D12451). Each cage was provided with the same amount of diet (70g). These feeding conditions were maintained for 12 weeks. Each animal and the amount of food left in the cage, were weighed once a week during the cage changing, to monitor weight trends and food intake respectively. The food intake assessment was obtained by dividing the amount (g) of food left in cage for the number of animals in the cage (n=2) and normalized for the body weight.

At the end of the experiment, mice were anesthetized with 300 mg/kg 2,2,2-tribromoethanol and decapitated to collect blood, hypothalamus and adipose tissues (iWAT, gWAT, iBAT), as described above for the time-course experiment. All the sacrifices were conducted between 12pm to 2 pm to minimize the impact of circadian rhythm on the analyses.

After the dissection, all the samples were quickly frozen in liquid nitrogen and stored at -80 °C to perform LC-MS for Oxt quantification in plasma and gene expression analyses for the assessment of *Oxt* expression in the hypothalamus.

4.18 Early Life Stress

Limited Bedding and Nesting (LBN) protocol

Pregnant dams were housed in single cages and monitored every 12h until labour. The day of pups' birth was termed P0. Cages were initially provided with standard bedding and nesting condition (STD) composed of: 50g of bedding material and 5g of nest. Control group was maintained in STD condition until the end of the experiment (P21). ELS group was housed in STD condition until P2, when the LBN protocol has started, and cages were then set up according to LBN paradigm [184]: minimal amount of bedding material, estimated ~ 15g for floor area of 2065cm^2/ 320.07 IN^2 ; 2g of nest equal to one third of the standard amount. ELS group was exposed to LBN until P9 and then transferred to STD cages until P21. Both the STD and ELS cages were observed at least twice a day for 30 minutes to monitor the dams and pups. The day of the weaning, at P21, the experiment was concluded, and pups' weight was recorded. Then, mice were anesthetized, and plasma was collected by intracardiac puncture to quantify plasma Oxt levels by LC-MS, as described in the previous sections of the paragraph. Animals were decapitated and hypothalamus and adipose tissues were collected and stored at -80 °c for future analysis. All the sacrifices were conducted among 12:00 and 2:00 pm to limit the effect of circadian rhythm on plasma Oxt release as described above.

4.19 Statistical Analysis and softwares

All data are reported as mean ± standard error of the mean (SEM). Comparisons between groups were performed with Student's t-test. A $p < 0.05$ was considered significant. All statistical analyses were performed with GraphPad Prism 6 software.

4.20 Tables

Table 1: *Sample size*

This study was conducted as a pilot, and therefore, formal sample size calculation was not performed. The data obtained from this pilot study will be utilized to inform sample size calculations for future, definitive studies.

Number (n)	Age	Male	Female
Oxt neurons counting	P21 2 months	n=9 P21 n=8 P60	n=11 P21 n=8 P60
p-Stat3	P21 2 months	n=2 Saline; n=3 Lep n=2 Saline ;n=3 Lep	n=2 Saline; n=3 Lep n=2 Saline ;n=3 Lep
c-Fos	P21 2 months	n=2 Saline; n=3 Lep n=2 Saline ;n=3 Lep	n=2 Saline; n=3 Lep n=2 Saline ;n=3 Lep
Time-course	2 months	n= 20 Saline; n=20 Lep (n=5 for each time-point)	n= 20 Saline; n=20 Lep (n=5 for each time-point)
IHC for TH and Oxt	2 months	n=3	/
POMC-fibers in SON	4-10 months	n=1	n=2
Lepr and MC4r in SON	2 months	n=2	n=2
Stereotaxic surgery and Ca^{2+} imaging	2 months	n=3 Tg(Pomc1-cre)16Lowl/J n=3 C57BL/6J	n=3 Tg(Pomc1-cre)16Lowl/J n=3 C57BL/6J
High-Fat Diet	4 months	n=4 ND n=6 HFD	n=4 ND n=6 HFD
Early Life Stress	2 months P21	n=2 Dums n=7 STD; n=8 ELS	

Table 2: *PCR customized primers for genotyping*

Mouse line	Primers sequences
C57BL/6J-Tg (Pomc-EGFP)1Low/J	Transgene GFP (F): AAG TTC ATC TGC ACC ACC G Transgene GFP (R): TCC TTG AAG AAG ATG GTG CG Internal positive control (F): CTA GGC CAC AGA ATT GAA AGA TCT Internal positive control (R): GTA GGT GGA AAT TCT AGC ATC ATC C
Tg(Pomc1-cre)16Lowl/J	Transgene Cre (F): GCG GTC TGG CAG TAA AAA CTA TC Transgene Cre (R): GTG AAA CAG CAT TGC TGT CAC TT Internal positive control (F): CTA GGC CAC AGA ATT GAA AGA TCT Internal positive control (R): GTA GGT GGA AAT TCT AGC ATC ATC C

Table 3: *Primary antibodies*

Antibody	Source	Dilution	Brand
Oxytocin	polyclonal guinea pig	1:7000 (IHC)	Synaptic System (Cat. No. 408 004)
p-Stat3	monoclonal rabbit	1:600 (IHC)	Cell Signaling (Cat. No. 9145)
c-Fos	monoclonal rabbit	1:3000 (IHC)	Cell Signaling (Cat. No. 2250)
GFP	monoclonal rabbit	1:300 (IHC)	Cell Signaling (Cat. No. 2956)
Cre-recombinase	polyclonal rabbit	1:500 (IHC)	Synaptic System (Cat. No. 257 003)
Oxytocin receptor	monoclonal mouse	1:100 (WB)	Santa Cruz (Cat. No. sc-515809)
β-Actin	monoclonal mouse	1:200 (WB)	Santa Cruz (Cat. No. sc-477778)
Th	polyclonal sheep	1:400 (IHC)	Merck (Cat. No. AB1542)

Table 4: *Secondary conjugated antibodies*

Conjugate	Source	Target	Dilution	Brand
Alexa Fluor 488	donkey	anti-guinea pig	1:200	Jackson ImmunoResearch (Cat. No. 706-546-148)
Cy3	donkey	anti-guinea pig	1:200	Jackson ImmunoResearch (Cat.No. 706-166-148)
Alexa Fluor 647	donkey	Anti-guinea pig	1:400	Jackson ImmunoResearch (Cat.No. 706-605-148)
Alexa Fluor 488	donkey	anti-rabbit	1:400	Invitrogen (Cat. No. A-21206)
Alexa Fluor 555	donkey	anti-rabbit	1:400	Invitrogen (Cat. No. A-31572)

Table 5: *q-PCR customized primers and TaqMan probes*

Target gene	Sequence or assay ID
Oxt	F: CTTACTGGCTCTGACCTCGG R: CACTTGCGCATATCCAGGTC
Avp	F: ACTTCCAGAACTGCCCAAGA R: GGTAGTTCTCCTCCTGGCAG
Socs3	F: ACCAAGAACCTACGCATCCA R: GTGGCAAAGAAAAGGAGGGG
Tata-Binding Protein (TBP)	F: GCAGCCTCAGTACAGCAATC R: CTGCGGTACAATTCCAGAGC
OxtR	Mm01182684_m1
B-actin	Mm01205647_g1

Table 6: *RNAscope Probes*

Probes	Assay ID
Oxt	Mm-oxytocin (Oxt) mRNA (493171)
Lepr	Mm-leptin receptor (Ob-r)-C2 (402731)
Mc4r	Mm-Mc4r-C2 (319181)
3-plex Positive control	Mm (32088)
3-plex Negative control	DapB (310043)

5. Results

5.1 *Oxytocin neurons distribution in the paraventricular and supraoptic nucleus is sexually dimorphic and changes during the postnatal development*

As part of the study of the crosstalk between Lep and Oxt, we first studied the morphology and the distribution of Oxt neurons to characterize any age- and sex- dependent differences in the hypothalamic Oxt system in male and female mice at P21 and P60. The P21 was selected as a time-point representative of the postnatal development, while P60 of adulthood.

The postnatal period is the timeframe between the day of the birth (P0) and the day of the weaning (P21) and during this critical period Oxt neurons progressively reach their maturation [157]. During such transformation, we expected that Oxt neurons may reach their maturation in a sex-dependent way, thus leading to the sex-dimorphism of the Oxt system in adulthood [185].

Therefore, IHC for Oxt antibody was employed to study both the PVN (Fig. 4A) and the SON (Fig. 4B) Oxt neurons in male and female mice at P21 and P60. Morphometric analysis revealed a significant higher number of Oxt neurons in both the PVN (Fig. 4C) and the SON (Fig. 4D) of male mice at P21, compared to females. Furthermore, male at P21 also displayed a higher number of Oxt neurons compared to adult males at P60 in both the PVN (Fig. 4C) and the SON (Fig. 4D). In contrast, the number of Oxt neurons was significantly higher only in the PVN in female mice at P60, as compared to females at P21 and males at P60 (Fig. 4C).

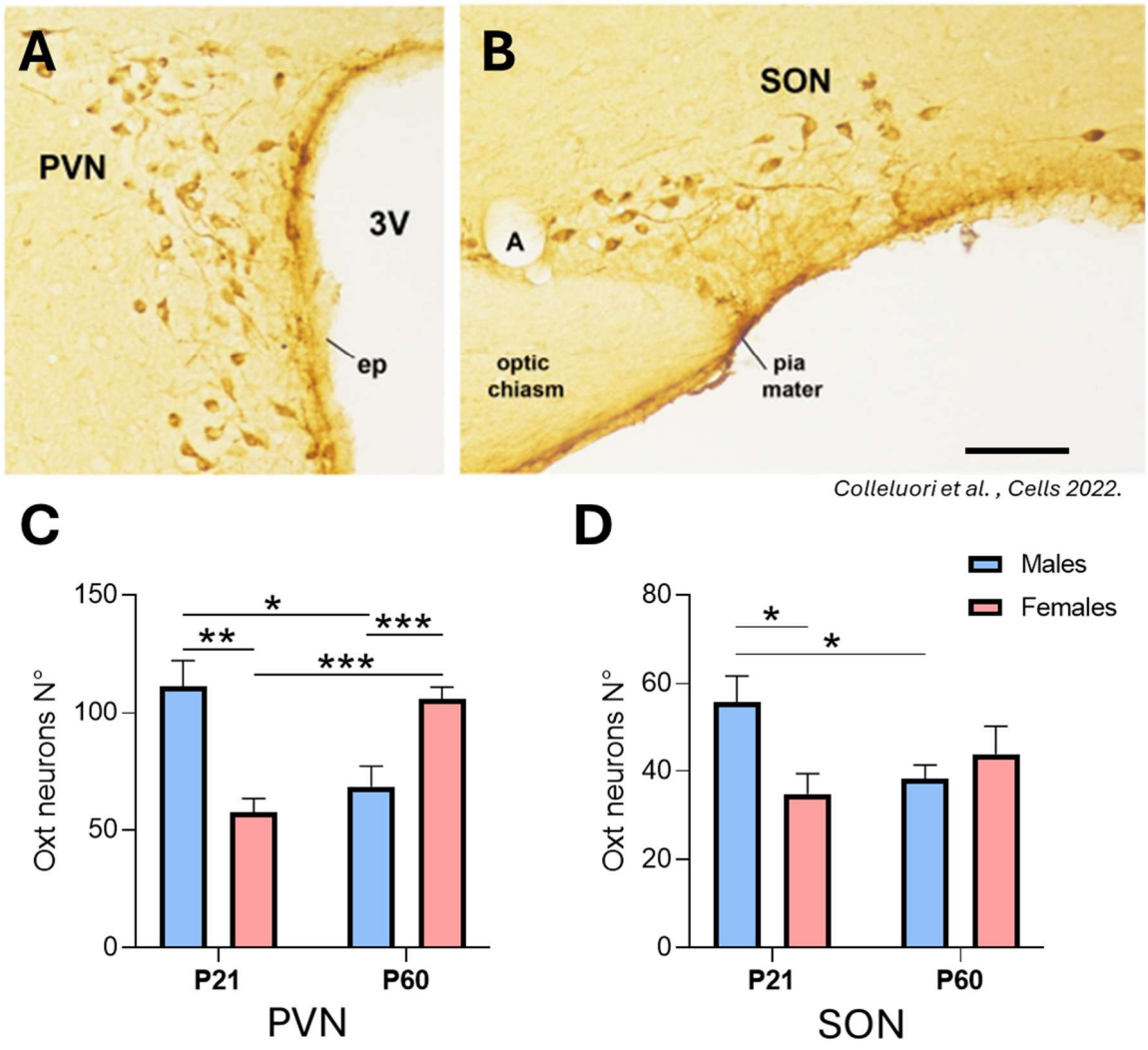

Figure 4:*Oxytocin neurons distribution in the PVN and the SON is sexually dimorphic and changes during the development*. Oxt IHC and light microscopy representative of Oxt neurons distribution in the PVN (**A**) and the SON **(B)** of adult mice. Morphometric analysis at P21 *versus (VS)* P60 in the PVN (**C**) and in the SON (**D**) of male and female mice. Sample size: P21 n=9-11; P60 n=8. Data were analysed using Student's *t*-test. *p<0.05;**p<0.01. *** p<0.001; P=postnatal day; 3V=third ventricle ; ep= ependyma; A=artery; The scale bar is included only in B and corresponds to: **A**,**B**=100 µm.

Based on these data, in female mice Oxt neurons in the PVN increase in number during growth to adulthood, when they display a higher absolute number of Oxt neurons compared to males. On the other side, male mice reduce the number of Oxt neurons in both the PVN and the SON moving from P21 to P60. Overall,

these data confirmed that Oxt neurons maturation occurs in a sex-dependent way and differently affects the PVN and the SON in the hypothalamus.

5.2 Leptin activates oxytocin neurons in the supraoptic nucleus

The crosstalk between Lep and Oxt in the hypothalamus were investigated in males and female mice at both P21 and P60, by studying the signalling factors activated by peripheral Lep administration in PVN- and SON- Oxt neurons.

Jak2-Stat3 is the main transduction pathway phosphorylated by Lep in the hypothalamus and related to its role in the regulation of the energy balance [39]. Therefore, an intraperitoneal-IP injection (0,5 mg/kg) of recombinant leptin was given to male and female mice to observe Stat3 activation. An abundant phosphorylation of Stat3 was observed in the arcuate nucleus (ARC) in mice injected with Lep, as compared to those treated with saline (Fig. 5 A-B), indicating that peripheral Lep administration successfully reached the hypothalamus. These results were confirmed in both male and female mice at P21 and P60.

Then, the colocalization between Oxt and p-Stat3 were studied in PVN and SON. Confocal microscopy showed that Lep failed to induce Stat3 activation in Oxt neurons of PVN (Fig. 5 C-D), due to the absence of colocalization between p-Stat3 positive nuclei and Oxt. In parallel, a total absence of p-Stat3 activation was found in SON, including in Oxt neurons, of both saline and Lep treated mice (Fig. 5 E-F). The absence of colocalization between Oxt and p-Stat3 antibodies was confirmed in both male and female mice at P21 and P60.

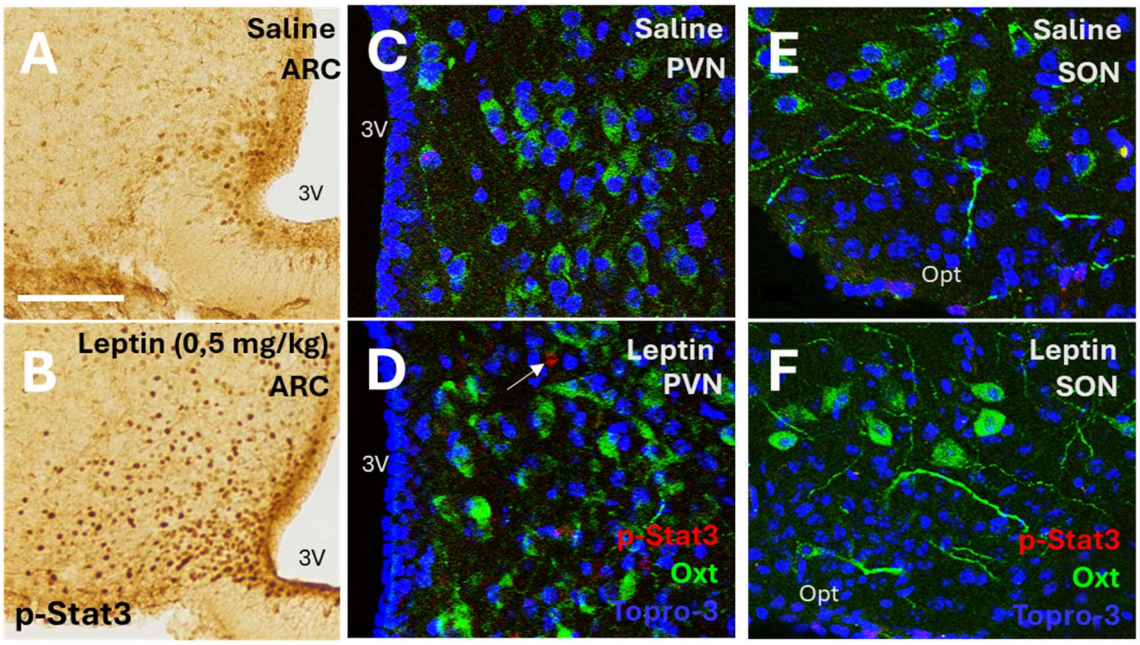

Figure 5: *Leptin activates p-Stat3 in ARC neurons but not in oxytocin neurons of the PVN and the SON*. p-Stat3 IHC and light microscopy in the ARC of P60 mice treated with saline **(A)** or Lep (IP: 0,5 mg/kg) **(B).** Double-labelled confocal microscopy representative of the absence of colocalization between Oxt (green cells) and p-Stat3 (red nuclei; white arrow) in the PVN and the SON in both saline **(C-E)** and leptin treated **(D-F)** P60 male and female mice**.** All pictures by confocal microscopy show blue nuclei stained by TO-PRO3. Sample size: n=2 saline n=3 Lep. 3V=third ventricle ; Opt= optic tract. The scale bar is included only in A and corresponds to: **A,B**=200 µm; **C,D,E,F**=50 µm.

Therefore, our morphological investigation revealed that peripheral Lep administration did not induce p-Stat3 activation either in PVN- or SON- Oxt neurons at P21 and P60.

Afterwards, the colocalization between Oxt and the "immediate early gene", c-Fos, was studied to assess the Lep-mediated Oxt neuron's activation in the PVN/SON [47, 186]. Rare or absent Oxt neurons nuclei were found to be c-Fos+ in the PVN of both saline (Fig. 6A) and Lep treated mice (Fig. 6B). On the other hand, several Oxt neurons were found to colocalize with c-Fos after Lep administration in the SON, but not after saline injection (Fig. 6 C-D) in both male and female mice at P60. Morphometric analyses were then

performed to quantify the Lep-induced activation in Oxt neurons. The neuronal c-Fos counting reported lack of significant difference in the number of Oxt neurons activated by Lep in the PVN of both male and female mice (Fig. 6E). On the other side, Lep treatment resulted in a significant increase in the number of c-Fos+ Oxt neurons in SON of both male and female mice at P60 (Fig. 6F). In summary, Lep was found to significantly activate c-Fos and not p-Stat3, exclusively in Oxt neurons in SON at P60.

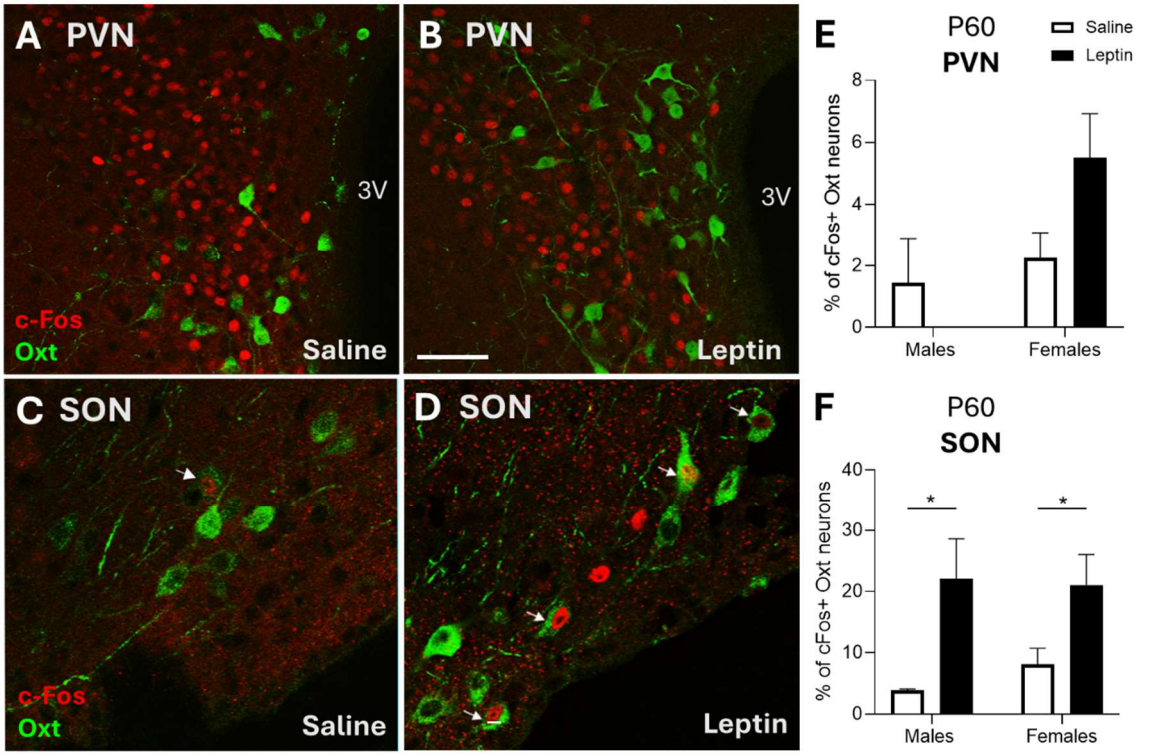

Figure 6: *Leptin activates c-Fos in oxytocin neurons in the SON in mice at P60.* Double-labelled confocal microscopy for c-Fos (red nuclei) and Oxt (green cells) in the PVN of saline **(A)** and Lep treated **(B)** mice. Double-labelled confocal microscopy for c-Fos and Oxt in SON of saline **(C)** and Lep treated **(D)** mice; arrows indicate cFos+ Oxt nuclei. Morphometric analysis of c-Fos+ nuclei in Oxt neurons, comparing saline and Lep treatment in the PVN (**E**) and in the SON **(F)** of male and female mice. Sample size: n=2 saline; n=3 Lep. Data were analysed using Student's *t*-test. *p<0.05. P=postnatal day; 3V= third ventricle. The scale bar is included only in B and corresponds to: **A,B**= 70µM; **C-D**= 35 µM

Furthermore, confocal microscopy and morphometric analysis for the study of c-Fos were performed also in P21 mice after saline or Lep treatment, to explore whether Oxt neurons were sensitive to Lep already during postnatal

development. Morphometric analysis revealed a non-significant difference in the number of c-Fos+ Oxt neurons between saline and Lep in the PVN of both male and female mice (Fig. 7A). Furthermore, c-Fos was not activated by Lep in the SON of male mice at P21, whereas its activation was confirmed in the SON of females (Fig. 7B).

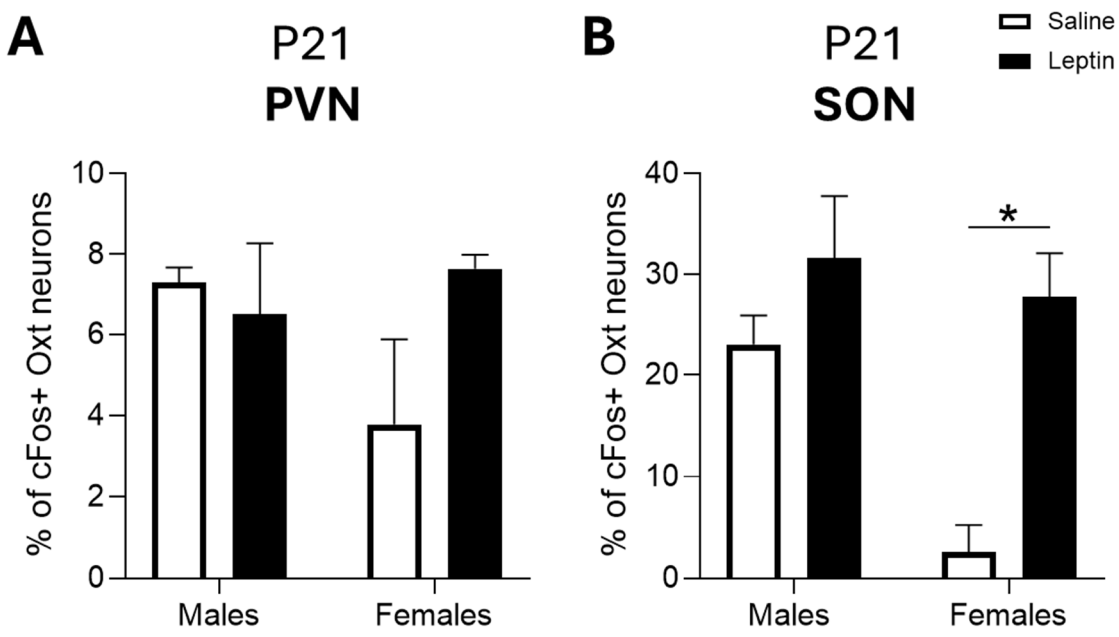

Figure 7: *Leptin activates c-Fos in oxytocin neurons in the SON of female mice at P21.* Morphometric analysis of c-Fos+ positive nuclei in the PVN (**A**) and the SON (**B**) of male and female mice at P21. P=postnatal day; Sample size: n=2 saline n=3 Lep. Data were analysed using Student's *t*-test. *p<0.05.

In conclusion, Lep was found to phosphorylate Stat3 neither in the PVN nor in the SON of male and female mice at both P21 and P60. In contrast, Lep significantly activates SON Oxt neurons of adult mice, while a sexual dimorphic response was found at P21, where Oxt neurons are significantly responsive to Lep only in the SON of female mice.

5.3 Leptin induces oxytocin plasma release in a time-dependent and sexually dimorphic manner

Since magnocellular Oxt neurons in the SON are the main source of circulating Oxt, a "*time-response*" experiment was conducted to assess whether recombinant Lep (IP; 0,5 mg/kg) may regulate Oxt synthesis in both male and female mice (Fig. 8 A). The following analyses of the "*time-response*" of Oxt to Lep was performed only in adult mice, at P60. Suppressor of cytokine signaling 3 (SOCS3) is a key feed-back inhibitor of the Jak-Stat pathway known to be activated by Lep signalling [187, 188]. In the hypothalamus of Lep-treated mice there was a significant increase in *Socs3 m-RNA* starting from 1,5h and up to 3 h from the injection in males (Fig. 8B) and up to 6h in females (Fig. 8C), indicating that Lep successfully entered the hypothalamus.

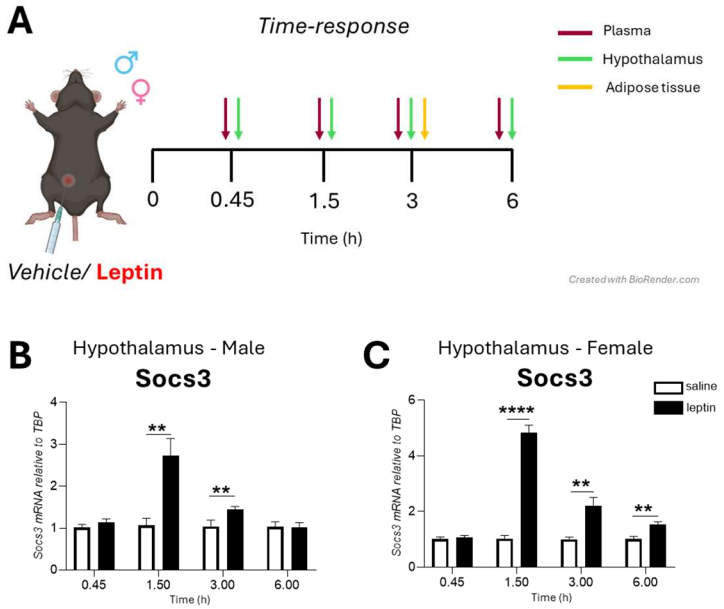

Figure 8: *Time-response to leptin intraperitoneal administration*. Male and female mice were intraperitoneally injected with saline or recombinant Lep (0,5mg/kg) to collect plasma, hypothalamus and adipose tissues (inguinal and gonadal white adipose depots and interscapular brown adipose depot) at different time-points (0,45h, 1.5h , 3h and 6h) **(A)**. *Socs3 m-RNA* levels in the hypothalamus of male **(B)** and female **(C)** mice. Sample size: n=5 for each time-point, group (saline/Lep) and sex. Data are shown as mean ± SEM. Data were analysed using Student's *t*-test. *p<0.05; **p<0.01;***p<0.001.

Gene expression assays in the hypothalamus revealed that Lep administration did not affect *Oxt m-RNA* expression levels in male mice (Fig. 9A), while it resulted in an increase of the hypothalamic content of Oxt at 1.5h after Lep administration in females (Fig. 9B). Oxt quantification in plasma by LC-MS was further assessed in the same animals. Interestingly, Lep increased Oxt plasma release after 1.5 hours in male mice (Fig. 9C), while it induced a trend (p=0,05) of increased plasma Oxt levels only after 6 hours from Lep administration in females (Fig. 9D).

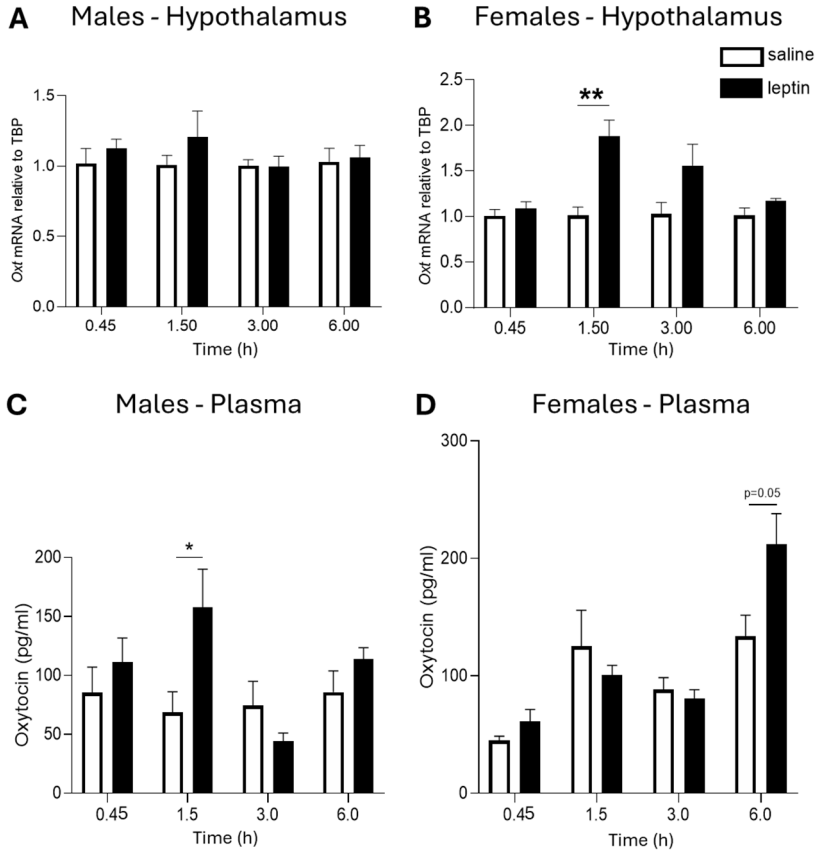

Figure 9*: *Leptin induces oxytocin mRNA synthesis and protein plasma release. Saline and Lep time-course for the analysis of *Oxt mRNA* in the hypothalamus by RT-qPCR in male (**A**) and female (**B**) mice. Oxt quantification in plasma by LC-MS in saline and Lep- treated male (**B**) and female (**D**) mice. Sample size: n=5 for each time-point, group (saline/Lep) and sex. Data are presented as mean ± SEM. Data were analysed using Student's *t*-test. *p<0.05; **p<0.01.

In conclusion, Lep induced an early Oxt release in plasma in male mice, where it did not affect the hypothalamic content of *Oxt mRNA*. In contrast, Lep increased the synthesis of *Oxt mRNA* in females, where it induced a trend for an increase in Oxt release in plasma at 6h post-injection.

However, SON neurons synthetized and release Oxt, as well as Avp. Therefore, we aimed to exclude that Lep administration was also responsible for *Avp mRNA* synthesis and protein release in plasma. We have obtained preliminary data for Avp only in male mice. Lep administration did not result in variation of *Avp mRNA* expression levels (Fig. 10 A). Furthermore, preliminary data on Avp quantification in plasma at 1.5 and 3h after Lep administration, showed that Lep did not affect Avp release in male mice (Fig. 10 B). However further analysis will be required to study Avp system after Lep administration in females.

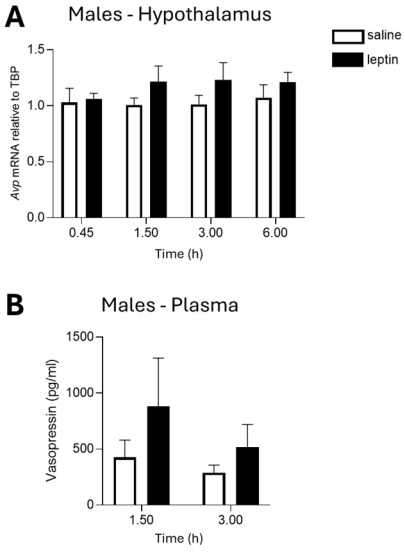

Figure 10: *Leptin does not affect Avp mRNA synthesis and protein plasma release.* Saline and Lep time-course for the analysis of *Avp mRNA* in the hypothalamus by RT-qPCR in male mice (**A**). Oxt quantification in plasma by LC-MS at 1.5 and 3h after saline/Lep administration in male mice (**B**)**.** Sample size: n=5 for each time-point, group (saline/Lep) and sex. Data are presented as mean ± SEM. Data were analysed using Student's *t*-test.

Furthermore, previous studies in literature reported that Oxt is not only synthetized by the hypothalamus, but also by sympathetic nerves in the adipose tissue, which are marked by tyrosine hydroxylase (Th) [137] and of the GI tract [135]. Since Lep administration increased Oxt release in plasma but failed to induce a variation of *Oxt mRNA* in the hypothalamus of male mice, IHC for Oxt were performed in both WAT and GI tract to assess whether peripheral Oxt synthesis may be involved in this process. Th + fibres were found in sections of iWAT stained with Th antibody compared to negative controls (Fig. 11A, B). In contrast, we did not observe Oxt+ fibers either in the iWAT (Fig. 11C) or in duodenum (Fig. 11D). These data were repeated and confirmed in both iWAT and gWAT and in stomach and duodenum of male adult mice at P60.

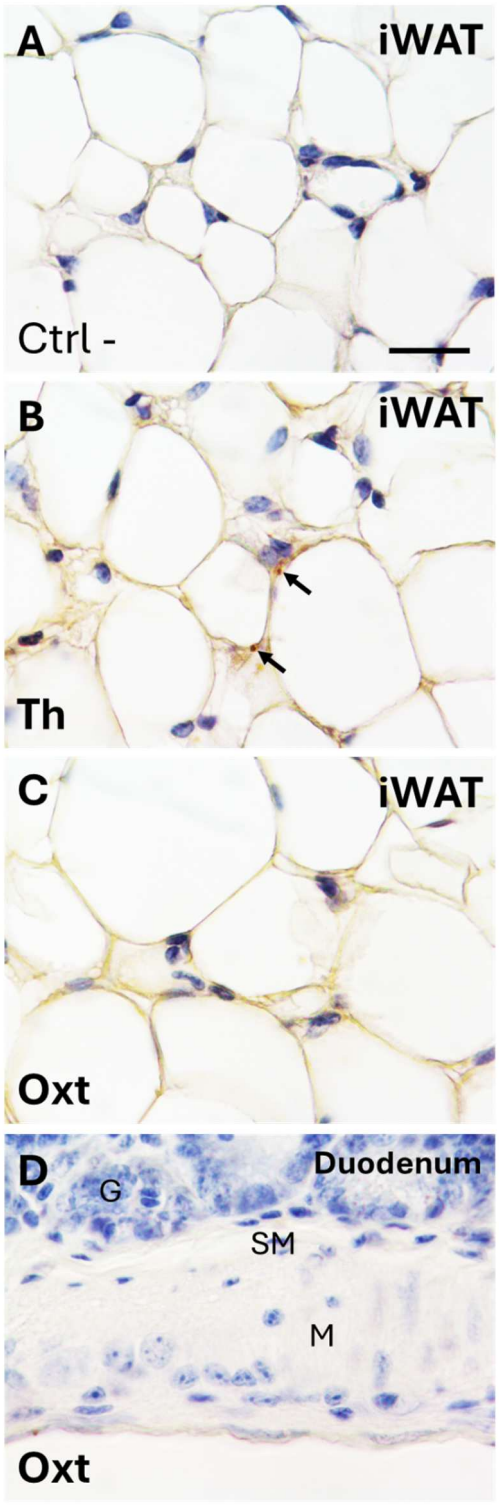

***Figure 11*: *IHC for Th and Oxt in WAT and GI tract*.** Negative control (no primary antibody) in iWAT (**A).** Th IHC showing some Th+ fibres (arrows) in iWAT **(B**). Oxt IHC in iWAT (**B)** and duodenum (**D**). Sample size: n=3. iWAT= inguinal (subcutaneous) white adipose tissue; Ctrl(-)= negative control; G=glands; SM=submucosa layer; M=muscular

layer; Th=Tyrosine Hydroxylase. The scale bar is included only in A and corresponds to: **A,B,C,D=** 130 μM.

In conclusion, the "time-course" experiment suggests that Lep specifically modulates Oxt release following a time-dependent and sexually dimorphic pattern. The absence of peripheral Oxt expression demonstrates that this process occurs mainly through hypothalamic Oxt release.

5.4 Leptin increases the expression of the oxytocin receptor in the white adipose tissue

Oxt secretion has multiple physiological functions and Oxtr is expressed by several peripheral tissues, including adipose tissue (AT) [189], where Oxt displays a lipolytic role [126, 189]. Thus, different depots of AT were collected after 3h from saline or Lep IP administration, to perform gene and protein expression analyses of Oxtr in iWAT, gWAT and iBAT. The following preliminary data were conducted only in female mice. Lep administration resulted in a significant decrease of *Oxtr mRNA* expression in both iWAT (Fig. 12A) and gWAT (Fig. 12B), but not in iBAT (data not shown). In contrast, Oxtr protein levels in Lep-treated mice displayed a trend of increased expression in iWAT (Fig. 12C), while it was significantly induced in gWAT (Fig. 12D). The reduced *Oxtr mRNA* levels coupled with increased protein expression in iWAT and gWAT suggest that Lep may increase Oxtr-protein synthesis in both the subcutaneous and visceral depots.

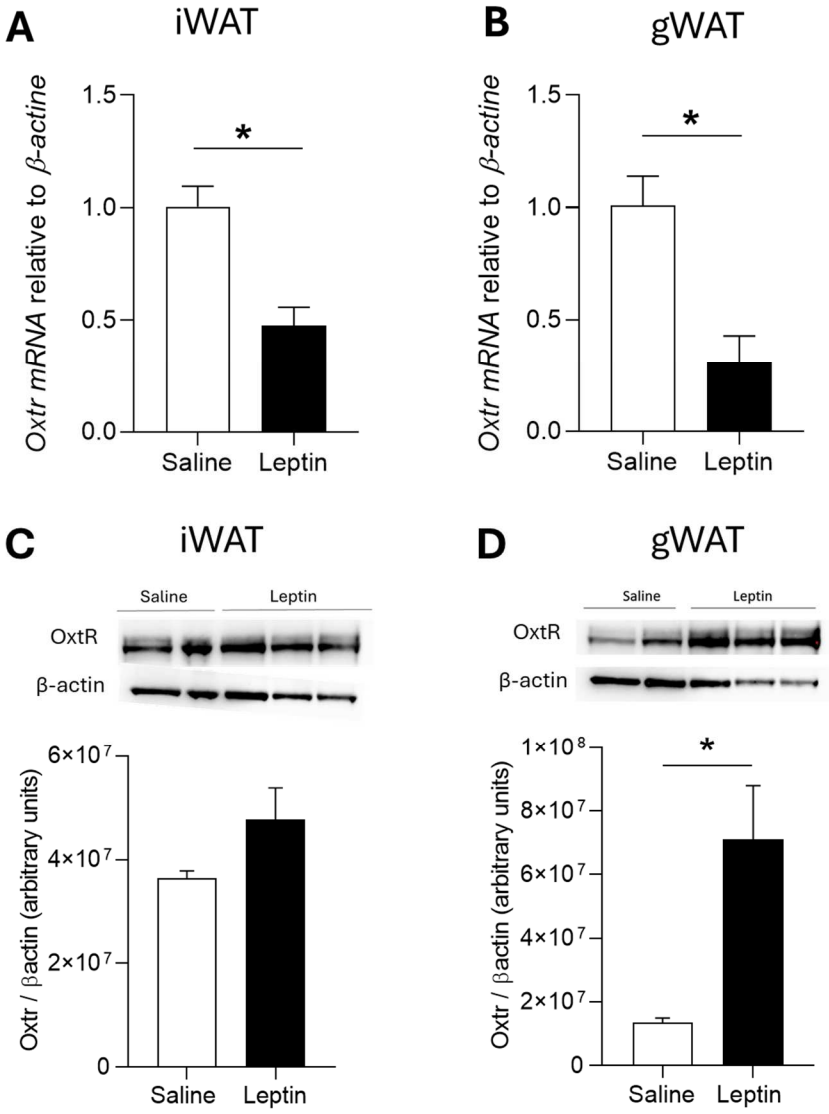

Figure 12: *Leptin regulates Oxtr mRNA and protein expression in adipose tissue.* RT-qPCR for Oxtr m-RNA expression analysis in iWAT (**A**) and gWAT (**B**), by comparing saline and Lep treatments in female mice. Representatives immunoblot and quantification of Oxtr expression in iWAT (**C**) and gWAT (**D**). iWAT= inguinal (subcutaneous) white adipose tissue; gWAT= gonadal white adipose tissue; Oxtr= oxytocin receptor. Sample size: n=2 saline; n=3 Lep. All data were analysed using Student's *t*-test. All data are mean ± SEM. *p < 0.05.

In conclusion, exogenous Lep increases Oxtr protein levels in WAT, possibly mediating a crosstalk between brain and white AT and perhaps to enhance the action of increased Oxt in plasma. These results suggest the existence of crosstalk between brain and WAT mediated by Lep and Oxt.

5.5 Leptin receptor is not express by oxytocin neurons

Leptin regulates energy balance binding to its receptor (*Lepr*) in the hypothalamus [190]. Since previous data demonstrated that Lep modulates Oxt production in the hypothalamus, the presence of Lepr in Oxt neurons was assessed by *in-situ* hybridization. First, *Lepr* was found to be abundantly expressed by the population of POMC neurons in the ARC (Fig. 13A). Furthermore, the presence of *Lepr* + cells was confirmed also in neurons of the PVN, although there was no colocalization between *Lepr* and *Oxt m-RNA* (Fig. 13B). Interestingly, *Lepr* was not expressed in SON (Fig. 13C). All data of *in-situ* hybridization were confirmed in both male and female mice. scRNA-seq dataset (provided by Prof. Tibor Harkany) [183], was used to assess the expression of Lepr in Oxt neurons. In agreement with our *in-situ* hybridization results, also data from the Sc-RNAseq reported the absence of *Lepr* in magnocellular hypothalamic cells (Fig. 13D-E) which express the *Oxt* gene (Fig. 13F). However, sc-RNA seq data were only performed on mice during pre- and post-natal development and not at P60. In conclusion, Lepr is not expressed by Oxt neurons either in the PVN or in the SON, although the latter was activated by Lep via c-Fos. Overall, these data suggest that Lep may act indirectly on Oxt neurons of the SON.

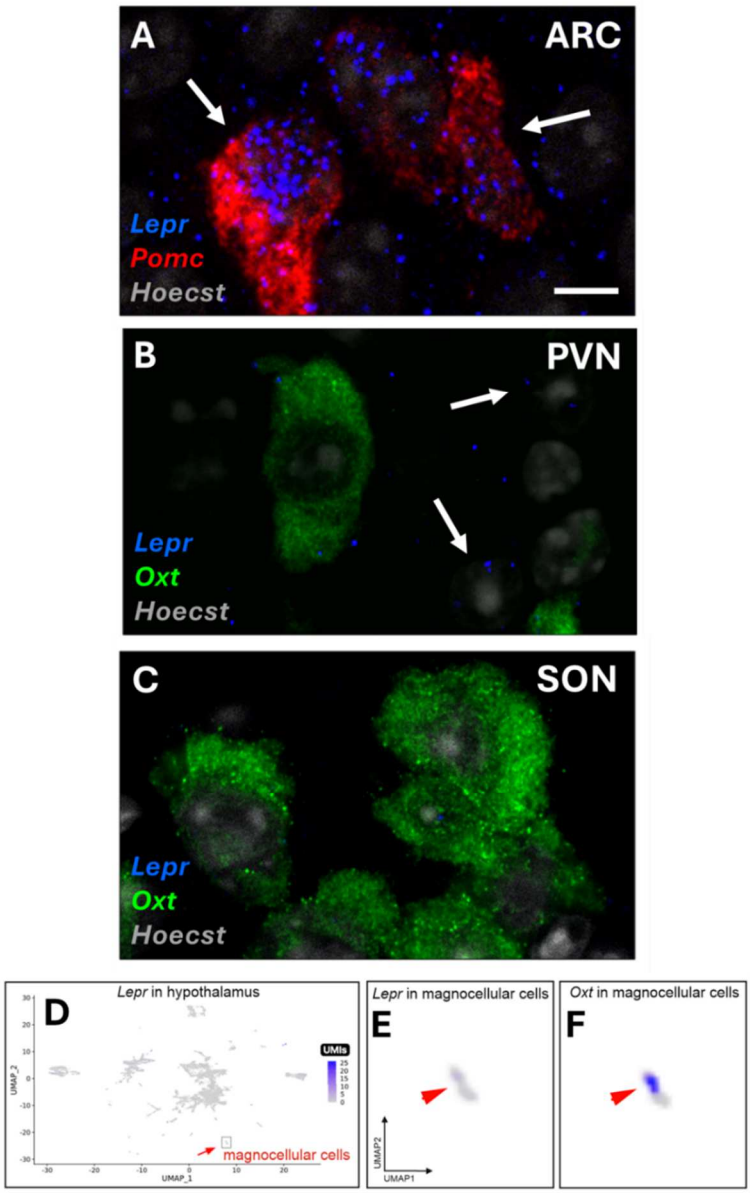

Figure 13: *Leptin receptor is not expressed by oxytocin neurons in the SON. In-Situ* hybridization and double-labelled confocal microscopy for *Lepr* (blue dots) and *POMC* (red dots; arrows) in the ARC **(A)** and for *Lepr* and *Oxt* (green dots) in the PVN (arrows indicate *Lepr* + cells) **(B)** and the SON **(C).** UMAP plot of *Lepr* expression in the hypothalamus from the single nucleus RNA-sequencing dataset (red arrow indicates the magnocellular fraction) **(D)**. Enlargement of the panel in D representing the expression of *Lepr* in the magnocellular cells of the hypothalamus (**E**). UMAP plot representing the expression of *Oxt* in magnocellular cells of the hypothalamus **(D)**. Nuclei are represented with grey dots by staining with Hoechst 33,342. Sample size for the RNA Scope n=2; Sample sizes for scRNA-seq experiments: n = 8 (E15.5), n = 7 (E17.5), n = 4 (P0), n = 4 (P2), n = 3 (P10), n = 3 (P23). UMIs=Unique Molecular Identifiers; The scale bar is included only in A and corresponds to: **A,B,C**= 7µM.

5.6 Pro-opiomelanocortin neurons project to Melanocortin 4-negative oxytocin neurons in the supraoptic nucleus

POMC neurons are the main population targeted by Lep in ARC [10]. To investigate whether Lep could indirectly target Oxt neurons in SON by acting on POMC neurons, C57BL/6J-Tg(Pomc-EGFP)1Low transgenic mice were employed to assess the presence of POMC projections in the SON. These transgenic mice express E-GFP in POMC neurons by the *Pomc* promoter region (Fig. 14A) [26] and green-fluorescent labelling was observed in the ARC (Fig. 14B) of these animals, as expected. POMC neurons projections were found in the SON, closed to Oxt neurons as shown by confocal microscopy (Fig. 14C). Employing the Stimulated Emission Depletion Microscopy (STED) which allows to study cell-cell relations with higher resolution (up to 35nm), we observed that the GFP-positive POMC neurons project to the SON Oxt neurons (Fig. 14D-G). Specifically, the overlay between GFP and Oxt revealed that POMC projections are in closed apposition to Oxt neurons somata and projections (Fig. 14G).

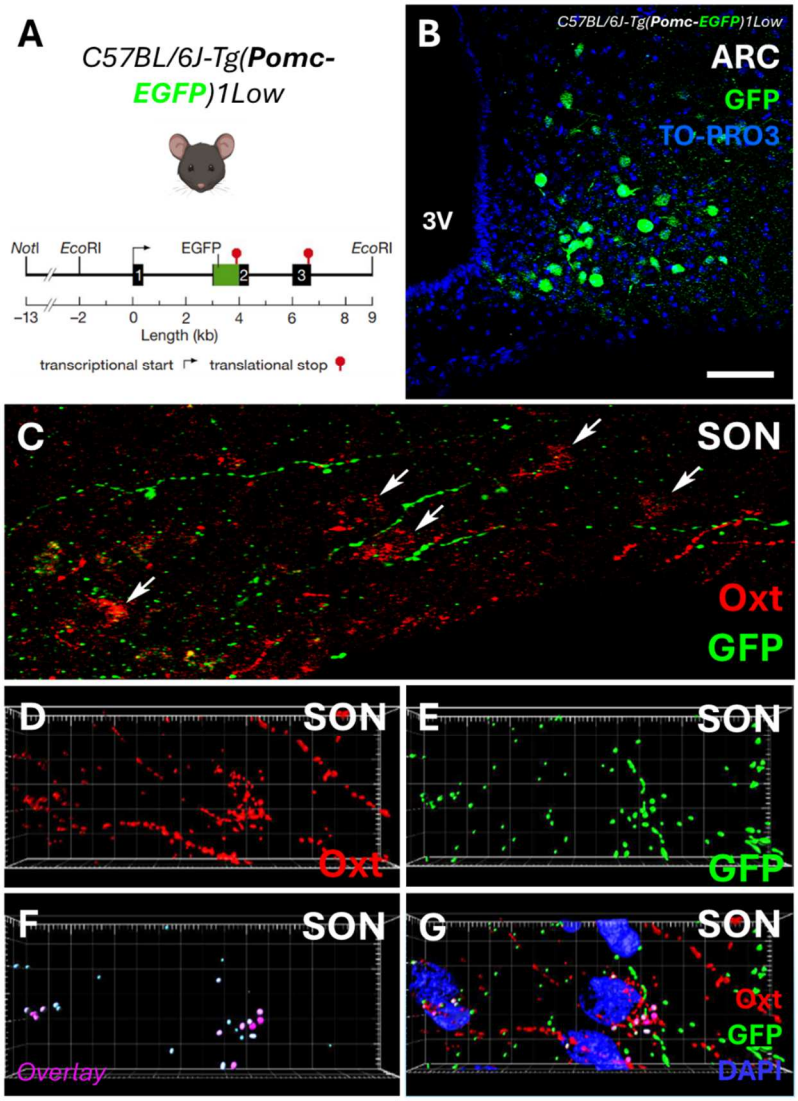

Figure 14: *POMC neurons project to the SON*. Transgene construct (Cowley et al. Nature, 2001) (**A**). Double-labelled confocal microscopy for GFP (green cells) in the ARC **(B)**. Double-labelled confocal microscopy for Oxt (red cells, white arrows) and GFP (green) antibodies in the SON **(C)**; arrows indicate POMC fibers in closed proximity to Oxt neurons. STED microscopy for Oxt (**D**) and GFP (**E**)**.** Overlay **(F)** and colocalization **(G)** between Oxt and GFP in the SON**.** All the analyses were made using C57BL/6J-Tg(Pomc-EGFP)1Low transgenic mice. Sample size: n=2. 3V=third ventricle; The scale bar is included only in A and corresponds to: **B**= 100 µM; **C**= 35 µM; **D,E,F,G** =10 µM.

POMC axon terminals produce and release alpha-melanocyte stimulating hormone (α-Msh), which in turn binds to melanocortin receptor 4 (Mc4r) [26]. Since POMC projection reaches Oxt neurons in SON where they may possibly release α-Msh, *in-situ* hybridization was employed to assess

whether *Mc4r* is expressed in Oxt neurons of the SON in both male and female mice. *Mc4r* was expressed in both, ARC (Fig. 15A) and in PVN (Fig. 15B) neurons. In the latter, *Mc4r* did not colocalize with *Oxt* suggesting that Oxt neurons do not express Mc4r *m-RNA* in the PVN. Furthermore, *Mc4r* was found to be completely absent in the SON (Fig. 15C).

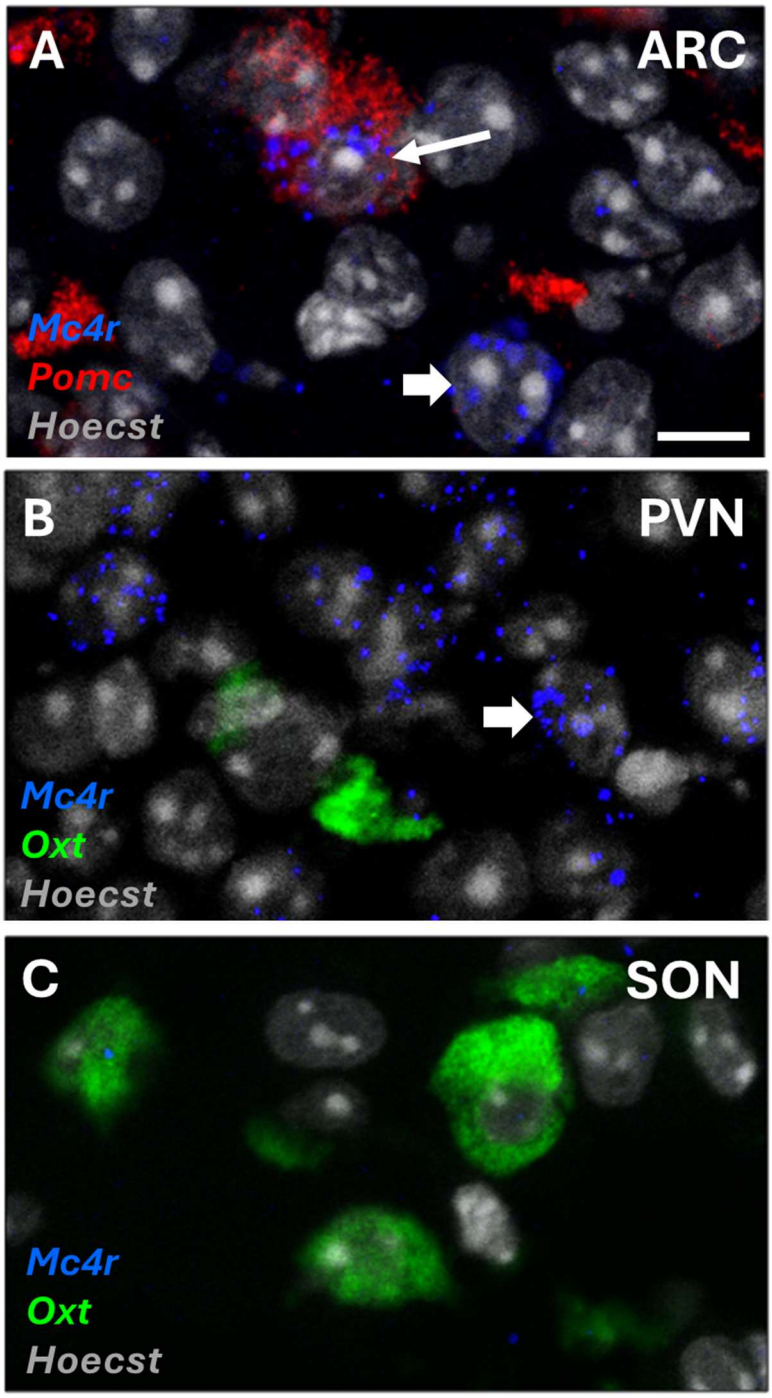

Figure 15**:** *Melanocortin-4 receptor is not expressed by oxytocin neurons in the SON. In-situ* hybridization for *Mc4r* and *Pomc*, showing that *Mc4r* is expressed by neurons in ARC (white, short arrow), also in those cells expressing *Pomc* (white, long arrow) (**A**). *In-situ* hybridization for *Mc4r* and *Oxt* in PVN (short arrow) (**B**) and in SON (**C**) neurons. All pictures show grey nuclei stained by Hoechst 33,342. Sample size: n=2. The scale bar is included only in A and corresponds to: **A,B,C** = 7 µm.

In conclusion, POMC neurons were found to project to Oxt neurons of the SON where *Mc4r* is not expressed, suggesting that the interaction between POMC and Oxt neurons is not hormone-mediated.

5.7 Leptin does not affect calcium signalling in the supraoptic nucleus ex vivo

Calcium imaging was performed to record any Lep-dependent variation of calcium activity in the ARC (as a control) and in the SON (target region), to further explore whether Lep activates Oxt neurons directly or indirectly.

Tg (Pomc 1-*Cre*)16Lowl transgenic mice were injected in the ARC with a *Cre*-dependent adeno-associated virus (AAV) to drive the expression of the GCaMP6 (510 nm of wavelength) and d-Tomato (581nm of wavelength) proteins (Fig. 16A), specifically in POMC neurons. The expression of the Ca^{2+}-sensor GCaMP6, allowed to easily assess Ca^{2+} release (hence neurons activation) in POMC neurons following Lep treatment and the red fluorescent protein d-Tomato helped to identify cells during the live imaging, as the basal signal of GCaMP6 could underestimate the presence of transfected cells.

Live imaging showed the basal fluorescence signal of GCaMP6 in POMC neurons, before Lep treatment (Fig. 16B). However, Lep perfusion via a-CSF (250 nM in female mice and 500 nM in male mice) on 300 µM thick brain slices resulted in increased Ca^{2+} levels and, hence fluorescence intensity, in POMC cells (Fig. 16C). Post-fixation with PFA and double-label confocal microscopy after Ca^{2+} confirmed the expression of both *Cre* recombinase and the d-Tomato protein in the ARC of transgenic mice (Fig. 16 D-F).

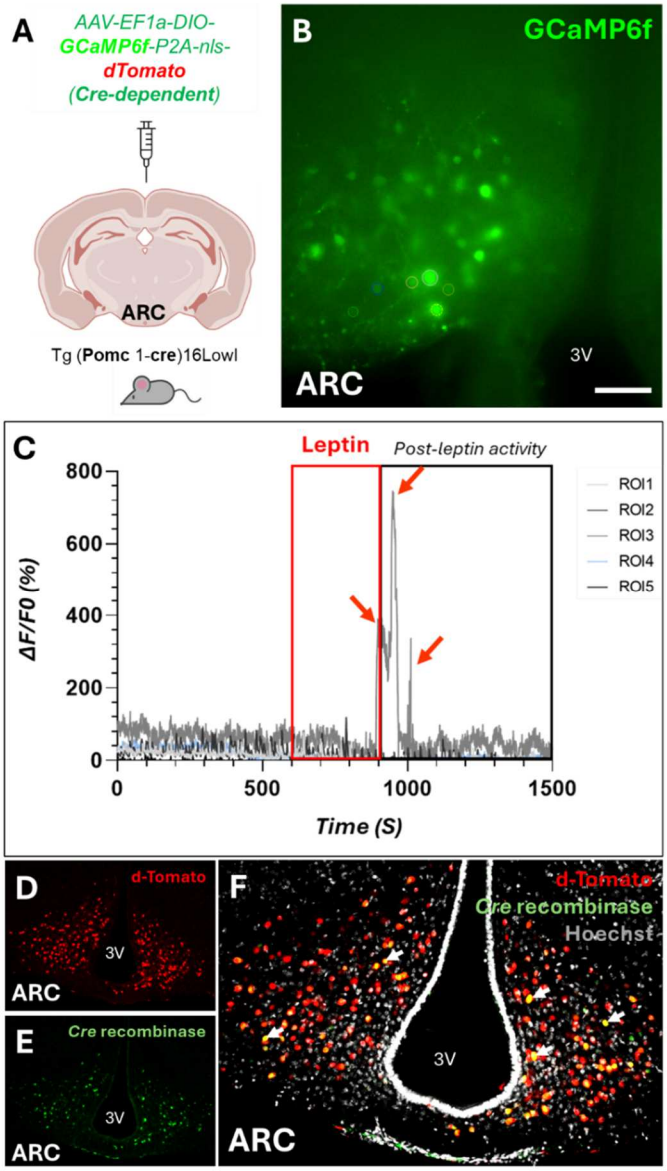

Figure 16: *Leptin induces* Ca^{2+} *increase in POMC neurons.* AAV-mediated and cre-dependent expression of GCaMP6f and d-Tomato in acute brain slices of ARC in Tg (Pomc 1-Cre)16Lowl transgene mice (**A**). Live Ca^{2+} imaging of POMC neurons expressing GCaMP6f calcium sensor in the ARC by fluorescence microscope (**B**). Circles are representative of selected region of interest (ROI). Representative traces of GCaMP6f fluorescence (calcium current) variation over time in selected ROI. Peaks of variation of fluorescence intensity (ΔF/F0) is indicated by red arrows (**C**). Immunofluorescence and confocal microscopy for d-Tomato (**D**) and *Cre*-recombinase (**E**) on thick sections of ARC. Both d-Tomato and Cre-recombinase are expressed in the ARC nucleus and they colocalize in numerous cells (yellow nuclei; short arrows) (**F**). Grey rectangles indicate the wash-out period; F0=initial resting (△F/F0) = variation of fluorescence intensity normalized to F0. 3V= third ventricle. Pictures by confocal microscopy show grey nuclei stained by Hoechst 33,342. Sample size: n=3 Tg(Pomc1-cre)16Lowl/J. The scale bar is included only in B and corresponds to: **B** =100 µm; **D,E**= 200 µm; **F**=100 µm.

In parallel, a non-*Cre* dependent AAV was injected in the SON of C57BL/6J mice (Fig. 17A). GCaMP6 fluorescent protein basal signal was recorded in neurons of the SON (Fig. 17B), as shown by the live imaging. Contrary to what observed in the ARC, Lep perfusion failed to induce a significant increase in Ca^{2+} activity in SON neurons (Fig. 17C). However, since the expression of the GCaMP6 was not driven by the *Cre*-recombinase, PFA-fixation and confocal microscopy for Oxt and d-Tomato was performed after Ca^{2+} imaging, to evaluate GCaMP6 expression in Oxt neurons of the SON. Colocalization of Oxt and the d-Tomato (Fig. 17 D-F) showed that AAV expression reached Oxt neurons in the SON, further suggesting that the Ca^{2+} activity of these neurons was recorded during the experiment.

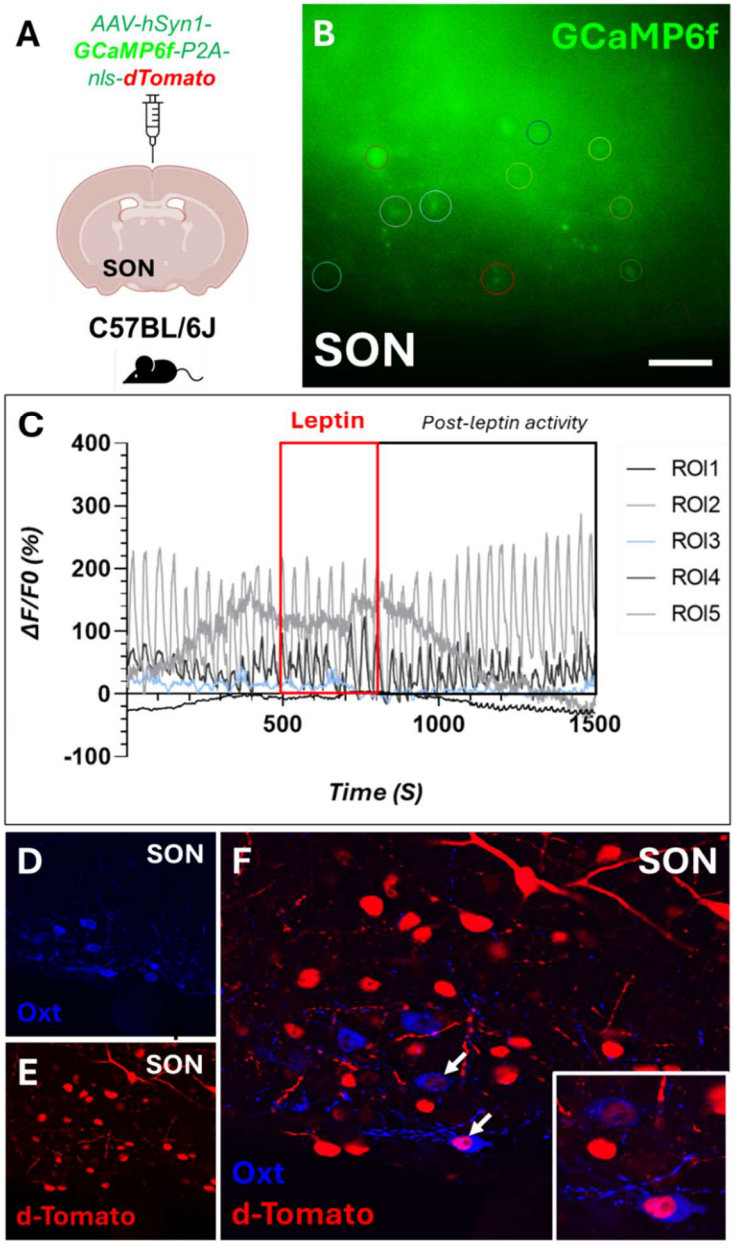

Figure 17: *Leptin does not affect [Ca^{2+}] signalling in SON neurons.* AAV-mediated GCaMP6f and d-Tomato expression in acute brain slices of SON in C57BL/6J mice (n=3 males and n=2 females) (**A**). Live [Ca^{2+}] imaging of SON neurons expressing GCaMP6f by fluorescence microscope (**B**). Representative traces of GCaMP6f fluorescence (calcium current) variation over time in five selected regions of interest (ROI). (**C**). Post- [Ca^{2+}] imaging immunofluorescence and confocal microscopy for Oxt (**D**) and d-Tomato (**E**). Oxt and d-Tomato antibodies colocalization in the SON (short arrows) (**F**). The insert in (F) represent the colocalization between Oxt neurons and d-Tomato at higher magnification. Grey rectangles indicate the wash-out period; F0=initial resting (△F/F0) = variation of fluorescence intensity normalized to F0. 3V= third ventricle. Sample size: n=3 C57BL/6J. The scale bar is included only in B and corresponds to: **B** =100 µm; **D,E**= 100 µm; **F**=35 µm; **insert in F**=15 µm.

In summary, 250 nM in female and 500 nM in male of Lep, were sufficient to activate POMC neurons in the ARC, but not Oxt neurons in the SON, thus suggesting that Lep acts indirectly on these neurons, possibly involving a further neuronal population far from the SON.

All the above-described experiments support the existence of a crosstalk between the fat-derived hormone Lep and Oxt neurons, pointing to a novel neuroendocrine pathway possibly implicated in the regulation of the energy balance.

As the overarching goal of this project was to assess Lep-Oxt interaction and its modification in condition of obesity and early postnatal stress, we performed preliminary experiment to assess possible variations of circulating Oxt in response to these two experimental settings.

5.8 Oxytocin hypothalamic synthesis and plasma secretion in mice exposed to high-fat diet

The "Lep time-course" experiment demonstrated that peripheral Lep levels affect Oxt production and secretion. Peripheral Lep levels are higher in mice exposed to HFD, where increased Lep production reflects an increased amount of body fat [31, 72, 191, 192]. Therefore, male and female mice were subjected to 12 weeks of normal or HFD to explore whether Oxt hypothalamic production and plasma secretion are affected by HFD consumption. Starting from the 9° week until the end of the protocol, body weight significantly increased in male mice exposed to HFD as compared to the control group (Fig. 18 A), while no variation was detected after HFD in females (Fig. 18 B). Food intake was significantly decreased in both male and female mice following the HFD

protocol as compared to ND, although females still consumed more food than males in both ND and HFD groups (Fig. 18 C).

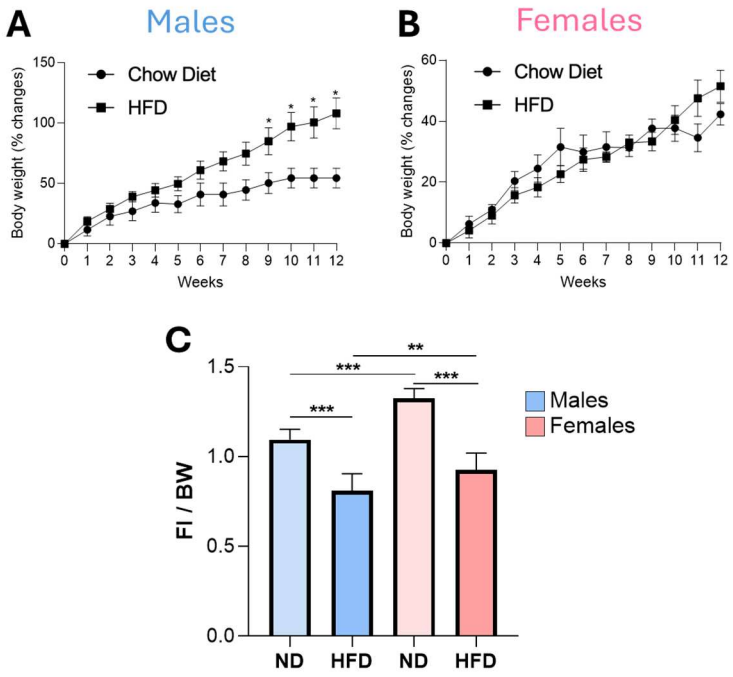

Figure 18: Body weight and food intake in mice exposed to HFD. Line graphs representing the percentage change in body weight from baseline during 12 weeks of CD or HFD in male (A) and female (B) mice. Grouped analysis comparing food intake change normalized to body weight in male and female mice subjected to CD or HFD (C). ND=normal diet; HFD=high-fat diet; FI= Food Intake; BW= Body Weight. Data are presented as mean ± SEM. Sample size: n=4 ND; n=6 HFD. Data were analysed using Student's *t*-test. *p<0.05; **p<0.01;***p<0,001.

No variation in the expression levels of the hypothalamic anorexigenic *pro-opiomelanocortin* (*Pomc*)(Fig. 19 A) and orexigenic *Neuropeptide Y* (*Npy*) (Fig. 19 B) genes were detected following HFD, in both males and females. Conversely, a trend towards increased levels of the anorexigenic *cocaine- and amphetamine-regulated transcript prepropeptide* (*Cartpt*) was found in HFD-fed females, which further displayed significantly increased expression levels as compared to HFD-exposed males (Fig. 19 C). At the same time, the expression of the orexigenic *agouti-related neuropeptide* (*Agrp*) was decreased in males and not in females in HFD, although expression levels were again

higher in HFD-exposed females than in males (Fig. 19 D). Oxt gene expression levels were not affected by HFD in either males or females (Fig. 19 E). Quantification of plasma Oxt levels, revealed a trend towards increased Oxt levels only in females exposed to HFD, which had significantly higher levels of the protein even compared to males exposed to HFD (Fig. 19 F).

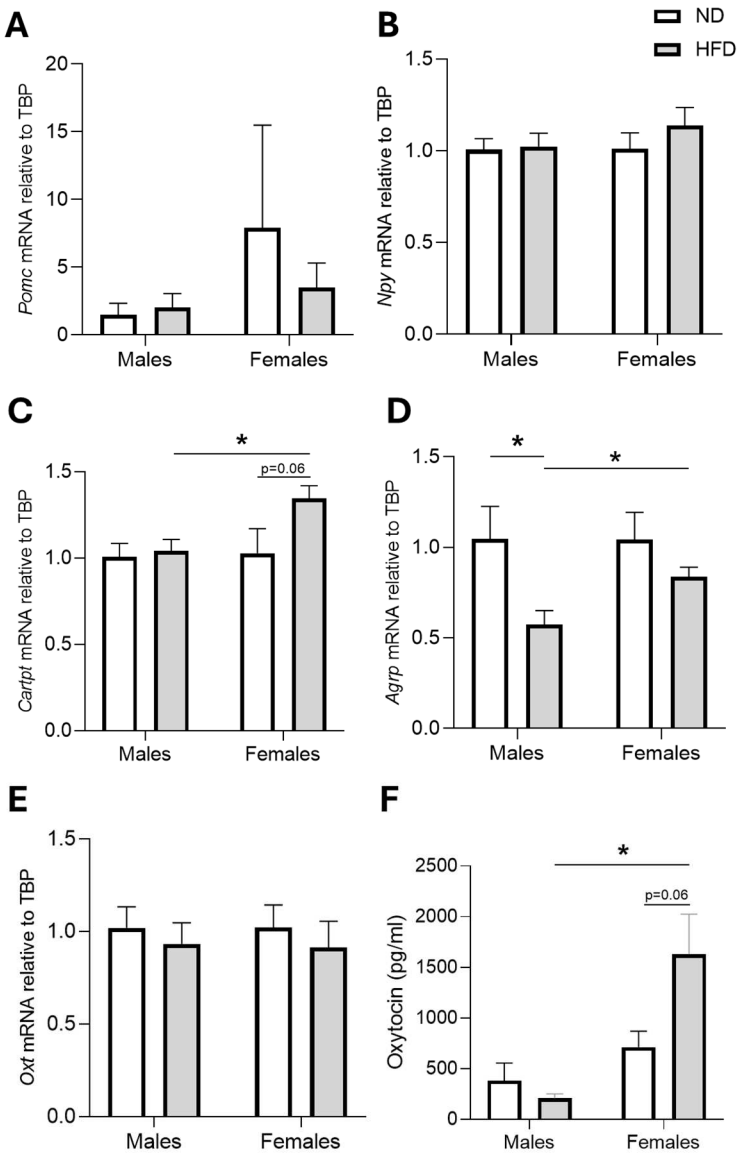

Figure 19 : Gene expression assays and Oxt quantification in plasma in mice exposed to HFD. RT-qPCR for Pomc (A) Npy (B) Cartpt (C) Agrp (D) and Oxt (E) gene expression analysis in ND and HFD male and female mice. Oxt quantification in plasma by LC-MS in ND and HFD male and female mice (F). Sample size: n=4 ND; n=6 HFD. ND=normal diet; HFD=high-fat diet; LC-MS= liquid chromatography and mass spectrometry. Data are presented as mean ± SEM. Data were analysed using Student's *t*-test. *p<0.05.

In summary, 12 weeks of HFD consumption led to a significant increase in body weight in males, but not in female mice. Furthermore, food intake was decreased in males, which displayed lower levels of the orexigenic *Agrp* and in even in females, which showed higher levels of the anorexigenic *Cartpt* after the HFD exposure. Importantly, circulating Oxt levels did not significantly vary following HFD in males and females, even though the last experienced a trend for higher plasma Oxt. Interestingly, *Cartpt* and *Agrp* hypothalamic expression levels and Oxt in plasma did not differ between males and females fed with ND, while they varied in a dimorphic way when comparing males and females exposed to HFD.

5.9 Oxytocin secretion in plasma in mice exposed to Early Life Stress

Environmental stimuli are known to affect Lep secretion and signalling and to directly impact Oxt system [157, 177, 193, 194]. All the data collected in this project, have laid the foundations for the study of the possible alterations induced by ELS on the Lep-Oxt crosstalk, which may predispose to obesity vulnerability in adulthood. Dams and pups belonging to the control group were housed in standard conditions (STD) until P21 (Fig. 20A), while the ELS group were exposed to the protocol of limited bedding and nesting (LBN) [184] for 7 days (P2-P9) and then returned to standard condition until P21 (Fig. 20B). Pups exposed to LBN weighed significantly less at P21 than controls (Fig. 20C), a typical feature of LBN-exposed pups which was also reported in previous studies [173, 195]. In contrast, preliminary data on Oxt quantification in plasma revealed that plasma Oxt levels were not significantly affected by LBN at P21 (Fig. 20D), although further experiments on a larger number of pups are required. All experiments were analysed by combining data from males and

females at P21. Future analyses will focus on determining the response of Oxt neurons to Lep in both males and females at P21 and P60 after LBN exposure, with the final aim of evaluating the vulnerability of ELS-exposed mice to obesity when exposed to HFD in adulthood.

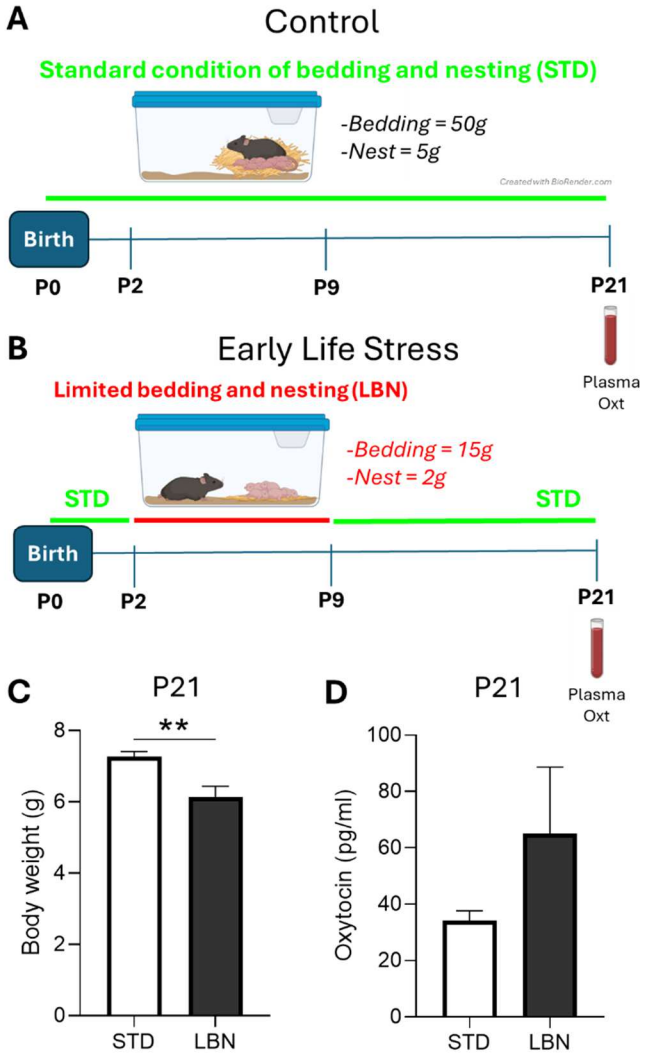

Figure 20 : Oxt quantification in plasma of mice exposed to LBN protocol. Timeline and experimental setting of control group exposed to STD (A) and ELS group exposed to LBN (B). Body weight (g) in P21 pups at the end of STD and LBN protocol (C). Oxt quantification in plasma by LC-MS in pups, at P21, which were exposed to STD and LBN (D). P=postnatal day; ELS= early life stress; LBN=limited bedding and nesting; STD=standard; LC-MS=liquid chromatography and mass spectrometry; Sample size: n=7 STD; n=8 ELS. Data are presented as mean ± SEM. Data were analysed using Student's *t*-test. **p<0.01.

6. Discussion

The regulation of the energy balance is a complex process integrating various peripheral signals within circuits in the central nervous system (CNS), primarily in the hypothalamus [196]. Disruption of this system, results in metabolic disorders, such as obesity [197].

Obesity is a highly complex, relapsing and multifactorial disease, which causes 4 million death each year due to the complications related to the comorbidities (e.g. cardiovascular diseases, type 2 diabetes and cancer) [4]. The CNS is the master regulator of the energy balance [197], and several studies focused on the brain to find the causes underlying the onset of obesity or target new pharmacological therapies [197, 198].

Oxt and Lep are both hormones involved in the regulation of various physiological processes, including energy balance [68, 199]. Oxt is an anti-obesogenic hormone, hypothesized to mediate the central anorexigenic role of Lep, while inducing lipolysis in the AT to control body weight. At the same time, Lep is an adipose-derived hormone produced proportionally to the amount of the fat mass [34]. Obesity is associated with the central Lep resistance, a condition which is reversed by the exogenous Oxt treatment in rodents [85, 93]. Thus, there are increasing evidence that exogenous Oxt administration interacts with Lep- related pathways [93, 122, 126, 200].

At the same time, the endogenous crosstalk between Oxt system and Lep may be a crucial aspect in obesity, where hyperleptinemia may affect Oxt synthesis and release.

Our study has demonstrated, for the first time, that Oxt secretion in plasma is induced by IP injection of Lep, following a time-dependent and a sex-dimorphic pattern. Lep significantly induced Oxt release in plasma after 1.5h in male mice, while it only induced a trend of Oxt release after 6h in females.

Oxt release in plasma was reported to be affected by Lep during particular physiological condition in female rodents, such as during pregnancy [201-203] and lactation [204, 205]. In contrast, previous studies failed to observe any changes in plasma Oxt concentrations in response to ICV treatment with Lep [206] or even observed a Lep-mediated inhibition of Oxt secretion in male rats [207].

However, the interpretation of data regarding plasma Oxt concentration, was heavily affected by methodological issues related to the assays available for the measurement of Oxt in biological samples [144, 208]. In the past years, the most common methods used to assess plasma Oxt were the commercially available radio immune-assays (RIA) or enzyme immuno-assays (EIA), which lead to inconsistent and uncorrelated results [209, 210].

Therefore, the strength of our study was to measure Oxt in plasma by LC-MS, which is recognized as the "gold-standard" technique to measure Oxt in biological samples [144, 153, 155, 156, 211, 212]. We optimized the protocol from Franke et al. [156] and performed the analysis with the addition of a stable isotope to increase the accuracy of the result.

At the same time, we also employed LC-MS to measure Avp release in plasma and found that Lep failed to induce Avp release in male mice, thus strengthening that Lep specifically target the Oxt system.

Therefore, our method provided us important results regarding the Lep-mediated increase in plasma Oxt, which we hypothesize is mediated by hypothalamic Oxt neurons.

However, our data showed that Oxt plasma release was uncoupled from *Oxt mRNA* synthesis in the hypothalamus: Lep induced *Oxt mRNA* synthesis in females, where Oxt plasma release was not significantly affected, while the

opposite results was observed in males, where Lep induced plasma Oxt release without affecting *Oxt mRNA* synthesis in the hypothalamus.

Since Oxt is known to be produced also by peripheral organs, such as the GI tract, we have hypothesized that Oxt release might be mediated by a peripheral source of Oxt in males [135, 136, 213, 214]. Importantly, a recent paper by Rosen lab reported the existence of a subpopulation of oxytocinergic Th+ sympathetic neurons that innervate WAT and release Oxt directly in AT to regulate lipolysis associated with fasting and cold-exposure [137]. They found that Oxt concentration in AT was increased during these conditions, while it was unchanged in serum. However, they measured Oxt in serum by using the "Enzyme Linked Immunosorbent Assay" (ELISA) kit, which was reported to have low sensitivity/specificity and to detect interference substances present in complex biological matrices, such as serum and plasma, and thus potentially confounding the results [148]. Furthermore, they studied the expression of Oxt in the WAT by using IHC and Oxt-*Cre* transgenic mice expressing the fluorescent proteins GFP or d-Tomato in the *Oxt* gene. However, we performed IHC for Oxt and TH antibodies on WAT, both inguinal and visceral, in male mice and we failed to find nerves containing Oxt in WAT but successfully observed Th+ fibers. Therefore, our data did not confirm that Oxt is expressed in the AT and further experiments would be needed to clarify these conflicting results.

As Oxt was reported to be produced also by the enteric nervous system [135], we assessed Oxt expression in several areas of the alimentary system. Based on our data, Oxt+ cells were not detectable in esophagus, stomach and duodenum. Therefore, a peripheral source of Oxt was not expected to be involved in the Oxt response to Lep in male mice.

The uncoupling between peripheral Oxt release and hypothalamic synthesis in male and female mice after Lep administration, remained a phenomenon which deserve further investigations. Interestingly, previous study on the behavioural effect of Oxt had already reported the existence of a mismatch between central and peripheral Oxt, demonstrating that emotional stress affects the central release of Oxt, in the CSF, but not in the plasma of male rats, while pharmacological stress affects only the peripheral release of Oxt [215]. Therefore, central and peripheral Oxt secretion might be independent of each other [123, 215].

Considering such a complex interaction between Lep and Oxt, we aimed to focus on the central mechanism behind the Lep-Oxt crosstalk, highlighting the Lepr-mediated signalling cascade in Oxt neurons of both male and female mice. Our data, showed that p-Stat3, which is the main signalling pathway activated by Lep for the regulation of the energy balance [57], is not activated in either PVN or SON Oxt neurons after the IP administration of Lep, in both male and female mice.

Our data are in contrast with those showed by Perello et al. [93], who gave an ICV injection of Lep to male rats and observed the activation of p-Stat3 in ~6% of Oxt neurons, only in the PVN.

However, since Lep is secreted from adipocytes into the bloodstream and accessed the brain by crossing the blood-brain barrier (BBB) or by directly accessing circumventricular organs [216, 217], the ICV injection is not a physiological route of administration and may induces artefactual effects in the brain.

At the same time, we have demonstrated that Lep acts on Oxt neurons by the activation of c-Fos in Oxt neurons in the SON, in both male and female mice.

The activation of c-Fos in Oxt neurons is consistent with the intracellular signalling pathways activated by Lep [35, 37, 52]. Indeed, Lep activates c-Fos as a downstream signal via the "extracellular signal-regulated kinase" (ERK 1/2) signalling cascade, *in vitro* [44]. ERK 1/2 is also among the most common signalling pathways activated by Lep for the regulation of the energy balance in the hypothalamus [37, 46] and Lep is responsible for c-Fos activation in hypothalamic regions involved in the energy balance regulation, such as the ARC [49-51], but also in the PVN [50, 52]. To our knowledge, none of these studies reported a Lep-induced activation of c-Fos in the SON and ours, is the first one describing cFos activation of Oxt neurons in the SON, but not in the PVN.

Our study demonstrated that ~20% of Oxt neurons were c-Fos+ in SON. In this regard, it is of importance to mention that the SON is enriched with gap junctions, which are used by Oxt magnocellular neurons under certain physiological condition to induce a synchronized neuronal firing, a phenomenon named "neuronal coupling" [218]. For example, lactation significantly increased intraneuronal coupling between Oxt neurons [219], while hyperosmotic stress increases Avp neuron activity in a gap junction-dependent manner [220]. Therefore, we speculate that the ability of Oxt neurons to engage in neuronal coupling could also play a pivotal role in mediating the response to Lep, possibly involving also those neurons where c-Fos is not activated.

The effect of Lep on magnocellular Oxt neurons in SON has been always poorly studied, although they are the main source of Oxt release from the neurohypophysis to the peripheral circulation [221]. Our study aimed to investigate the mechanism behind Lep activation of Oxt neurons in SON, by

assessing the presence of Lepr in these neurons. Previous studies assumed that Lep directly act on Oxt neurons in SON, by binding to Lepr, which was reported to be expressed in this region by using IHC against Lepr [100]. In our experience, there are no commercially available antibodies against Lepr suitable for the immunohistochemical detection of Lepr in the mouse brain. This observation is in line with a previous study in literature which investigated Lepr distribution in several hypothalamic regions, by inducing the expression of the GFP on Lepr-positive neurons [222]. This study observed Lepr expression in PVN, but not in SON neurons. Furthermore, several studies preferred the use of *in-situ* hybridization to study Lepr expression rather than IHC [190, 222-225].

Our data of *in-situ* hybridization and sc-RNA seq failed to observe the expression of Lepr in Oxt neurons in both PVN and SON neurons, a finding which raised the hypothesis that Lep may indirectly act on Oxt neurons in the SON. Consistently, we failed to observe an increased Ca^{2+} activity after Lep perfusion in SON neurons *ex-vivo*, thus confirming that Lep is not able to directly activate Oxt neurons in the SON.

The paper from Sabatier et al. [123], observed that a strong c-Fos expression, coupled with increased Ca^{2+} activity, was induced by the α-Melanocyte-stimulating hormone (α-Msh) in Oxt neurons in the SON, *ex vivo*. Interestingly, the α-Msh is produced and released by POMC neurons of the ARC and Lep is known to induce α-Msh release [26, 226, 227]. Therefore, Oxt neurons in the SON may receive projections from POMC neurons, which may further release α-Msh in response to Lep. In literature, POMC neurons were reported to project only to the PVN [228, 229], although we showed for the first time that they also project to the SON, where axon terminals are in proximity of Oxt neurons.

Therefore, we hypothesized that Lep may indirectly target these neurons through POMC projections, which could in turn release the α-Msh and bind to Mc4r in Oxt neurons in SON. Although Mc4r [102, 230] is reported to be expressed in SON, we failed to find the expression of *Mc4r mRNA* in Oxt neurons by *in-situ* hybridization.

Therefore, our study supports that Lep may indirectly target Oxt neurons by a mechanism which is possibly not mediated by a "peptidergic" transmission. Indeed, POMC neurons can also express the neurotransmitters GABA and glutamate [231] and can rapidly affect the activity of downstream neurons via their release [232].

At the same time, the peptide α-Msh also binds to other melanocortin receptors [233] such as Mc3r [234], whose expression in Oxt neurons in SON has not yet been documented. Interestingly, Mc1r expression was observed in Oxt neurons in both the PVN and the SON [124] and its role in Oxt neurons is currently unknown. Therefore, the next step would be to assess the expression of further melanocortin receptors and/or of GABA/glutamate transporters in Oxt neurons in SON, to gain new insight into the central mechanism behind Lep-Oxt crosstalk.

Lep-Oxt crosstalk has been investigated by others [17, 128] and was shown to be associated with an effect on the energy balance regulation. Specifically, the existence of a neural circuit including Lep-responsive Oxt neurons of the PVN projecting to the nucleus of the solitary tract (NTS), a region that integrates gut-derived satiety signals to the CNS, was documented [95]. Our study points to the existence of a novel, additional pathway involving Oxt neurons of the SON activated by Lep. An in-depth study of the mechanism responsible for the observed Lep-induced activation of Oxt neurons in the SON, would be of

paramount importance to unravel novel mechanisms possibly involved in the energy balance regulation.

Despite Lep may interact with Oxt for multiple physiological functions [201, 235], several evidences demonstrate that Oxt mediates the central anorexigenic effect of Lep [17, 87, 93, 97, 236, 237] and Oxt administration is able to reverse the Lep resistance [17, 93, 237]. Thus, we exposed mice to HFD to observe whether Oxt system could be subjected to any alteration in diet-induced obese mice, known to display chronic hyperleptinemia. Surprisingly, HFD-induced obesity did not affect central and peripheral Oxt levels in male mice [191].
Our data may suggest that the physiological response to the HFD is to increase Oxt in plasma to counteract the chronic positive energy balance. The lack of increased Oxt in plasma in male mice following HFD, could be due to the Lep resistance, hence Oxt neurons unresponsiveness to Lep in periphery, differently from females [57, 238]. Indeed, in diet-induced obese female mice, who are less prone to develop Lep resistance [239], we found a tendency towards increased plasma Oxt, which is in accordance with previous studies reporting higher levels of Oxt in obesity [144]. Such data may also explain the different weight gain experienced by males and females after HFD exposure: female mice appeared more resistant to fat accumulation after HFD compared to males and the sex-dependent protective role of females towards HFD-induced obesity is not related to an increased food intake [240] . Our data suggest that higher Oxt levels in plasma may contribute to the reduced body weight observed in females during HFD and we also speculate that the plasmatic Oxt release may be a neuroendocrinological reflex in response to hyperleptinemia and high energy state, possibly responsible for the reduction of plasma Lep levels [241] and further counteracting the onset of the Lep resistance. This data are also in

accordance with the hypothesis that Oxt can act as a signal of energy availability [144], in parallel with its lipolytic role [126, 137].

Indeed, our study demonstrated that Lep administration increases Oxtr protein levels in iWAT. It is thus possible that Lep increases not only circulating Oxt levels, but also the expression of its receptor in the white adipose tissues to promote Oxt lipolytic action. The Lep-induced Oxt release and the neuropeptide potential action on adipose tissues, may hence be considered as feedback negatively regulating fat mass.

At the same time, it is of importance to underline that Lep-Oxt crosstalk may have different physiological roles in males and females, since we observed a dimorphic pattern in both physiological system and in obesity. However, our data are in contrast with those reported by Wu et al. [94], who found that ablation of Oxt neurons activity driven by the diphtheria toxin (DTX) resulted in body weight increase during HFD only in males and not in females.

We believe that the total ablation of Oxt neurons not only in the SON but also in the PVN, may interfere with several neuro-endocrinological responses and not discriminate the exclusive SON-mediated response to obesity. Furthermore, it is possible that the different dietary approach used in this paper consisting of a higher percentage/different type of fat and a higher percentage of carbohydrates may have resulted in a different metabolic response.

In conclusion, the discovery of a new central mechanism regulating Lep-Oxt crosstalk is of importance to comprehend the central regulation of the energy balance not only in physiologic conditions, but also in condition of obesity and related metabolic diseases. However, further studies are needed to elucidate the physiological implication of the Lep-mediated endogenous Oxt release.

The neuronal networks behind the regulation of the energy balance, develop during the pre- and post-natal period, when the brain is highly plastic [172, 242, 243]. Since brain development is strongly dependent on environmental factors [172], our future studies will be focused on investigating the effect of adverse stimuli during brain development, such as ELS, in the central regulation of the energy balance in adulthood [157]. Interestingly, both Lep [177, 193] and Oxt [244, 245] system are reported to be affected by the ELS, which is related to an higher risk of obesity in adulthood [160]. However, our preliminary data failed to detect a significant difference of Oxt secretion in ELS-exposed mice, although further experiments with a larger samples size are required.

Lep exerts a trophic function during the postnatal development, by shaping neuronal network involved in the regulation of the energy balance [169]. It is currently unknown whether Lep may impact the development of the Oxt system during brain maturation [157]. Importantly, our study demonstrated that Oxt neurons are responsive to Lep already at P21. Furthermore, the different number of Oxt neurons described in males and females at P21 compared to P60, suggest a distinct and sex-specific maturation of Oxt neurons during this critical period. Therefore, Lep may differently affect Oxt neurons development in a time and sex-specific pattern.

Moreover, ELS may negatively affect such crosstalk between Lep and Oxt during the postnatal development and further impact the central regulation of the energy balance. The disruption of Lep-Oxt crosstalk induced by ELS, may provide new insights into comprehending the aetiology of obesity in adulthood.

7. Conclusions

Our study demonstrated for the first time that Lep regulates Oxt synthesis and release in circulation, following a time- and sex- dimorphic pattern. Such activation is associated with an increased c-Fos expression in Oxt neurons in the SON of both sexes, suggesting that Lep modulate Oxt release by targeting Oxt neurons in the SON. Moreover, we found that Lep may target Oxt neurons indirectly and that POMC neurons project to Oxt neurons in the SON, where Mc4r was not expressed, thus suggesting that Lep-Oxt interaction is not "hormone-mediated". In conclusion, our study points to the existence of a novel neuroendocrine pathway between Lep and Oxt neurons in the SON. Furthermore, we have demonstrated that Lep regulates Oxtr expression in AT in females and that Oxt synthesis is affected by HFD exposure in female but not in male mice. Further studies regarding the crosstalk between Lep and Oxt, would be of critical relevance for the study of obesity.

8. Bibliography

1. Solomon, B.L., *The hypothalamus and the pituitary gland: an overview.* Nurs Clin North Am, 1980. **15**(3): p. 435-51.
2. Rodriguez-Rodriguez, R. and C. Miralpeix, *Hypothalamic Regulation of Obesity.* Int J Mol Sci, 2021. **22**(24).
3. Apovian, C.M., *Obesity: definition, comorbidities, causes, and burden.* Am J Manag Care, 2016. **22**(7 Suppl): p. s176-85.
4. Collaborators, G.B.D.R.F., *Global burden of 87 risk factors in 204 countries and territories, 1990-2019: a systematic analysis for the Global Burden of Disease Study 2019.* Lancet, 2020. **396**(10258): p. 1223-1249.
5. The Lancet Gastroenterology, H., *Obesity: another ongoing pandemic.* Lancet Gastroenterol Hepatol, 2021. **6**(6): p. 411.
6. Schneeberger, M., R. Gomis, and M. Claret, *Hypothalamic and brainstem neuronal circuits controlling homeostatic energy balance.* J Endocrinol, 2014. **220**(2): p. T25-46.
7. Berthoud, H.R., *Metabolic and hedonic drives in the neural control of appetite: who is the boss?* Curr Opin Neurobiol, 2011. **21**(6): p. 888-96.
8. Boer, G.A., D.L. Hay, and A. Tups, *Obesity pharmacotherapy: incretin action in the central nervous system.* Trends Pharmacol Sci, 2023. **44**(1): p. 50-63.

9. Argente, J., et al., *Hypothalamic obesity: from basic mechanisms to clinical perspectives.* Lancet Diabetes Endocrinol, 2024.
10. Elias, C.F., et al., *Leptin differentially regulates NPY and POMC neurons projecting to the lateral hypothalamic area.* Neuron, 1999. **23**(4): p. 775-86.
11. Hill, J.W., *Gene Expression and the Control of Food Intake by Hypothalamic POMC/CART Neurons.* Open Neuroendocrinol J, 2010. **3**: p. 21-27.
12. Rafiei, N., et al., *Chemogenetic activation of arcuate nucleus NPY and NPY/AgRP neurons increases feeding behaviour in mice.* Neuropeptides, 2024. **107**: p. 102454.
13. Aponte, Y., D. Atasoy, and S.M. Sternson, *AGRP neurons are sufficient to orchestrate feeding behavior rapidly and without training.* Nat Neurosci, 2011. **14**(3): p. 351-5.
14. Krashes, M.J., et al., *Rapid, reversible activation of AgRP neurons drives feeding behavior in mice.* J Clin Invest, 2011. **121**(4): p. 1424-8.
15. Zhan, C., et al., *Acute and long-term suppression of feeding behavior by POMC neurons in the brainstem and hypothalamus, respectively.* J Neurosci, 2013. **33**(8): p. 3624-32.
16. Qualls-Creekmore, E. and H. Munzberg, *Modulation of Feeding and Associated Behaviors by Lateral Hypothalamic Circuits.* Endocrinology, 2018. **159**(11): p. 3631-3642.
17. Altirriba, J., A.L. Poher, and F. Rohner-Jeanrenaud, *Chronic Oxytocin Administration as a Treatment Against Impaired Leptin Signaling or Leptin Resistance in Obesity.* Front Endocrinol (Lausanne), 2015. **6**: p. 119.
18. Crawley, J.N. and R.L. Corwin, *Biological actions of cholecystokinin.* Peptides, 1994. **15**(4): p. 731-55.
19. Seabrook, L.T. and S.L. Borgland, *The orbitofrontal cortex, food intake and obesity.* J Psychiatry Neurosci, 2020. **45**(5): p. 304-312.
20. Kwon, E. and Y.H. Jo, *Activation of the ARC(POMC)-->MeA Projection Reduces Food Intake.* Front Neural Circuits, 2020. **14**: p. 595783.
21. Hwang, Y.G. and H.S. Lee, *Neuropeptide Y (NPY) or cocaine- and amphetamine-regulated transcript (CART) fiber innervation on central and medial amygdaloid neurons that project to the locus coeruleus and dorsal raphe in the rat.* Brain Res, 2018. **1689**: p. 75-88.
22. Narayanan, N.S., D.J. Guarnieri, and R.J. DiLeone, *Metabolic hormones, dopamine circuits, and feeding.* Front Neuroendocrinol, 2010. **31**(1): p. 104-12.
23. Boekhoudt, L., et al., *Does activation of midbrain dopamine neurons promote or reduce feeding?* Int J Obes (Lond), 2017. **41**(7): p. 1131-1140.
24. Domingo-Rodriguez, L., et al., *A specific prelimbic-nucleus accumbens pathway controls resilience versus vulnerability to food addiction.* Nat Commun, 2020. **11**(1): p. 782.
25. Caron, A., et al., *Leptin and brain-adipose crosstalks.* Nat Rev Neurosci, 2018. **19**(3): p. 153-165.
26. Cowley, M.A., et al., *Leptin activates anorexigenic POMC neurons through a neural network in the arcuate nucleus.* Nature, 2001. **411**(6836): p. 480-4.
27. Zhang, Y., et al., *Positional cloning of the mouse obese gene and its human homologue.* Nature, 1994. **372**(6505): p. 425-32.
28. Ingalls, A.M., M.M. Dickie, and G.D. Snell, *Obese, a new mutation in the house mouse.* J Hered, 1950. **41**(12): p. 317-8.

29. Zhang, F., et al., *Crystal structure of the obese protein leptin-E100.* Nature, 1997. **387**(6629): p. 206-9.
30. Klein, S., et al., *Adipose tissue leptin production and plasma leptin kinetics in humans.* Diabetes, 1996. **45**(7): p. 984-7.
31. Maffei, M., et al., *Leptin levels in human and rodent: measurement of plasma leptin and ob RNA in obese and weight-reduced subjects.* Nat Med, 1995. **1**(11): p. 1155-61.
32. Cinti, S., *The adipose organ: endocrine aspects and insights from transgenic models.* Eat Weight Disord, 2001. **6**(3 Suppl): p. 4-8.
33. Trayhurn, P., *Endocrine and signalling role of adipose tissue: new perspectives on fat.* Acta Physiol Scand, 2005. **184**(4): p. 285-93.
34. Maffei, M. and A. Giordano, *Leptin, the brain and energy homeostasis: From an apparently simple to a highly complex neuronal system.* Rev Endocr Metab Disord, 2022. **23**(1): p. 87-101.
35. Bjorbaek, C. and B.B. Kahn, *Leptin signaling in the central nervous system and the periphery.* Recent Prog Horm Res, 2004. **59**: p. 305-31.
36. Baumann, H., et al., *The full-length leptin receptor has signaling capabilities of interleukin 6-type cytokine receptors.* Proc Natl Acad Sci U S A, 1996. **93**(16): p. 8374-8.
37. Kwon, O., K.W. Kim, and M.S. Kim, *Leptin signalling pathways in hypothalamic neurons.* Cell Mol Life Sci, 2016. **73**(7): p. 1457-77.
38. Maniscalco, J.W. and L. Rinaman, *Systemic leptin dose-dependently increases STAT3 phosphorylation within hypothalamic and hindbrain nuclei.* Am J Physiol Regul Integr Comp Physiol, 2014. **306**(8): p. R576-85.
39. Bates, S.H., et al., *STAT3 signalling is required for leptin regulation of energy balance but not reproduction.* Nature, 2003. **421**(6925): p. 856-9.
40. Vaisse, C., et al., *Leptin activation of Stat3 in the hypothalamus of wild-type and ob/ob mice but not db/db mice.* Nat Genet, 1996. **14**(1): p. 95-7.
41. Hubschle, T., et al., *Leptin-induced nuclear translocation of STAT3 immunoreactivity in hypothalamic nuclei involved in body weight regulation.* J Neurosci, 2001. **21**(7): p. 2413-24.
42. Morton, G.J., et al., *Leptin regulates insulin sensitivity via phosphatidylinositol-3-OH kinase signaling in mediobasal hypothalamic neurons.* Cell Metab, 2005. **2**(6): p. 411-20.
43. Hill, J.W., et al., *Acute effects of leptin require PI3K signaling in hypothalamic proopiomelanocortin neurons in mice.* J Clin Invest, 2008. **118**(5): p. 1796-805.
44. Banks, A.S., et al., *Activation of downstream signals by the long form of the leptin receptor.* J Biol Chem, 2000. **275**(19): p. 14563-72.
45. Takahashi, Y., et al., *Leptin induces mitogen-activated protein kinase-dependent proliferation of C3H10T1/2 cells.* J Biol Chem, 1997. **272**(20): p. 12897-900.
46. Rahmouni, K., et al., *Hypothalamic ERK mediates the anorectic and thermogenic sympathetic effects of leptin.* Diabetes, 2009. **58**(3): p. 536-42.
47. Kovacs, K.J., *Measurement of immediate-early gene activation- c-fos and beyond.* J Neuroendocrinol, 2008. **20**(6): p. 665-72.
48. Hoffman, G.E., M.S. Smith, and J.G. Verbalis, *c-Fos and related immediate early gene products as markers of activity in neuroendocrine systems.* Front Neuroendocrinol, 1993. **14**(3): p. 173-213.

49. Rezai-Zadeh, K., et al., *Leptin receptor neurons in the dorsomedial hypothalamus are key regulators of energy expenditure and body weight, but not food intake.* Mol Metab, 2014. **3**(7): p. 681-93.
50. Elias, C.F., et al., *Leptin activates hypothalamic CART neurons projecting to the spinal cord.* Neuron, 1998. **21**(6): p. 1375-85.
51. Elmquist, J.K., et al., *Leptin activates neurons in ventrobasal hypothalamus and brainstem.* Endocrinology, 1997. **138**(2): p. 839-42.
52. Wang, L., et al., *Fos expression in the brain induced by peripheral injection of CCK or leptin plus CCK in fasted lean mice.* Brain Res, 1998. **791**(1-2): p. 157-66.
53. Funcke, J.B., et al., *Monogenic forms of childhood obesity due to mutations in the leptin gene.* Mol Cell Pediatr, 2014. **1**(1): p. 3.
54. Clement, K., et al., *A mutation in the human leptin receptor gene causes obesity and pituitary dysfunction.* Nature, 1998. **392**(6674): p. 398-401.
55. Halaas, J.L., et al., *Physiological response to long-term peripheral and central leptin infusion in lean and obese mice.* Proc Natl Acad Sci U S A, 1997. **94**(16): p. 8878-83.
56. Gruzdeva, O., et al., *Leptin resistance: underlying mechanisms and diagnosis.* Diabetes Metab Syndr Obes, 2019. **12**: p. 191-198.
57. Bjorbaek, C., et al., *Identification of SOCS-3 as a potential mediator of central leptin resistance.* Mol Cell, 1998. **1**(4): p. 619-25.
58. Zhou, Y. and L. Rui, *Leptin signaling and leptin resistance.* Front Med, 2013. **7**(2): p. 207-22.
59. Balthasar, N., et al., *Leptin receptor signaling in POMC neurons is required for normal body weight homeostasis.* Neuron, 2004. **42**(6): p. 983-91.
60. Banks, W.A., C.R. DiPalma, and C.L. Farrell, *Impaired transport of leptin across the blood-brain barrier in obesity.* Peptides, 1999. **20**(11): p. 1341-5.
61. Jurek, B. and I.D. Neumann, *The Oxytocin Receptor: From Intracellular Signaling to Behavior.* Physiol Rev, 2018. **98**(3): p. 1805-1908.
62. Jirikowski, G.F., *Diversity of central oxytocinergic projections.* Cell Tissue Res, 2019. **375**(1): p. 41-48.
63. Dale, H.H., *On some physiological actions of ergot.* J Physiol, 1906. **34**(3): p. 163-206.
64. Veenema, A.H. and I.D. Neumann, *Central vasopressin and oxytocin release: regulation of complex social behaviours.* Prog Brain Res, 2008. **170**: p. 261-76.
65. Inada, K., *Neurobiological mechanisms underlying oxytocin-mediated parental behavior in rodents.* Neurosci Res, 2024. **207**: p. 1-12.
66. Hagihara, M., K. Miyamichi, and K. Inada, *The importance of oxytocin neurons in the supraoptic nucleus for breastfeeding in mice.* PLoS One, 2023. **18**(3): p. e0283152.
67. Hidema, S., et al., *Oxytocin Receptor-Expressing Neurons in the Medial Preoptic Area Are Essential for Lactation, whereas Those in the Lateral Septum Are Not Critical for Maternal Behavior.* Neuroendocrinology, 2024. **114**(6): p. 517-537.
68. Lawson, E.A., et al., *The role of oxytocin in regulation of appetitive behaviour, body weight and glucose homeostasis.* J Neuroendocrinol, 2020. **32**(4): p. e12805.
69. Parmaksiz, D. and Y. Kim, *Navigating Central Oxytocin Transport: Known Realms and Uncharted Territories.* Neuroscientist, 2024: p. 10738584241268754.

70. Zhang, B., et al., *Reconstruction of the Hypothalamo-Neurohypophysial System and Functional Dissection of Magnocellular Oxytocin Neurons in the Brain.* Neuron, 2021. **109**(2): p. 331-346 e7.
71. Li, H., et al., *Single-neuron projectomes of mouse paraventricular hypothalamic nucleus oxytocin neurons reveal mutually exclusive projection patterns.* Neuron, 2024. **112**(7): p. 1081-1099 e7.
72. Ahren, B., et al., *Regulation of plasma leptin in mice: influence of age, high-fat diet, and fasting.* Am J Physiol, 1997. **273**(1 Pt 2): p. R113-20.
73. Vigh-Teichmann, I., B. Vigh, and S. Koritsanszky, *[Liquor contacting neurons in the paraventricular nucleus].* Z Zellforsch Mikrosk Anat, 1970. **103**(4): p. 483-501.
74. Xiao, M., et al., *The distribution of neural nitric oxide synthase-positive cerebrospinal fluid-contacting neurons in the third ventricular wall of male rats and coexistence with vasopressin or oxytocin.* Brain Res, 2005. **1038**(2): p. 150-62.
75. Leng, G., C. Caquineau, and N. Sabatier, *Regulation of oxytocin secretion.* Vitam Horm, 2005. **71**: p. 27-58.
76. Veening, J.G., T. de Jong, and H.P. Barendregt, *Oxytocin-messages via the cerebrospinal fluid: behavioral effects; a review.* Physiol Behav, 2010. **101**(2): p. 193-210.
77. Arata, M., et al., *The Effects of Testosterone on Hypothalamic and Serum Oxytocin Levels Are Affected by the Estrogen Milieu in Female Rats.* Nutrients, 2024. **16**(15).
78. Tokui, T., et al., *Effects of gonadal status and the estrogen milieu on hypothalamic oxytocin gene expression and serum oxytocin levels in female rats.* Horm Behav, 2021. **133**: p. 105005.
79. Haussler, H.U., G.F. Jirikowski, and J.D. Caldwell, *Sex differences among oxytocin-immunoreactive neuronal systems in the mouse hypothalamus.* J Chem Neuroanat, 1990. **3**(4): p. 271-6.
80. Liao, P.Y., et al., *Mapping Central Projection of Oxytocin Neurons in Unmated Mice Using Cre and Alkaline Phosphatase Reporter.* Front Neuroanat, 2020. **14**: p. 559402.
81. Vincent, J.L. and F. Su, *Physiology and pathophysiology of the vasopressinergic system.* Best Pract Res Clin Anaesthesiol, 2008. **22**(2): p. 243-52.
82. Song, Z. and H.E. Albers, *Cross-talk among oxytocin and arginine-vasopressin receptors: Relevance for basic and clinical studies of the brain and periphery.* Front Neuroendocrinol, 2018. **51**: p. 14-24.
83. Donaldson, Z.R. and L.J. Young, *Oxytocin, vasopressin, and the neurogenetics of sociality.* Science, 2008. **322**(5903): p. 900-4.
84. Arletti, R., A. Benelli, and A. Bertolini, *Influence of oxytocin on feeding behavior in the rat.* Peptides, 1989. **10**(1): p. 89-93.
85. Deblon, N., et al., *Mechanisms of the anti-obesity effects of oxytocin in diet-induced obese rats.* PLoS One, 2011. **6**(9): p. e25565.
86. Blevins, J.E. and D.G. Baskin, *Translational and therapeutic potential of oxytocin as an anti-obesity strategy: Insights from rodents, nonhuman primates and humans.* Physiol Behav, 2015. **152**(Pt B): p. 438-49.
87. Morton, G.J., et al., *Peripheral oxytocin suppresses food intake and causes weight loss in diet-induced obese rats.* Am J Physiol Endocrinol Metab, 2012. **302**(1): p. E134-44.

88. Takayanagi, Y., et al., *Oxytocin receptor-deficient mice developed late-onset obesity.* Neuroreport, 2008. **19**(9): p. 951-5.
89. Camerino, C., *Low sympathetic tone and obese phenotype in oxytocin-deficient mice.* Obesity (Silver Spring), 2009. **17**(5): p. 980-4.
90. Swaab, D.F., J.S. Purba, and M.A. Hofman, *Alterations in the hypothalamic paraventricular nucleus and its oxytocin neurons (putative satiety cells) in Prader-Willi syndrome: a study of five cases.* J Clin Endocrinol Metab, 1995. **80**(2): p. 573-9.
91. Michaud, J.L., et al., *Sim1 haploinsufficiency causes hyperphagia, obesity and reduction of the paraventricular nucleus of the hypothalamus.* Hum Mol Genet, 2001. **10**(14): p. 1465-73.
92. Maejima, Y., et al., *The Anorexigenic Neural Pathways of Oxytocin and Their Clinical Implication.* Neuroendocrinology, 2018. **107**(1): p. 91-104.
93. Perello, M. and J. Raingo, *Leptin activates oxytocin neurons of the hypothalamic paraventricular nucleus in both control and diet-induced obese rodents.* PLoS One, 2013. **8**(3): p. e59625.
94. Wu, Z., et al., *An obligate role of oxytocin neurons in diet induced energy expenditure.* PLoS One, 2012. **7**(9): p. e45167.
95. Blevins, J.E., M.W. Schwartz, and D.G. Baskin, *Evidence that paraventricular nucleus oxytocin neurons link hypothalamic leptin action to caudal brain stem nuclei controlling meal size.* Am J Physiol Regul Integr Comp Physiol, 2004. **287**(1): p. R87-96.
96. Llewellyn-Smith, I.J., et al., *Oxytocin-immunoreactive innervation of identified neurons in the rat dorsal vagal complex.* Neurogastroenterol Motil, 2012. **24**(3): p. e136-46.
97. Matarazzo, V., et al., *Inactivation of Socs3 in the hypothalamus enhances the hindbrain response to endogenous satiety signals via oxytocin signaling.* J Neurosci, 2012. **32**(48): p. 17097-107.
98. Blevins, J.E., et al., *Oxytocin innervation of caudal brainstem nuclei activated by cholecystokinin.* Brain Res, 2003. **993**(1-2): p. 30-41.
99. Maejima, Y., et al., *Oxytocinergic circuit from paraventricular and supraoptic nuclei to arcuate POMC neurons in hypothalamus.* FEBS Lett, 2014. **588**(23): p. 4404-12.
100. Hakansson, M.L., et al., *Leptin receptor immunoreactivity in chemically defined target neurons of the hypothalamus.* J Neurosci, 1998. **18**(1): p. 559-72.
101. Caquineau, C., et al., *Effects of alpha-melanocyte-stimulating hormone on magnocellular oxytocin neurones and their activation at intromission in male rats.* J Neuroendocrinol, 2006. **18**(9): p. 685-91.
102. Siljee, J.E., et al., *Melanocortin 4 receptor distribution in the human hypothalamus.* Eur J Endocrinol, 2013. **168**(3): p. 361-9.
103. Shah, B.P., et al., *MC4R-expressing glutamatergic neurons in the paraventricular hypothalamus regulate feeding and are synaptically connected to the parabrachial nucleus.* Proc Natl Acad Sci U S A, 2014. **111**(36): p. 13193-8.
104. Perello, M., et al., *Maintenance of the thyroid axis during diet-induced obesity in rodents is controlled at the central level.* Am J Physiol Endocrinol Metab, 2010. **299**(6): p. E976-89.
105. Moos, F., et al., *Release of oxytocin within the supraoptic nucleus during the milk ejection reflex in rats.* Exp Brain Res, 1989. **76**(3): p. 593-602.

106. Takahashi, A., et al., *Cholinergic input to the supraoptic nucleus increases Fos expression and body temperature in rats.* Pflugers Arch, 2001. **442**(3): p. 451-8.
107. Stricker, E.M. and J.G. Verbalis, *Interaction of osmotic and volume stimuli in regulation of neurohypophyseal secretion in rats.* Am J Physiol, 1986. **250**(2 Pt 2): p. R267-75.
108. Qiu, J., et al., *Transcriptomic analysis of the osmotic and reproductive remodeling of the female rat supraoptic nucleus.* Endocrinology, 2011. **152**(9): p. 3483-91.
109. Pan, Y.J., et al., *Oxytocin in hypothalamic supraoptic nucleus is transferred to the caudate nucleus to influence pain modulation.* Neuropeptides, 2016. **58**: p. 61-5.
110. Brown, C.H., et al., *Physiological regulation of magnocellular neurosecretory cell activity: integration of intrinsic, local and afferent mechanisms.* J Neuroendocrinol, 2013. **25**(8): p. 678-710.
111. McCann, M.J., J.G. Verbalis, and E.M. Stricker, *LiCl and CCK inhibit gastric emptying and feeding and stimulate OT secretion in rats.* Am J Physiol, 1989. **256**(2 Pt 2): p. R463-8.
112. Hill, J.M., et al., *Autoradiographic localization of insulin receptors in rat brain: prominence in olfactory and limbic areas.* Neuroscience, 1986. **17**(4): p. 1127-38.
113. Unger, J., et al., *Distribution of insulin receptor-like immunoreactivity in the rat forebrain.* Neuroscience, 1989. **31**(1): p. 143-57.
114. Song, Z., et al., *Supraoptic oxytocin and vasopressin neurons function as glucose and metabolic sensors.* Am J Physiol Regul Integr Comp Physiol, 2014. **306**(7): p. R447-56.
115. Sladek, C.D., et al., *The "metabolic sensor" function of rat supraoptic oxytocin and vasopressin neurons is attenuated during lactation but not in diet-induced obesity.* Am J Physiol Regul Integr Comp Physiol, 2016. **310**(4): p. R337-45.
116. Serter Kocoglu, S., et al., *Glutamate receptor antagonist suppresses the activation of nesfatin-1 neurons following refeeding or glucose administration.* Folia Morphol (Warsz), 2022. **81**(2): p. 379-386.
117. Nichols, C.G., *KATP channels as molecular sensors of cellular metabolism.* Nature, 2006. **440**(7083): p. 470-6.
118. Matschinsky, F.M., *Glucokinase as glucose sensor and metabolic signal generator in pancreatic beta-cells and hepatocytes.* Diabetes, 1990. **39**(6): p. 647-52.
119. Levin, B.E., et al., *Metabolic sensing and the brain: who, what, where, and how?* Endocrinology, 2011. **152**(7): p. 2552-7.
120. Honda, K., et al., *Leptin affects the electrical activity of neurones in the hypothalamic supraoptic nucleus.* Brain Res Bull, 2002. **57**(5): p. 721-5.
121. Hristov, M., B. Landzhov, and K. Yakimova, *Effect of leptin on nitrergic neurons in the lateral hypothalamic area and the supraoptic nucleus of rats.* Biotech Histochem, 2024. **99**(3): p. 125-133.
122. Velmurugan, S., J.A. Russell, and G. Leng, *Systemic leptin increases the electrical activity of supraoptic nucleus oxytocin neurones in virgin and late pregnant rats.* J Neuroendocrinol, 2013. **25**(4): p. 383-90.
123. Sabatier, N., et al., *Alpha-melanocyte-stimulating hormone stimulates oxytocin release from the dendrites of hypothalamic neurons while inhibiting oxytocin release from their terminals in the neurohypophysis.* J Neurosci, 2003. **23**(32): p. 10351-8.

124. Romanova, I.V., et al., *Type 1 melanocortin receptors in pro-opiomelanocortin-, vasopressin-, and oxytocin-immunopositive neurons in different areas of mouse brain.* Anat Rec (Hoboken), 2023. **306**(9): p. 2388-2399.
125. Eliava, M., et al., *A New Population of Parvocellular Oxytocin Neurons Controlling Magnocellular Neuron Activity and Inflammatory Pain Processing.* Neuron, 2016. **89**(6): p. 1291-1304.
126. Assinder, S.J. and B.B. Boumelhem, *Oxytocin stimulates lipolysis, prostaglandin E(2) synthesis, and leptin secretion in 3T3-L1 adipocytes.* Mol Cell Endocrinol, 2021. **534**: p. 111381.
127. Szeto, A., et al., *Oxytocin reduces adipose tissue inflammation in obese mice.* Lipids Health Dis, 2020. **19**(1): p. 188.
128. Altirriba, J., et al., *Divergent effects of oxytocin treatment of obese diabetic mice on adiposity and diabetes.* Endocrinology, 2014. **155**(11): p. 4189-201.
129. Yi, K.J., et al., *The regulation of oxytocin receptor gene expression during adipogenesis.* J Neuroendocrinol, 2015. **27**(5): p. 335-42.
130. Rodbell, M., *Metabolism of Isolated Fat Cells. I. Effects of Hormones on Glucose Metabolism and Lipolysis.* J Biol Chem, 1964. **239**: p. 375-80.
131. Ding, C., M.K. Leow, and F. Magkos, *Oxytocin in metabolic homeostasis: implications for obesity and diabetes management.* Obes Rev, 2019. **20**(1): p. 22-40.
132. Zeng, W., et al., *Sympathetic neuro-adipose connections mediate leptin-driven lipolysis.* Cell, 2015. **163**(1): p. 84-94.
133. Zhang, H., et al., *Treatment of obesity and diabetes using oxytocin or analogs in patients and mouse models.* PLoS One, 2013. **8**(5): p. e61477.
134. Plessow, F., et al., *Intranasal Oxytocin for Obesity.* NEJM Evid, 2024. **3**(5): p. EVIDoa2300349.
135. Ohlsson, B., et al., *Oxytocin is expressed throughout the human gastrointestinal tract.* Regul Pept, 2006. **135**(1-2): p. 7-11.
136. Welch, M.G., et al., *Expression and developmental regulation of oxytocin (OT) and oxytocin receptors (OTR) in the enteric nervous system (ENS) and intestinal epithelium.* J Comp Neurol, 2009. **512**(2): p. 256-70.
137. Li, E., et al., *Control of lipolysis by a population of oxytocinergic sympathetic neurons.* Nature, 2024. **625**(7993): p. 175-180.
138. Zhang, G., et al., *Neuropeptide exocytosis involving synaptotagmin-4 and oxytocin in hypothalamic programming of body weight and energy balance.* Neuron, 2011. **69**(3): p. 523-35.
139. Gajdosechova, L., et al., *Hypooxytocinaemia in obese Zucker rats relates to oxytocin degradation in liver and adipose tissue.* J Endocrinol, 2014. **220**(3): p. 333-43.
140. Stock, S., et al., *Elevated plasma levels of oxytocin in obese subjects before and after gastric banding.* Int J Obes, 1989. **13**(2): p. 213-22.
141. Schorr, M., et al., *Oxytocin and Its Relationship to Body Composition, Bone Mineral Density, and Hip Geometry Across the Weight Spectrum.* J Clin Endocrinol Metab, 2017. **102**(8): p. 2814-2824.
142. Yuan, G., et al., *Reduced circulating oxytocin and High-Molecular-Weight adiponectin are risk factors for metabolic syndrome.* Endocr J, 2016. **63**(7): p. 655-62.

143. Qian, W., et al., *Decreased circulating levels of oxytocin in obesity and newly diagnosed type 2 diabetic patients.* J Clin Endocrinol Metab, 2014. **99**(12): p. 4683-9.
144. Lawson, E.A., *The effects of oxytocin on eating behaviour and metabolism in humans.* Nat Rev Endocrinol, 2017. **13**(12): p. 700-709.
145. McCullough, M.E., P.S. Churchland, and A.J. Mendez, *Problems with measuring peripheral oxytocin: can the data on oxytocin and human behavior be trusted?* Neurosci Biobehav Rev, 2013. **37**(8): p. 1485-92.
146. Beardwell, C.G., et al., *Radioimmunoassay of plasma vasopressin in physiological and pathological states in man.* J Endocrinol, 1975. **67**(2): p. 189-202.
147. Baylis, P.H. and D.A. Heath, *The development of a radioimmunoassay for the measurement of human plasma arginine vasopressin.* Clin Endocrinol (Oxf), 1977. **7**(2): p. 91-102.
148. Leng, G. and N. Sabatier, *Measuring Oxytocin and Vasopressin: Bioassays, Immunoassays and Random Numbers.* J Neuroendocrinol, 2016. **28**(10).
149. Chard, T., *The radioimmunoassay of oxytocin and vasopressin.* J Endocrinol, 1973. **58**(1): p. 143-60.
150. Bagdy, G. and K.T. Kalogeras, *Stimulation of 5-HT1A and 5-HT2/5-HT1C receptors induce oxytocin release in the male rat.* Brain Res, 1993. **611**(2): p. 330-2.
151. Zhang, D., et al., *Development and validation of a highly sensitive LC-MS/MS assay for the quantification of arginine vasopressin in human plasma and urine: Application in preterm neonates and child.* J Pharm Biomed Anal, 2014. **99**: p. 67-73.
152. Rooke, P. and P.H. Baylis, *A new sensitive radioimmunoassay for plasma arginine vasopressin.* J Immunoassay, 1982. **3**(2): p. 115-31.
153. Brandtzaeg, O.K., et al., *Proteomics tools reveal startlingly high amounts of oxytocin in plasma and serum.* Sci Rep, 2016. **6**: p. 31693.
154. Takiwaki, M., et al., *Development of a sensitive liquid chromatography-tandem mass spectrometry method for quantification of human plasma arginine vasopressin.* J Chromatogr B Analyt Technol Biomed Life Sci, 2021. **1181**: p. 122903.
155. Zhang, G., et al., *Ultra sensitive quantitation of endogenous oxytocin in rat and human plasma using a two-dimensional liquid chromatography-tandem mass spectrometry assay.* Anal Biochem, 2011. **416**(1): p. 45-52.
156. Franke, A.A., et al., *Oxytocin analysis from human serum, urine, and saliva by orbitrap liquid chromatography-mass spectrometry.* Drug Test Anal, 2019. **11**(1): p. 119-128.
157. Colleluori, G., et al., *Early Life Stress, Brain Development, and Obesity Risk: Is Oxytocin the Missing Link?* Cells, 2022. **11**(4).
158. Dehorter, N. and I. Del Pino, *Shifting Developmental Trajectories During Critical Periods of Brain Formation.* Front Cell Neurosci, 2020. **14**: p. 283.
159. Hensch, T.K., *Critical period plasticity in local cortical circuits.* Nat Rev Neurosci, 2005. **6**(11): p. 877-88.
160. Miller, A.L. and J.C. Lumeng, *Pathways of Association from Stress to Obesity in Early Childhood.* Obesity (Silver Spring), 2018. **26**(7): p. 1117-1124.
161. Entringer, S., C. Buss, and C. Heim, *[Early-life stress and vulnerability for disease in later life].* Bundesgesundheitsblatt Gesundheitsforschung Gesundheitsschutz, 2016. **59**(10): p. 1255-61.

162. Moreno-Mendez, E., et al., *Early-life programming of adipose tissue.* Nutr Res Rev, 2020. **33**(2): p. 244-259.
163. Bluher, M., *Obesity: global epidemiology and pathogenesis.* Nat Rev Endocrinol, 2019. **15**(5): p. 288-298.
164. Blum, H.P., *Separation-individuation theory and attachment theory.* J Am Psychoanal Assoc, 2004. **52**(2): p. 535-53.
165. Yamamoto, Y., et al., *Neonatal manipulations of oxytocin alter expression of oxytocin and vasopressin immunoreactive cells in the paraventricular nucleus of the hypothalamus in a gender-specific manner.* Neuroscience, 2004. **125**(4): p. 947-55.
166. Bouret, S.G., *Neurodevelopmental actions of leptin.* Brain Res, 2010. **1350**: p. 2-9.
167. Pinto, S., et al., *Rapid rewiring of arcuate nucleus feeding circuits by leptin.* Science, 2004. **304**(5667): p. 110-5.
168. Bouret, S.G., S.J. Draper, and R.B. Simerly, *Trophic action of leptin on hypothalamic neurons that regulate feeding.* Science, 2004. **304**(5667): p. 108-10.
169. Ahima, R.S., et al., *Regulation of neuronal and glial proteins by leptin: implications for brain development.* Endocrinology, 1999. **140**(6): p. 2755-62.
170. Frontini, A., et al., *Leptin-dependent STAT3 phosphorylation in postnatal mouse hypothalamus.* Brain Res, 2008. **1215**: p. 105-15.
171. Kamitakahara, A., et al., *A critical period for the trophic actions of leptin on AgRP neurons in the arcuate nucleus of the hypothalamus.* J Comp Neurol, 2018. **526**(1): p. 133-145.
172. Nelson, C.A., 3rd and L.J. Gabard-Durnam, *Early Adversity and Critical Periods: Neurodevelopmental Consequences of Violating the Expectable Environment.* Trends Neurosci, 2020. **43**(3): p. 133-143.
173. Walker, C.D., et al., *Chronic early life stress induced by limited bedding and nesting (LBN) material in rodents: critical considerations of methodology, outcomes and translational potential.* Stress, 2017. **20**(5): p. 421-448.
174. Kim, S., et al., *Early adverse experience and substance addiction: dopamine, oxytocin, and glucocorticoid pathways.* Ann N Y Acad Sci, 2017. **1394**(1): p. 74-91.
175. Ellis, B.J., et al., *Developmental programming of oxytocin through variation in early-life stress: Four meta-analyses and a theoretical reinterpretation.* Clin Psychol Rev, 2021. **86**: p. 101985.
176. Lapp, H.E., et al., *Early experience alters developmental trajectory of central oxytocin systems involved in hypothalamic-pituitary-adrenal axis regulation in Long-Evans rats.* Horm Behav, 2020. **126**: p. 104822.
177. Yam, K.Y., et al., *Exposure to chronic early-life stress lastingly alters the adipose tissue, the leptin system and changes the vulnerability to western-style diet later in life in mice.* Psychoneuroendocrinology, 2017. **77**: p. 186-195.
178. Leachman, J.R., et al., *Exacerbated obesogenic response in female mice exposed to early life stress is linked to fat depot-specific upregulation of leptin protein expression.* Am J Physiol Endocrinol Metab, 2020. **319**(5): p. E852-E862.
179. Bouillon-Minois, J.B., et al., *Leptin as a Biomarker of Stress: A Systematic Review and Meta-Analysis.* Nutrients, 2021. **13**(10).
180. Zhang, G. and D. Cai, *Circadian intervention of obesity development via resting-stage feeding manipulation or oxytocin treatment.* Am J Physiol Endocrinol Metab, 2011. **301**(5): p. E1004-12.

181. S.E., B., *The Concentrations of Circulating Plasma Oxytocin and the Pattern of Oxytocin Release in Mare during Oestrus and after Ovulation.*, in *EKC 2009 Proceedings of the EU-Korea Conference on Science and Technology*. 2010, Springer, Berlin, Heidelberg.
182. Tachibana, A., et al., *Changes in Serum Oxytocin Levels under Physiological and Supraphysiological Gonadal Steroid Hormone Conditions in Women of Reproductive Age: A Preliminary Study.* Nutrients, 2022. **14**(24).
183. Romanov, R.A., et al., *Molecular design of hypothalamus development.* Nature, 2020. **582**(7811): p. 246-252.
184. Rice, C.J., et al., *A novel mouse model for acute and long-lasting consequences of early life stress.* Endocrinology, 2008. **149**(10): p. 4892-900.
185. Scott, N., et al., *A sexually dimorphic hypothalamic circuit controls maternal care and oxytocin secretion.* Nature, 2015. **525**(7570): p. 519-22.
186. Bullitt, E., *Expression of c-fos-like protein as a marker for neuronal activity following noxious stimulation in the rat.* J Comp Neurol, 1990. **296**(4): p. 517-30.
187. Yang, Z., et al., *Regulation of insulin and leptin signaling by muscle suppressor of cytokine signaling 3 (SOCS3).* PLoS One, 2012. **7**(10): p. e47493.
188. Ernst, M.B., et al., *Enhanced Stat3 activation in POMC neurons provokes negative feedback inhibition of leptin and insulin signaling in obesity.* J Neurosci, 2009. **29**(37): p. 11582-93.
189. Tysoe, O., *Oxytocin regulates adipose tissue lipolysis.* Nat Rev Endocrinol, 2024. **20**(3): p. 126.
190. Mercer, J.G., et al., *Localization of leptin receptor mRNA and the long form splice variant (Ob-Rb) in mouse hypothalamus and adjacent brain regions by in situ hybridization.* FEBS Lett, 1996. **387**(2-3): p. 113-6.
191. Frederich, R.C., et al., *Leptin levels reflect body lipid content in mice: evidence for diet-induced resistance to leptin action.* Nat Med, 1995. **1**(12): p. 1311-4.
192. Lin, S., et al., *Development of high fat diet-induced obesity and leptin resistance in C57Bl/6J mice.* Int J Obes Relat Metab Disord, 2000. **24**(5): p. 639-46.
193. Daniels, T.E., et al., *Associations of early life stress with leptin and ghrelin in healthy young adults.* Psychoneuroendocrinology, 2023. **149**: p. 106007.
194. Wei, F., et al., *Experiences affect social behaviors via altering neuronal morphology and oxytocin system.* Psychoneuroendocrinology, 2021. **129**: p. 105247.
195. Arp, J.M., et al., *Blocking glucocorticoid receptors at adolescent age prevents enhanced freezing between repeated cue-exposures after conditioned fear in adult mice raised under chronic early life stress.* Neurobiol Learn Mem, 2016. **133**: p. 30-38.
196. Roh, E., D.K. Song, and M.S. Kim, *Emerging role of the brain in the homeostatic regulation of energy and glucose metabolism.* Exp Mol Med, 2016. **48**(3): p. e216.
197. Timper, K. and J.C. Bruning, *Hypothalamic circuits regulating appetite and energy homeostasis: pathways to obesity.* Dis Model Mech, 2017. **10**(6): p. 679-689.
198. Barreto-Vianna, A.R., M.B. Aguila, and C.A. Mandarim-de-Lacerda, *Effects of liraglutide in hypothalamic arcuate nucleus of obese mice.* Obesity (Silver Spring), 2016. **24**(3): p. 626-33.
199. Friedman, J.M., *Leptin and the endocrine control of energy balance.* Nat Metab, 2019. **1**(8): p. 754-764.

200. Chiodera, P., et al., *Effect of systemic oxytocin administration on dexamethasone-induced leptin secretion in normal and obese men.* J Clin Endocrinol Metab, 2000. **85**(10): p. 3683-6.
201. Henson, M.C. and V.D. Castracane, *Leptin in pregnancy: an update.* Biol Reprod, 2006. **74**(2): p. 218-29.
202. Grattan, D.R., S.R. Ladyman, and R.A. Augustine, *Hormonal induction of leptin resistance during pregnancy.* Physiol Behav, 2007. **91**(4): p. 366-74.
203. Lacroix, M., et al., *Higher maternal leptin levels at second trimester are associated with subsequent greater gestational weight gain in late pregnancy.* BMC Pregnancy Childbirth, 2016. **16**: p. 62.
204. Cagiran Yilmaz, F. and A.O. Ozcelik, *The relationships between leptin levels in maternal serum and breast milk of mothers and term infants.* Ann Med, 2021. **53**(1): p. 1309-1315.
205. Brogan, R.S., et al., *Suppression of leptin during lactation: contribution of the suckling stimulus versus milk production.* Endocrinology, 1999. **140**(6): p. 2621-7.
206. Yamamoto, S., et al., *Centrally administered murine leptin stimulates plasma arginine-vasopressin secretion and increases the level of mRNA expression in the supraoptic nucleus of conscious rats.* Neuroendocrinology, 1999. **70**(3): p. 207-12.
207. Kutlu, S., et al., *Leptin modulates noradrenaline release in the paraventricular nucleus and plasma oxytocin levels in female rats: a microdialysis study.* Brain Res, 2010. **1317**: p. 87-91.
208. MacLean, E.L., et al., *Challenges for measuring oxytocin: The blind men and the elephant?* Psychoneuroendocrinology, 2019. **107**: p. 225-231.
209. Szeto, A., et al., *Evaluation of enzyme immunoassay and radioimmunoassay methods for the measurement of plasma oxytocin.* Psychosom Med, 2011. **73**(5): p. 393-400.
210. Gnanadesikan, G.E., et al., *Specificity of plasma oxytocin immunoassays: A comparison of commercial assays and sample preparation techniques using oxytocin knockout and wildtype mice.* Psychoneuroendocrinology, 2021. **132**: p. 105368.
211. Karbiwnyk, C.M., et al., *Determination of oxytocin in a dilute IV solution by LC-MS(n).* J Pharm Biomed Anal, 2008. **48**(3): p. 672-7.
212. Liu, D., et al., *Measurement of ultra-trace level of intact oxytocin in plasma using SALLE combined with nano-LC-MS.* J Pharm Biomed Anal, 2019. **173**: p. 62-67.
213. Paiva, L., et al., *Identification of peripheral oxytocin-expressing cells using systemically applied cell-type specific adeno-associated viral vector.* J Neuroendocrinol, 2021. **33**(5): p. e12970.
214. Mohan, S., et al., *Oxytocin is present in islets and plays a role in beta-cell function and survival.* Peptides, 2018. **100**: p. 260-268.
215. Ivanyi, T., V.M. Wiegant, and D. de Wied, *Differential effects of emotional and physical stress on the central and peripheral secretion of neurohypophysial hormones in male rats.* Life Sci, 1991. **48**(13): p. 1309-16.
216. Meister, B. and M.L. Hakansson, *Leptin receptors in hypothalamus and circumventricular organs.* Clin Exp Pharmacol Physiol, 2001. **28**(7): p. 610-7.
217. Golden, P.L., T.J. Maccagnan, and W.M. Pardridge, *Human blood-brain barrier leptin receptor. Binding and endocytosis in isolated human brain microvessels.* J Clin Invest, 1997. **99**(1): p. 14-8.
218. Wang, P., et al., *Role of Connexin 36 in Autoregulation of Oxytocin Neuronal Activity in Rat Supraoptic Nucleus.* ASN Neuro, 2019. **11**: p. 1759091419843762.

219. Hatton, G.I., Q.Z. Yang, and P. Cobbett, *Dye coupling among immunocytochemically identified neurons in the supraoptic nucleus: increased incidence in lactating rats.* Neuroscience, 1987. **21**(3): p. 923-30.
220. Yuan, H., et al., *Acute hyperosmotic stimulus-induced Fos expression in neurons depends on activation of astrocytes in the supraoptic nucleus of rats.* J Neurosci Res, 2010. **88**(6): p. 1364-73.
221. Brownstein, M.J., J.T. Russell, and H. Gainer, *Synthesis, transport, and release of posterior pituitary hormones.* Science, 1980. **207**(4429): p. 373-8.
222. Patterson, C.M., et al., *Molecular mapping of mouse brain regions innervated by leptin receptor-expressing cells.* Brain Res, 2011. **1378**: p. 18-28.
223. Udagawa, J., et al., *Expression of the long form of leptin receptor (Ob-Rb) mRNA in the brain of mouse embryos and newborn mice.* Brain Res, 2000. **868**(2): p. 251-8.
224. Yoo, S., et al., *Tanycyte-Independent Control of Hypothalamic Leptin Signaling.* Front Neurosci, 2019. **13**: p. 240.
225. Leon Mercado, L., et al., *Identification of Leptin Receptor-Expressing Cells in the Nodose Ganglion of Male Mice.* Endocrinology, 2019. **160**(5): p. 1307-1322.
226. Kim, M.S., et al., *The central melanocortin system affects the hypothalamo-pituitary thyroid axis and may mediate the effect of leptin.* J Clin Invest, 2000. **105**(7): p. 1005-11.
227. Guo, L., et al., *N-acetylation of hypothalamic alpha-melanocyte-stimulating hormone and regulation by leptin.* Proc Natl Acad Sci U S A, 2004. **101**(32): p. 11797-802.
228. Metz, M.J., et al., *Individual arcuate nucleus proopiomelanocortin neurons project to select target sites.* Am J Physiol Regul Integr Comp Physiol, 2021. **321**(6): p. R982-R989.
229. Wang, D., et al., *Whole-brain mapping of the direct inputs and axonal projections of POMC and AgRP neurons.* Front Neuroanat, 2015. **9**: p. 40.
230. Mountjoy, K.G., et al., *Melanocortin receptor-mediated mobilization of intracellular free calcium in HEK293 cells.* Physiol Genomics, 2001. **5**(1): p. 11-9.
231. Quarta, C., et al., *POMC neuronal heterogeneity in energy balance and beyond: an integrated view.* Nat Metab, 2021. **3**(3): p. 299-308.
232. Dicken, M.S., R.E. Tooker, and S.T. Hentges, *Regulation of GABA and glutamate release from proopiomelanocortin neuron terminals in intact hypothalamic networks.* J Neurosci, 2012. **32**(12): p. 4042-8.
233. Dall'Olmo, L., et al., *Alpha-melanocyte stimulating hormone (alpha-MSH): biology, clinical relevance and implication in melanoma.* J Transl Med, 2023. **21**(1): p. 562.
234. West, K.S., et al., *Alpha-melanocyte stimulating hormone increases the activity of melanocortin-3 receptor-expressing neurons in the ventral tegmental area.* J Physiol, 2019. **597**(12): p. 3217-3232.
235. Harris, M., et al., *Transcriptional regulation of the thyrotropin-releasing hormone gene by leptin and melanocortin signaling.* J Clin Invest, 2001. **107**(1): p. 111-20.
236. Labyb, M., et al., *Oxytocin Administration Alleviates Acute but Not Chronic Leptin Resistance of Diet-Induced Obese Mice.* Int J Mol Sci, 2018. **20**(1).
237. Iwasaki, Y., et al., *Peripheral oxytocin activates vagal afferent neurons to suppress feeding in normal and leptin-resistant mice: a route for ameliorating hyperphagia and obesity.* Am J Physiol Regul Integr Comp Physiol, 2015. **308**(5): p. R360-9.

238. Munzberg, H., J.S. Flier, and C. Bjorbaek, *Region-specific leptin resistance within the hypothalamus of diet-induced obese mice.* Endocrinology, 2004. **145**(11): p. 4880-9.
239. Harris, R.B., H.M. Bowen, and T.D. Mitchell, *Leptin resistance in mice is determined by gender and duration of exposure to high-fat diet.* Physiol Behav, 2003. **78**(4-5): p. 543-55.
240. Oraha, J., et al., *Sex-specific changes in metabolism during the transition from chow to high-fat diet feeding are abolished in response to dieting in C57BL/6J mice.* Int J Obes (Lond), 2022. **46**(10): p. 1749-1758.
241. Andreoli, M.F., et al., *Leptin resensitisation: a reversion of leptin-resistant states.* J Endocrinol, 2019. **241**(3): p. R81-R96.
242. Jernigan, T.L., et al., *Postnatal brain development: structural imaging of dynamic neurodevelopmental processes.* Prog Brain Res, 2011. **189**: p. 77-92.
243. Higa, G.S.V., et al., *5-HT-dependent synaptic plasticity of the prefrontal cortex in postnatal development.* Sci Rep, 2022. **12**(1): p. 21015.
244. Jin, Y., et al., *The Role of Oxytocin in Early-Life-Stress-Related Neuropsychiatric Disorders.* Int J Mol Sci, 2023. **24**(13).
245. Baracz, S.J., N.A. Everett, and J.L. Cornish, *The impact of early life stress on the central oxytocin system and susceptibility for drug addiction: Applicability of oxytocin as a pharmacotherapy.* Neurosci Biobehav Rev, 2020. **110**: p. 114-132.

9. Acknowledgements

I am grateful to Prof. Antonio Giordano e Dr. Georgia Colleluori, who were the mentor and the supervisor of this PhD project respectively. I am also grateful to Prof. Ilenia Severi, Prof. Jessica Perugini and Dr. Martina Senzacqua for their contribution to this project, providing me with conceptual and technical assistance during the experiments. Furthermore, I am grateful to Prof. Tibor Harkany and Dr. Valentina Cinquina, who kindly hosted me in their laboratory of Molecular Neurosciences at the Medical University of Vienna and for providing me with instruments and techniques which were crucial to the realization of this project.